

Uncertainties in Supernova Yields I: 1D Explosions

Patrick A. Young^{1,2}, Chris L. Fryer^{1,3}

payoung@lanl.gov, fryer@lanl.gov

ABSTRACT

Theoretical nucleosynthetic yields from supernovae are sensitive to both the details of the progenitor star and the explosion calculation. We attempt to comprehensively identify the sources of uncertainties in these yields. In this paper we concentrate on the variations in yields from a single progenitor arising from common 1-dimensional methods of approximating a supernova explosion. Subsequent papers will examine 3-dimensional effects in the explosion and the progenitor, and trends in mass and composition. For the 1-dimensional explosions we find that both elemental and isotopic yields for Si and heavier elements are a sensitive function of explosion energy. Also, piston-driven and thermal bomb type explosions have different yields for the same explosion energy. Yields derived from 1-dimensional explosions are non-unique.

Subject headings: nuclear reactions, nucleosynthesis, abundances — stars: evolution — supernovae: general — supernova remnants

1. INTRODUCTION

The amount of observational data on chemical abundances is growing at an enormous rate. The Sloan Digital Sky Survey has produced spectra for $> 10^5$ galaxies at low redshifts. Information is also becoming available for smaller numbers of galaxies to redshifts > 6 with the current generation of large telescopes (Berger et al. 2006). Observations at high to moderate redshift show a gradual build-up in metallicity (Erb et al. 2006), from which conclusions about the star formation histories of galaxies are drawn. Comparison of metallicities between elliptical and spiral galaxies, members of groups and clusters, and abundance

¹Theoretical Astrophysics, Los Alamos National Laboratories, Los Alamos, NM 87545

²Steward Observatory, University of Arizona, Tucson AZ 85721

³Physics Dept., University of Arizona, Tucson AZ 85721

gradients within individual galaxies are used to probe their formation, interaction history, and evolution. Large telescopes are providing detailed abundances for Milky Way halo stars and dwarf galaxies and globular clusters in the local group. The dwarfs and globular clusters show a range of nearly a dex in $[\alpha/\text{Fe}]$ at a given $[\text{Fe}/\text{H}]$ (Pritzl, Venn, & Irwin 2005). Several ultra-metal-poor stars are now known with $[\text{Fe}/\text{H}] < -4$ (Aoki et al. 2006). Each has unique abundance anomalies that suggest they have been enriched by only one or a few stars.

Chemical evolution over a large fraction of the age of the universe is becoming a quantitative field of study. The conclusions that can be drawn from this data, however, are only as good as our understanding of how chemical elements are produced in stars. The best currently practical approach to producing theoretical yields would be to take a set of progenitor stars and explode them in 1-dimension with a range of free parameters such as explosion energy or mass cut. Then a linear combination of the models, weighted by an initial mass function (IMF) would be chosen which produces the desired abundance pattern, i.e solar, and these would then form a table of yields with mass and metallicity. In fact, the common approach is to take a single set of yields without any exploration of parameter space. (Garnett 2002)¹. In either scenario, these yields are fit, not predicted. The local group results indicate that very different enrichment histories with very different abundance ratios can lead to the same *total* enrichment in metallicity. Exploring these pathways require predictive yields. Identifying the star or stars that enriched the ultra-metal-poor halo stars even more clearly requires predictive yields with a unique correspondence to a progenitor.

Unfortunately, it is not presently possible routinely (or perhaps at all) to produce a truly predictive yield for an ensemble of stars. The nucleosynthesis is sensitive to a number of properties of the progenitor and explosion models, both physical and numerical. The structure of progenitors integrated over the evolution changes dramatically if hydrodynamic processes are included (Young et al. 2005). The evolution also depends upon rotation and mass loss (i.e. Meynet & Maeder 2000). The dynamics of the progenitor before and during collapse will also leave an imprint on the explosion. Hydrodynamic motions can result in asymmetries in the shell burning regions of $> 10\%$ at the onset of collapse (Meakin & Arnett 2006). The integrated effects can be incorporated into a stellar evolution code after an analytic framework is derived from examining simulations, but the late stage dynamics must be simulated directly with a computationally expensive multi-dimensional hydrodynamics code. The composition and mass of the progenitor of course also play a role.

¹The common standard for yields is Woosley & Weaver (1995). This compilation only presents yields for a single explosion energy, except at progenitor masses of 30 - 40 M_{\odot} .

The idea that the convection above the proto-neutron star plays an important role in understanding supernova energetics is gradually becoming accepted (Herant et al. 1994; Fryer & Warren 2002; Blondin & Mezcappa 2006; Burrows et al. 2006). If so, understanding the explosion and obtaining accurate explosion energetics will require 3-dimensional calculations. We are far from modeling all of the physics, including the convection, with enough detail in 2-dimensions, let alone 3, to accurately estimate explosion energies. 2-dimensional simulations assuming a 90° wedge geometry (Buras et al. 2003) have obtained different results when modeled using a 180° domain. (Janka - pvt. communication). The convective instabilities depend sensitively on the equation of state, resolution and, probably, implementation of the gravitational force (Fryer & Kusenko 2006; Fryer 2006). The convective instabilities also depend on the effects of rotation and asymmetries in the collapsing core (Shimizu et al. 1994; Fryer & Heger 2000; Kotake et al. 2003; Fryer & Warren 2004).

In addition to being important for our understanding of the explosive engine, multi-dimensional simulations are required to understand the outward mixing of heavy elements and, ultimately, the amount of this material that is ejected in a supernova (Kifonidis et al. 2000; Hungerford, Fryer, & Warren 2003) This effect is enhanced by explosion asymmetries (Nagataki et al. 1998; Kifonidis et al. 2003; Hungerford, Fryer, & Warren 2003; Hungerford, Fryer, & Rockefeller 2005). Multi-dimensional studies of the explosion are just now beginning to put in the relevant physics, and these new studies will no doubt bring new surprises in supernovae explosions. Detailed multi-dimensional models are required both to understand the supernova engine and the resultant explosion and, at this point in time, much more work must be done before we can predict either the explosive energies or the yields from supernovae. For massive stars, explosion mechanisms beyond the standard supernova engine (e.g. Woosley 1993, the collapsar model), will also play a role in nucleosynthetic yields.

Clearly, progress in the fields of chemical evolution, stellar populations, and galaxy assembly is not going to be put on hold while all the outstanding issues in supernovae and nucleosynthesis are resolved. We can, however, attempt to quantify the uncertainties arising from various assumptions in the yield calculations. In this series of papers we will identify sources of uncertainty from each aspect of the calculations so that we may include error bars in a new generation of integrated yields. In this first paper we will examine changes in yields for a single progenitor arising from various methods of performing 1D explosion calculations. Even though we are able to produce a weak explosion of a $23 M_\odot$ star in 3D, the simulation requires approximately seven months of computer time on a moderately sized cluster. Doing multi-D explosions for even a sparse sampling of a population will not be feasible for some time, so we still must rely on 1D models for integrated yields. In the second paper we will examine a full 3D collapse and explosion of the same progenitor and compare it to the 1D explosions. Paper three will study trends with changes in progenitor mass, composition and

evolution code physics. A final paper will compare our initially spherically symmetric 3D explosion with one with realistic progenitor dynamics as initial conditions.

2. PROGENITOR AND EXPLOSION CALCULATIONS

2.1. Progenitor

We use a $23 M_{\odot}$ progenitor of Grevesse & Sauval (1998) solar composition, aspects of which we have examined in Young et al. (2005). The model was produced with the TYCHO stellar evolution code (Young & Arnett 2005). The model is non-rotating and includes hydrodynamic mixing processes (Young & Arnett 2005; Young et al. 2005). Mass loss uses the prescriptions of Kudritzki et al. (1989) for OB mass loss and Blöcker (1995) for red giant/supergiant mass loss. The final stellar mass is $14.4 M_{\odot}$. Figure 1 shows the mean atomic weight (\bar{A} , top) and density (bottom) versus enclosed mass. A 177 element network terminating at ${}^{74}\text{Ge}$ is used throughout the evolution. The network uses the NOSMOKER rates from Rauscher & Thielemann (2001), weak rates from Langanke & Martinez-Pinedo (2000), and screening from Graboske et al. (1973). Neutrino cooling from plasma processes and the Urca process is included.

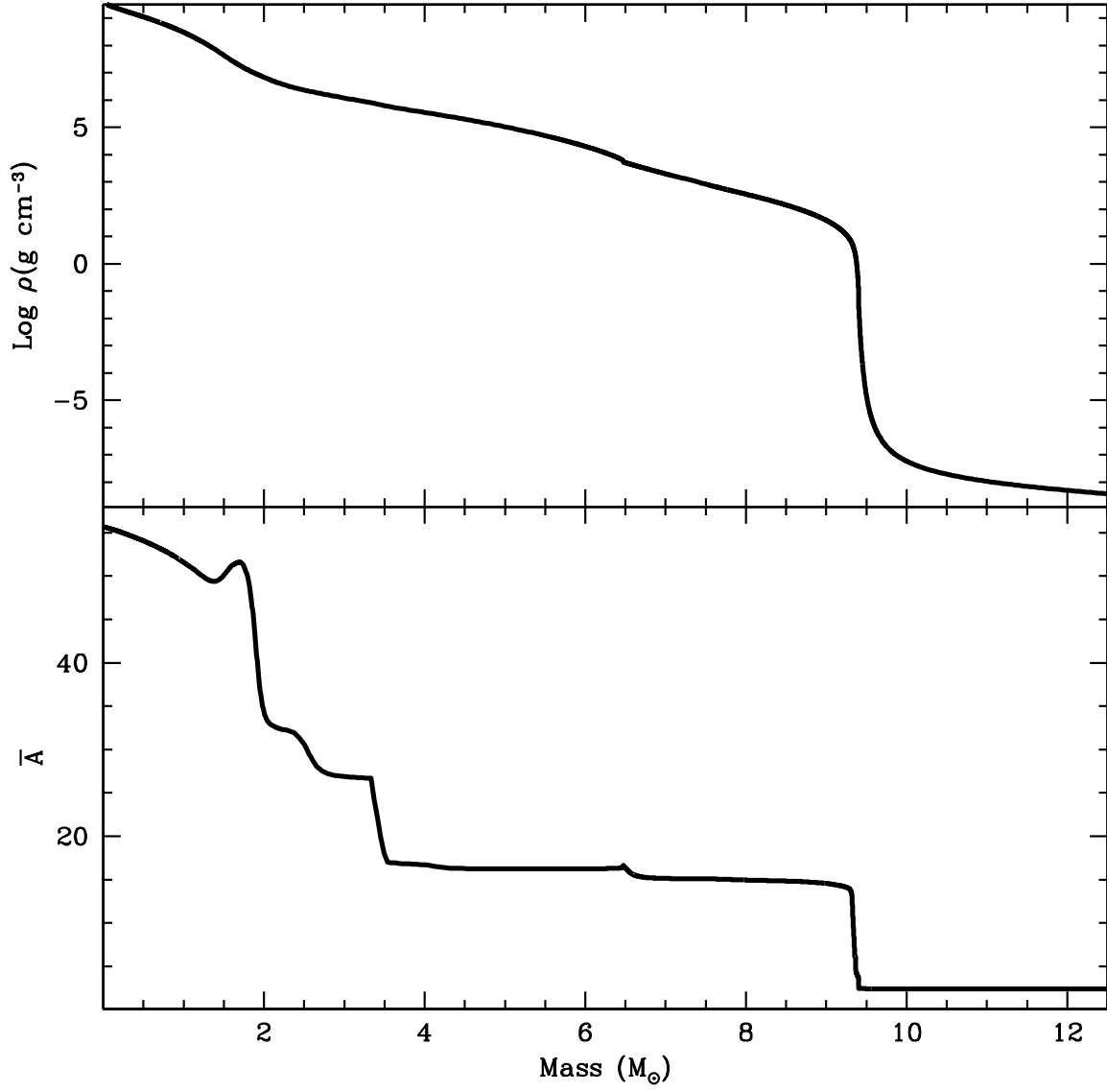


Fig. 1.— Mean atomic weight \bar{A} (top) and density (bottom) vs. mass coordinate for the progenitor model.

2.2. Explosion Calculations

To model collapse and explosion, we use a 1-dimensional Lagrangian code developed by Herant et al. (1994). This code includes 3-flavor neutrino transport using a flux-limited diffusion calculation and a coupled set of equations of state to model the wide range of densities in the collapse phase (see Herant et al. 1994; Fryer et al. 1999a, for details). It includes a 14-element nuclear network (Benz, Thielemann, & Hills 1989) to follow the energy generation. This code was used to follow the collapse of the star through bounce. For our neutrino driven explosions, we enhanced the neutrino heating by artificially turning up the neutrino energy. For these explosions, we found that either we got a very strong explosion (10^{52} erg) or no explosion at all. This was because if the explosion did not occur quickly, we were unable to drive a supernova explosion due to the quick decay in the electron neutrino and anti-neutrino fluxes. But such a result (either strong or no explosion) can be overcome if we did not increase the neutrino energy throughout the star (including the proto-neutron star core) or if we were adding this heating in a multi-dimensional calculation. In a calculation that modifies the neutrino transport by assuming convection can redistribute the energy in the neutron star and separately modifies the neutrino transport above the neutron star, one can easily get a range of explosion energies by increasing the neutrino energy (Fröhlich et al. 2006).

To get a range of explosion energies, we opted to remove the neutron star and drive an explosion by one of two ways: injecting energy in the innermost 15 zones (roughly $0.035 M_{\odot}$) or by driving a piston at the innermost zone (outer edge of the proto-neutron star). The duration and magnitude (piston velocity or energy injection) of these artificial explosions were altered to produce the different explosion energies. During energy injection, the proto-neutron star is modeled as a hard surface. We do not include the neutrino flux from the proto-neutron star, but the energy injected by this neutrino flux is minimal compared to our artificial energy injection. Shortly after the end of the energy injection, we turn the hard neutron star surface to an absorbing boundary layer, mimicking the accretion of infalling matter due to neutrino cooling onto the proto-neutron star. In this manner, we can model the explosion out to late times, even if there is considerable fallback.

In this paper, we have focused on the energy-injection model for explosions. We have produced 3 sets of explosions (each with a range of energy) using the same base model where the collapse, bounce, and fail of the bounce shock is followed with no energy injection (first 380ms after start of collapse). The first set of models assumes a fast explosion where the energy is injected in just 20 ms, producing an explosion just 400ms after collapse (roughly 150ms after bounce). By varying the energy injected, we produce a range of explosion energies. We then modeled two additional sets of explosions where we injected energy into

those inner 15 zones for longer times: 200 ms (roughly 330 ms after bounce) and 700 ms (roughly 830 ms after bounce). Of course, to produce the same final explosion energy, the rate of energy input for longer injection times is much lower than that of our fast explosions.

The 1D explosions are summarized in Table 1. All of our models assume the same initial mass of the compact remnant: $\sim 1.75M_{\odot}$, corresponding to a gravitational mass of the neutron star roughly equal to $1.6M_{\odot}$. But unless the explosion is extremely energetic, material falling back onto the proto-neutron star always produces a much more massive compact remnant, generally producing a black hole. We expect such massive progenitors to produce black holes. Although it is likely that all stars above $12 M_{\odot}$ have some fallback (Fryer et al. 1999b), above $20 M_{\odot}$, we expect the fallback to be considerable. When an explosion is launched, the inner material all has energy (mostly internal) in excess of the escape energy. However, this material deposits much of its energy into the layers above it. Fallback occurs when this material loses so much energy that it eventually becomes bound again and *falls back* back onto the compact remnant (see Fryer & Kalogera (2001) for details).

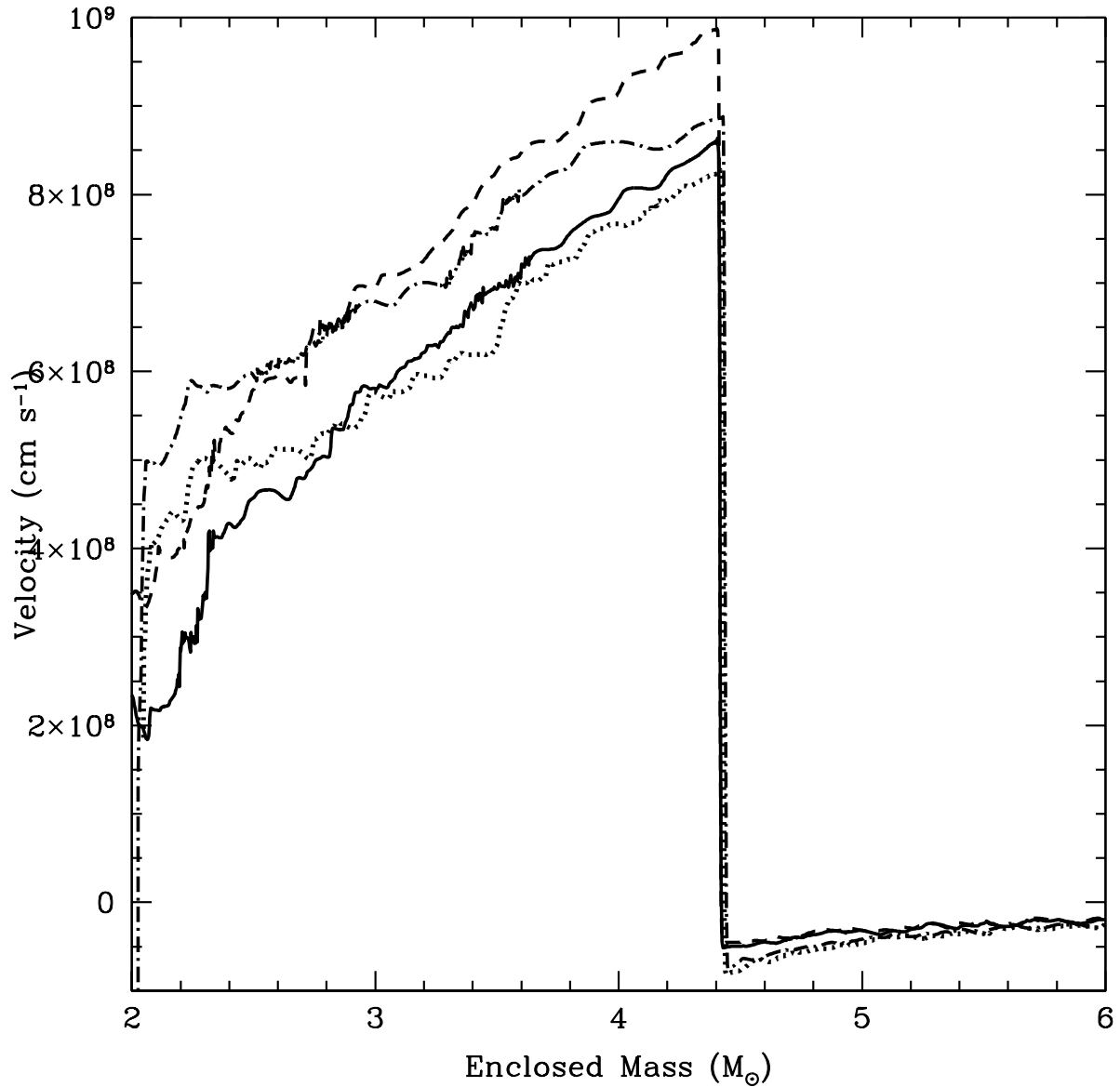


Fig. 2.— Velocity of the ejecta as a function of enclosed mass for two 200 ms explosions: 23e-0.2-0.8 (solid), 23e-0.2-1.5 (dashed) and two 700 ms explosions: 23e-0.7-0.8 (dotted), 23e-0.7-1.5 (long-dashed). The results are compared when all the shocks are at the same spot. This occurs at different times for the different simulations. Although the more energetic explosions tend to have higher velocities, the duration that the energy is injected also changes the velocity profile.

Our different explosion methods lead to different amounts of fallback that, while not physical, allow us probe a range of effects that may occur in nature. First off, the piston model moves the material outward in radius, reducing the potential well that this matter must climb out to be ejected. In general, this smaller potential well leads to less fallback for a given energy than thermal bomb models. Thielemann et al. (1997, 2002) and Timmes (private communication) note that there are differences in yields from piston and thermal bomb explosions. Depending on how one works the piston engine, one could prevent any fallback at all, although many piston engines do allow for fallback (Fryer et al. 1999b). Aufderheide, Baron, & Thielemann (1991) find that pistons and thermal bombs can produce differences in yields on the order of tens of percent, despite imposing a mass cut to get the desired Fe peak yields. Comparing the different simulations using a thermal bomb, we see that the simulations with a longer energy injection also produce less massive remnants. Because we continue to inject energy into the inner cells for longer timescales, these zones move further out of the potential well and are less likely to fall back.

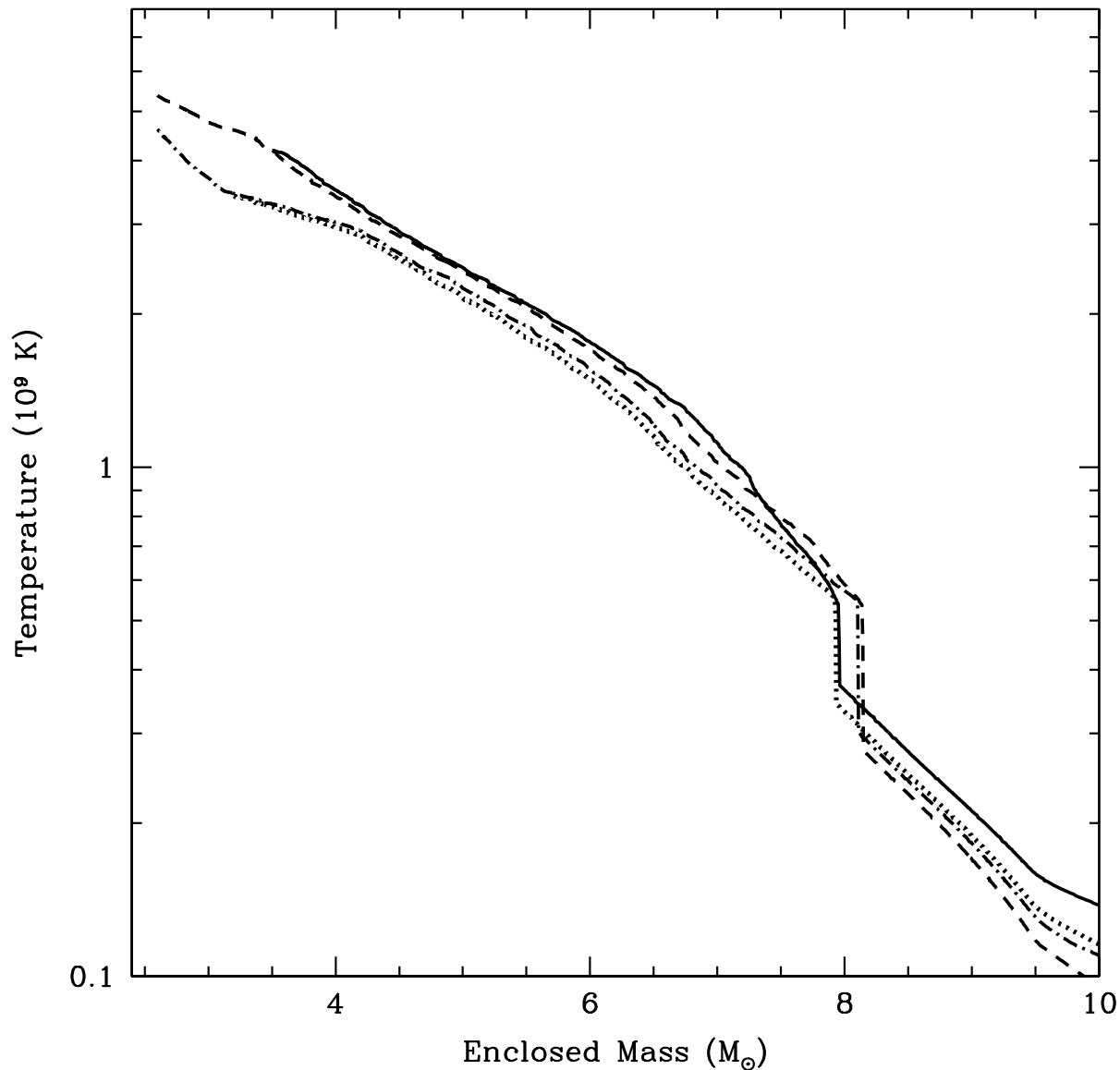


Fig. 3.— Maximum temperature reached by ejecta material as a function of enclosed mass for two 200 ms explosions: 23e-0.2-0.8 (solid), 23e-0.2-1.5 (dashed) and two 700 ms explosions: 23e-0.7-0.8 (dotted), 23e-0.7-1.5 (long-dashed). Note that the weaker shocks in the longer duration explosions produced lower peak temperatures. The difference between the maximum temperature based on the explosion energy is much less than the difference caused by the duration.

But the remnant mass is not the only difference caused by the duration of the energy injection. Figure 2 shows the velocity profiles of 4 of our simulations as a function of enclosed mass when the shock reaches roughly 1.2×10^9 cm. Comparing the weak (0.8 foe^2) explosions (solid, dotted lines) to their normal (1.5 foe) explosion counterparts, we see the obvious trend: the more energetic explosion has faster velocities. But note that the shorter delays in the 200 ms explosions produces faster velocities than their 700 ms counterparts. The quicker explosions deposit the energy faster, leading to a faster initial explosion. How will this effect the nuclear yield? The shock velocity determines the temperature of the gas when it is shocked, so the faster velocities mean higher peak temperatures. The peak temperatures for these models is shown in figure 2. Not surprisingly, the quicker explosions produce higher peak temperatures.

It should be noted that neither the thermal bomb or piston models are physically motivated in the sense of representing an actual supernova mechanism. Both are arbitrary methods of inserting enough energy into the star to disrupt it. Although we are far from solving the supernova mechanism, it is believed that stars in the $18\text{-}23 M_{\odot}$ range lie at the boundary where the neutrino-driven supernova mechanism can successfully drive strong supernova explosions (Fryer et al. 1999a). Following the intuition of the collapse community, one would assume that this particular star would have weak or no explosions. This would severely restrict the range of allowable energies for this star. However, stars that fail to produce strong supernovae have another way to explode, the collapsar black-hole accretion disk engine (Woosley 1993). This engine can drive extremely energetic explosions. On the observational side, Hamuy (2003) derive a wide range of energies for Type IIp supernovae. Nomoto et al. (2003) find two branches of supernovae at progenitor masses relevant to this study. The two populations suggest that two mechanisms might be at work, one that produces strong explosions and one weak. Without an understanding of the explosion mechanism we are free to choose final kinetic energies for the explosion, and time histories for the thermal energy deposition or piston.

2.3. Nucleosynthesis Post-Processing

The network in the explosion code terminates at ^{56}Ni and cannot follow neutron excess so to accurately calculate the yields from these models, so we turn to a post-process step. Nucleosynthesis post-processing was performed with the Burn code (Fryer et al. 2006), using

²A foe is a unit made up by Hans Bethe in his normal sense of humor to denote ten to the fifty one ergs (10^{51} erg). The foe has also been termed a “Bethe”.

a 524 element network terminating at ^{99}Tc . The network uses the current NOSMOKER rates described in Rauscher & Thielemann (2001), weak rates from Langanke & Martinez-Pinedo (2000), and screening from Graboske et al. (1973). Reverse rates are calculated from detailed balance and allow a smooth transition to a nuclear statistical equilibrium (NSE) solver at $T > 10^{10}\text{K}$. For this work Burn chooses an appropriate timestep based on the rate of change of abundances and performs a log-linear interpolation in the thermodynamic trajectory of each zone in the explosion calculation. The code also has available modes for analytic adiabatic trajectories, arbitrary density trajectories coupled with the equation of state solver in TYCHO (Young & Arnett 2005), Big Bang conditions, and hydrostatic (stellar) burning. Neutrino cooling from plasma processes and the Urca process is calculated. The initial abundances are those of the 177 nuclei in the initial stellar model, and the network machinery is identical to that in TYCHO.

3. Yields

Table 2 and Table 3 give final yields for the thermal bomb and piston models, respectively. The tables terminate at ^{74}Ge . Heavier elements were not tracked during the star's evolution, so the final yield of those species would not be complete. The extra extent of the tables does allow us to track the neutron-rich iron peak correctly, without nuclei we tabulate building up artificially at a network boundary. In this paper we will concentrate on the iron peak and intermediate mass elements and defer any discussion of r and s process to a later paper. Figures 4-9 show the graphical yields for the thermal bomb models. Figures 10-12 show yields for piston models.

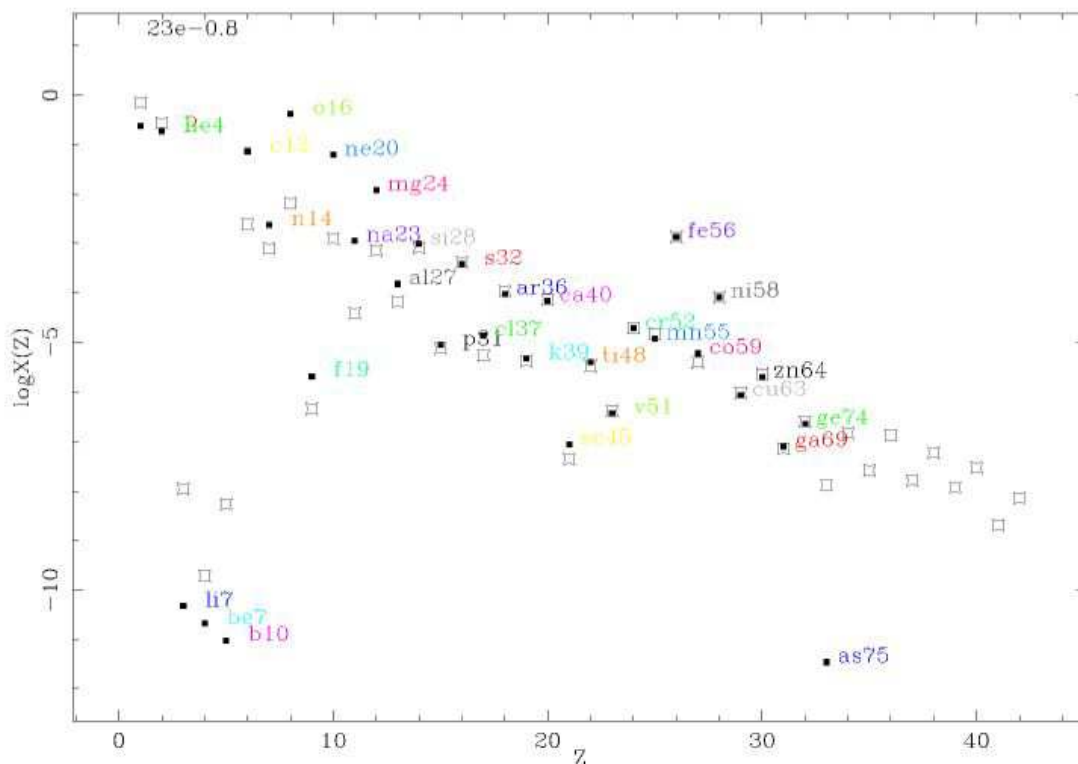


Fig. 4.— Mass fraction of elemental yields X/X_{\odot} versus proton number Z for the 0.8foe thermal bomb model. Figures 5-9 show the same for the other thermal bomb explosions) Each element is labeled with the most abundant isotope of that element. A clear trend is seen with energy. The 0.8 foe explosion ejects the H, He, and part of the C/O layers. The heavier elements are represented only by their initial abundances in the star. As explosion energy increases the yields of C/O increase, followed by the intermediate mass elements. Only at 1.5 foe does ejecta reach Si burning temperatures during the explosion, and produces mostly ^{54}Fe , characteristic of high entropy QSE nucleosynthesis. At 2 foe there is ejecta that reaches NSE conditions and produces ^{56}Ni as the dominant Fe peak isotope.

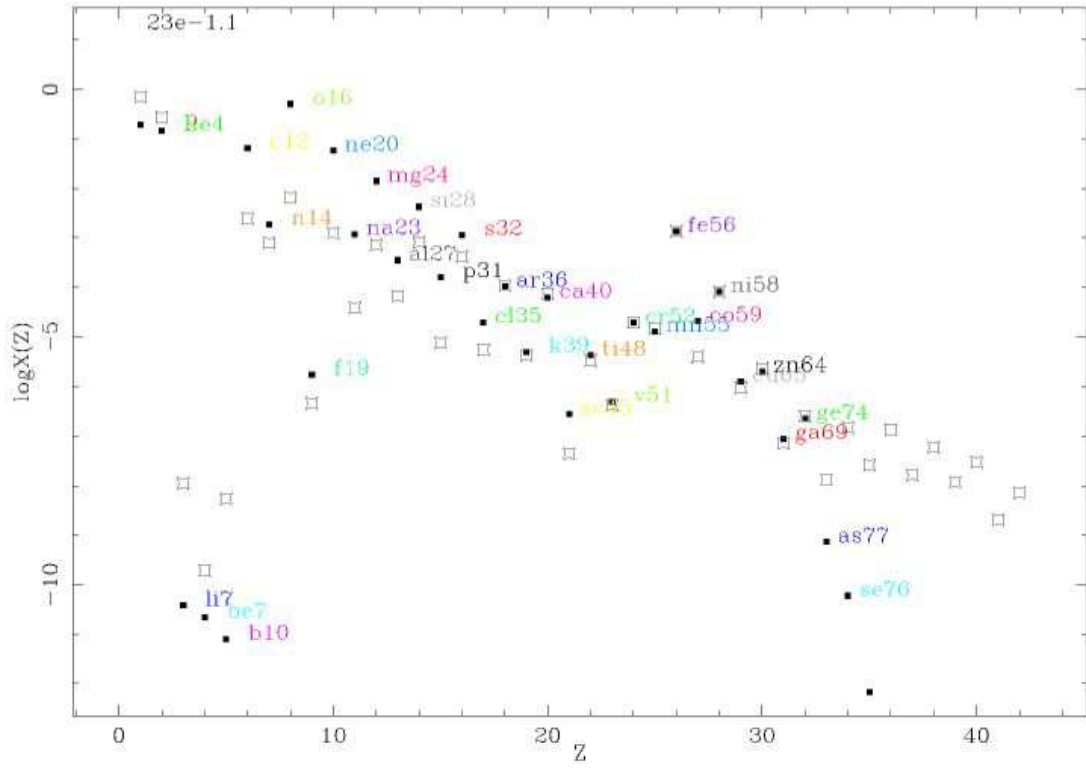


Fig. 5.— Mass fraction of elemental yields X/X_{\odot} versus proton number Z for the 1.1foe thermal bomb model.

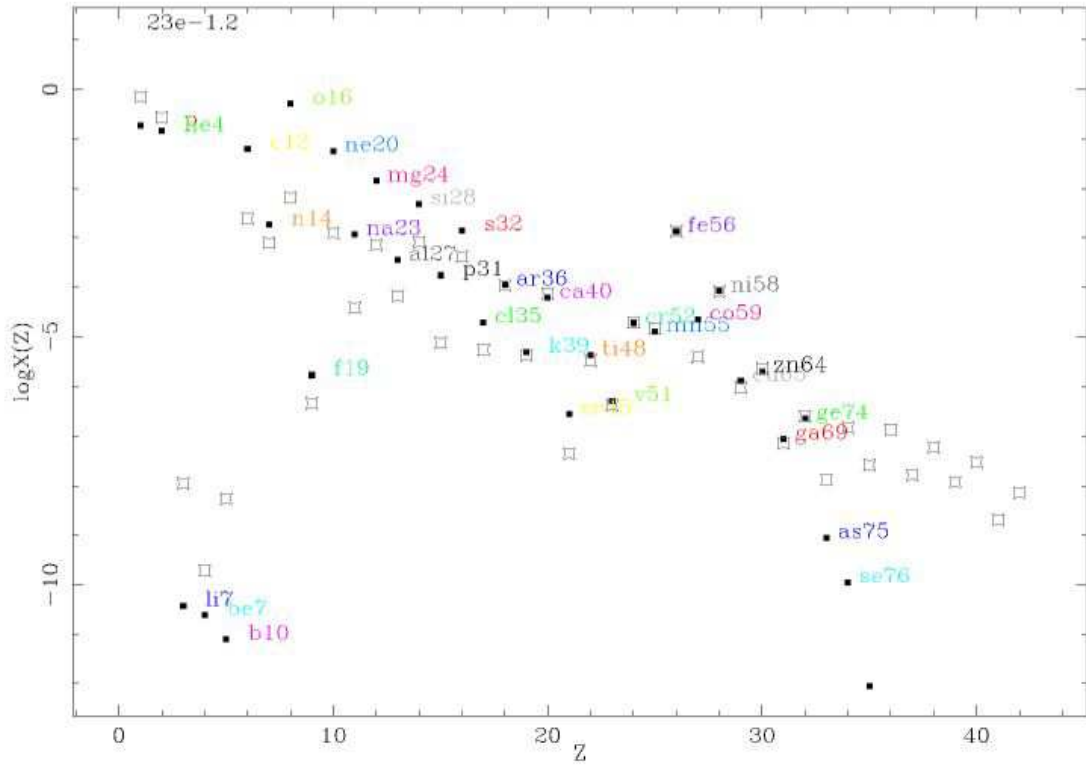


Fig. 6.— Mass fraction of elemental yields X/X_{\odot} versus proton number Z for the 1.2foe thermal bomb model.

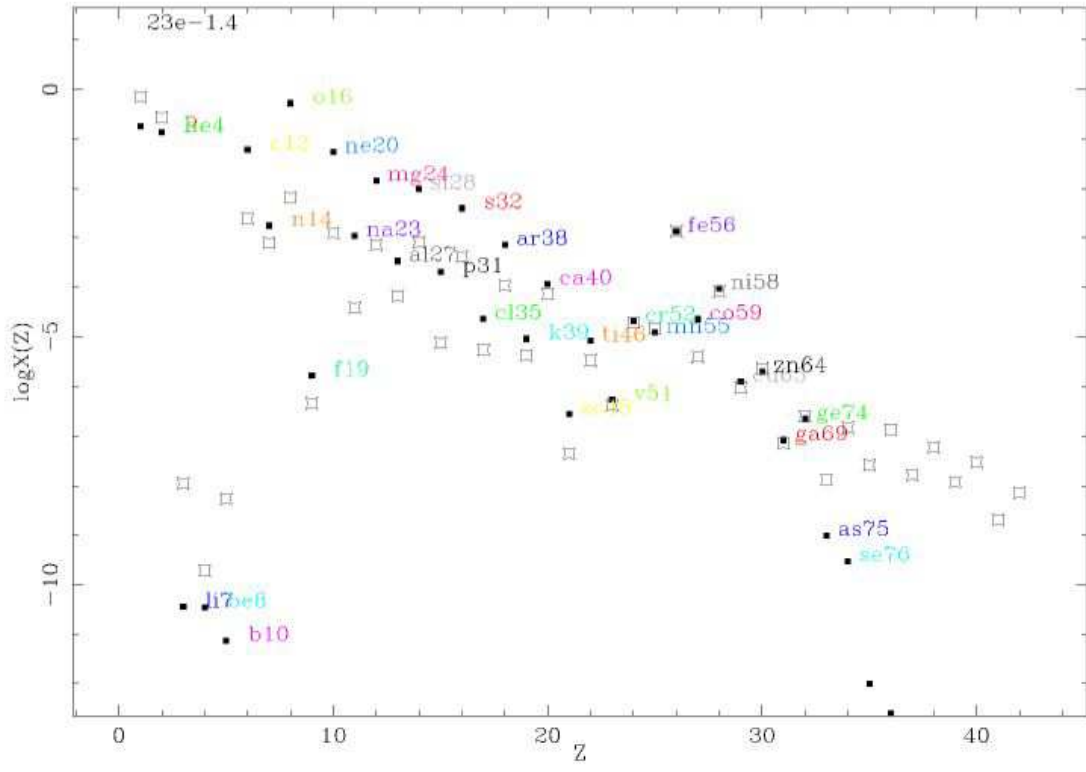


Fig. 7.— Mass fraction of elemental yields X/X_{\odot} versus proton number Z for the 1.4foe thermal bomb model.

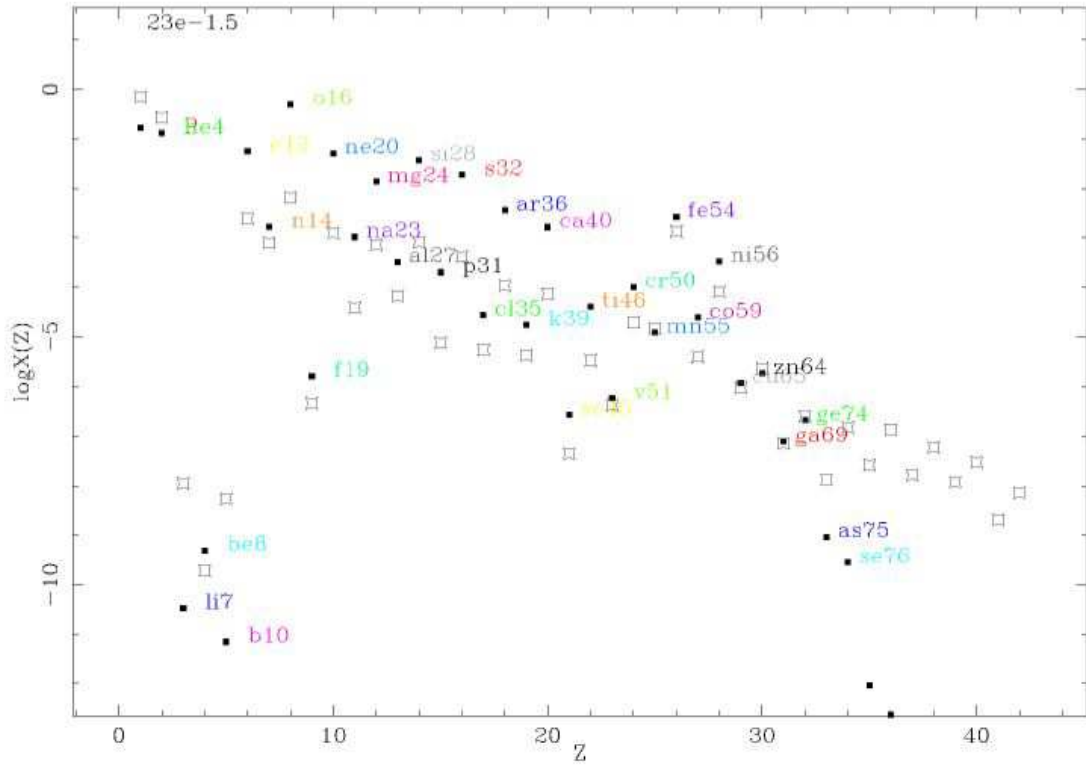


Fig. 8.— Mass fraction of elemental yields X/X_{\odot} versus proton number Z for the 1.5foe thermal bomb model.

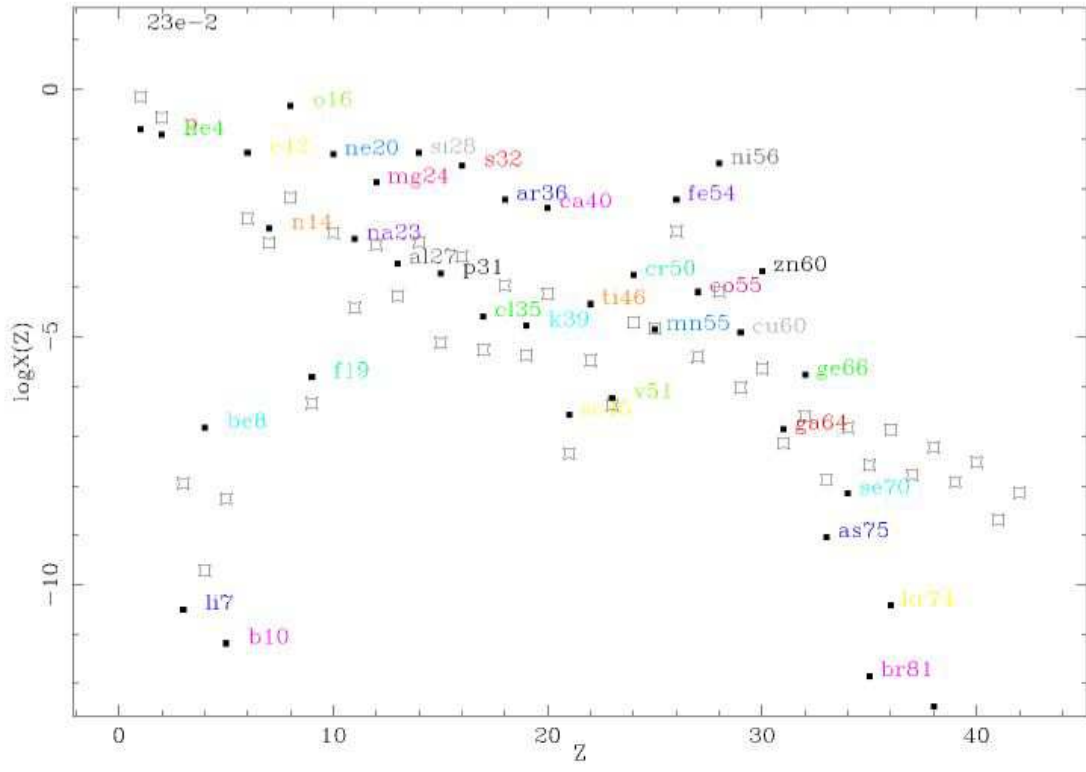


Fig. 9.— Mass fraction of elemental yields X/X_{\odot} versus proton number Z for the 2.0foe thermal bomb model.

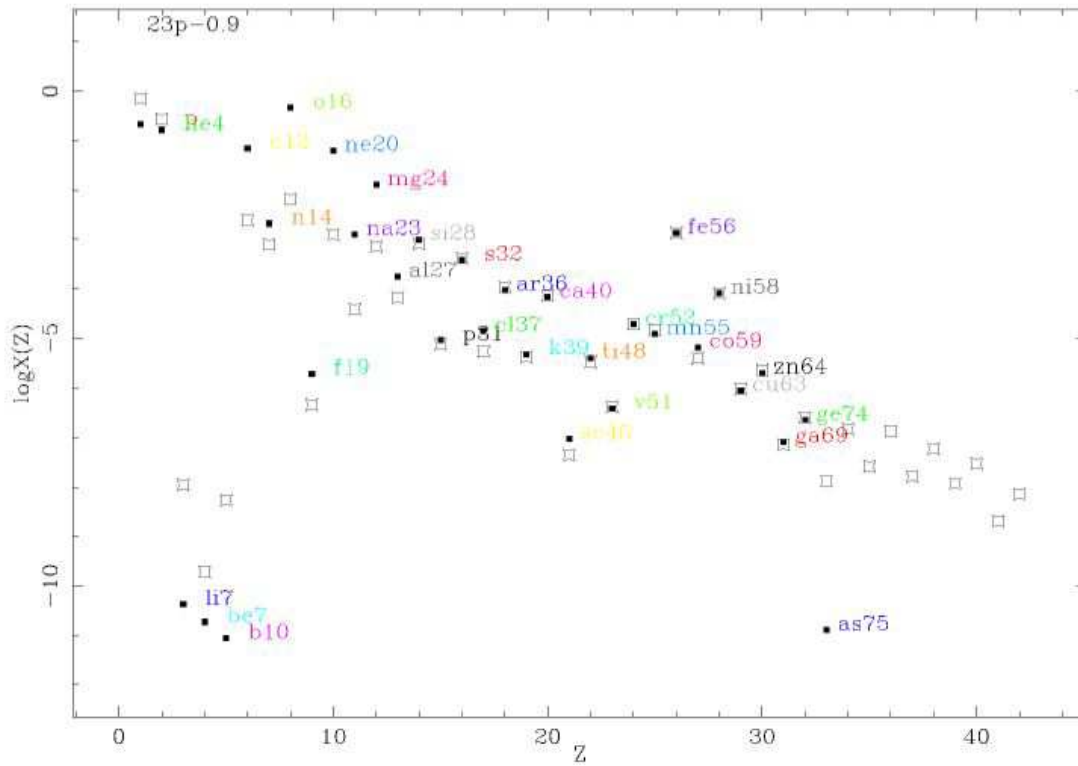


Fig. 10.— Mass fraction of elemental yields X/X_{\odot} versus proton number Z for the 0.9foe piston model. (Figures 11 and 12 show the same for the other piston explosions.) Each element is labeled with the most abundant isotope of that element. Trends with energy are similar to the thermal bombs, but offset to lower energies.

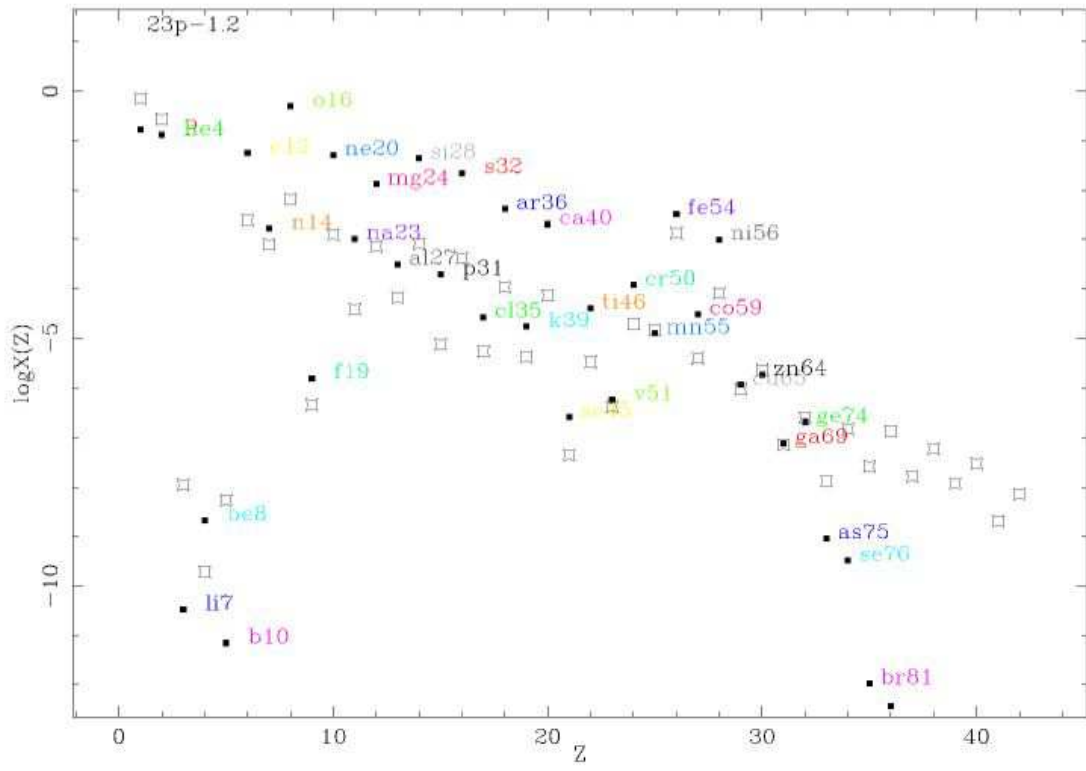


Fig. 11.— Mass fraction of elemental yields X/X_{\odot} versus proton number Z for the 0.9foe piston model.

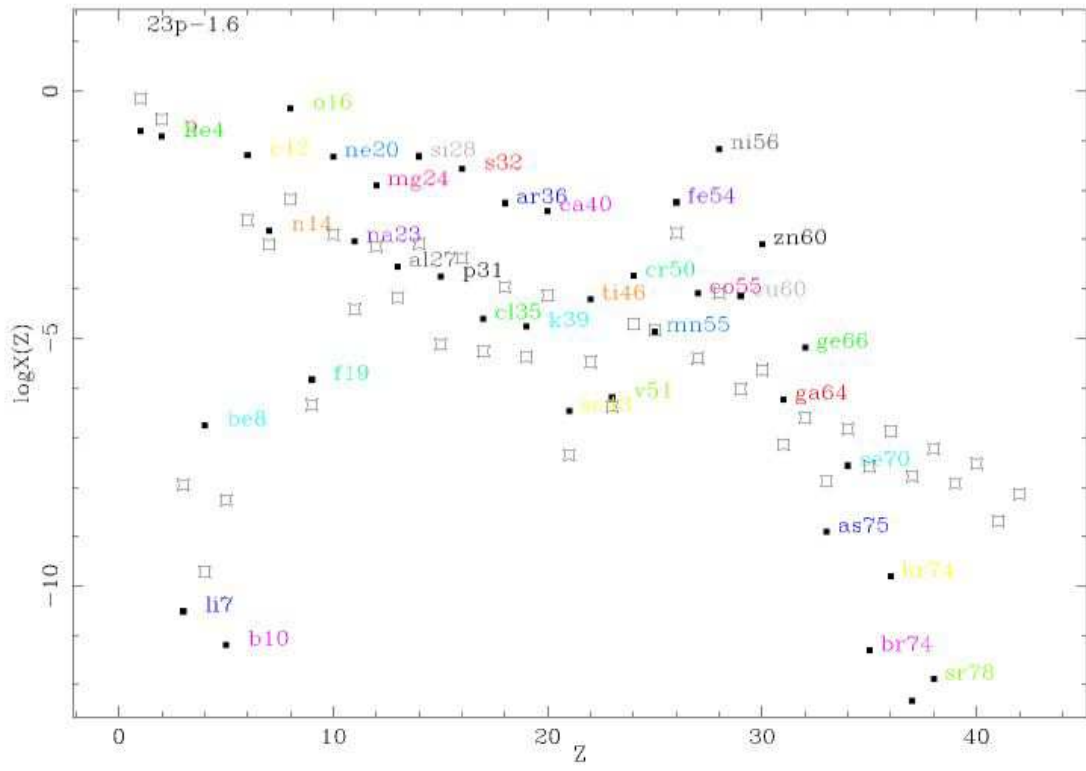


Fig. 12.— Mass fraction of elemental yields X/X_{\odot} versus proton number Z for the 0.9foe piston model.

The thermal bomb models show a clear trend with final explosion energy. This behavior is simple to interpret. Figure 13 indicates the material which escapes for different thermal bomb explosion energies on a plot of mean atomic weight \bar{A} vs enclosed mass for the progenitor. This ignores of course 3D effects and mixing during the explosion. Figure 14 shows the peak temperature reached by each mass zone ejected for the 0.8, 1.2, 1.5, and 2.0 foe explosions. The explosions with less than 1.4 foe do not reach even oxygen burning temperatures in the material which escapes as ejecta. Elements heavier than oxygen are represented only by their initial abundances in the star. With increasing explosion energy a larger fraction of the unprocessed material from the original star is gravitationally unbound, and abundances of intermediate mass elements begin to come up above solar, progressing towards larger A in order of synthesis temperature. In the 0.8 foe explosion only about half of the O-rich mantle escapes. By 1.4 foe Si-rich material makes it out in the explosion. At 1.5 foe some Si-rich material in the ejecta reaches quasi-statistical equilibrium temperatures ($> 3 \times 10^9\text{K}$) and is burned to the Fe peak. In the high entropy QSE regime the material is dominated by ^{54}Fe with a smaller component of ^{56}Ni . At 2.0 foe some of the ejecta reaches full NSE ($T > 5 \times 10^9\text{K}$) and is dominated by ^{56}Ni ($0.3 M_{\odot}$).

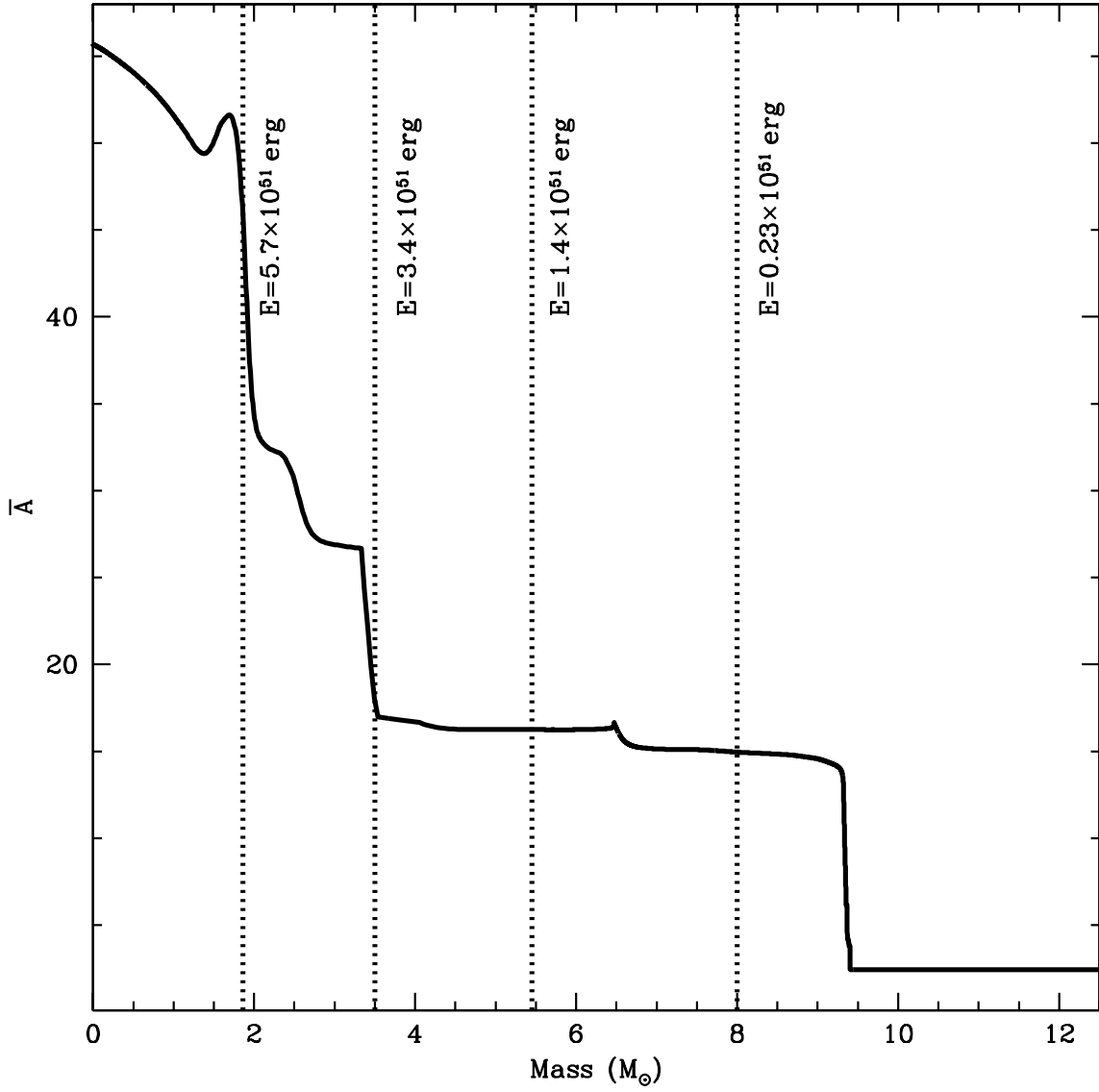


Fig. 13.— Mean atomic mass \bar{A} vs. enclosed mass in the progenitor. Dashed vertical lines indicate the material that escapes for thermal bomb explosions of the indicated energies, ignoring 3D effects and mixing.

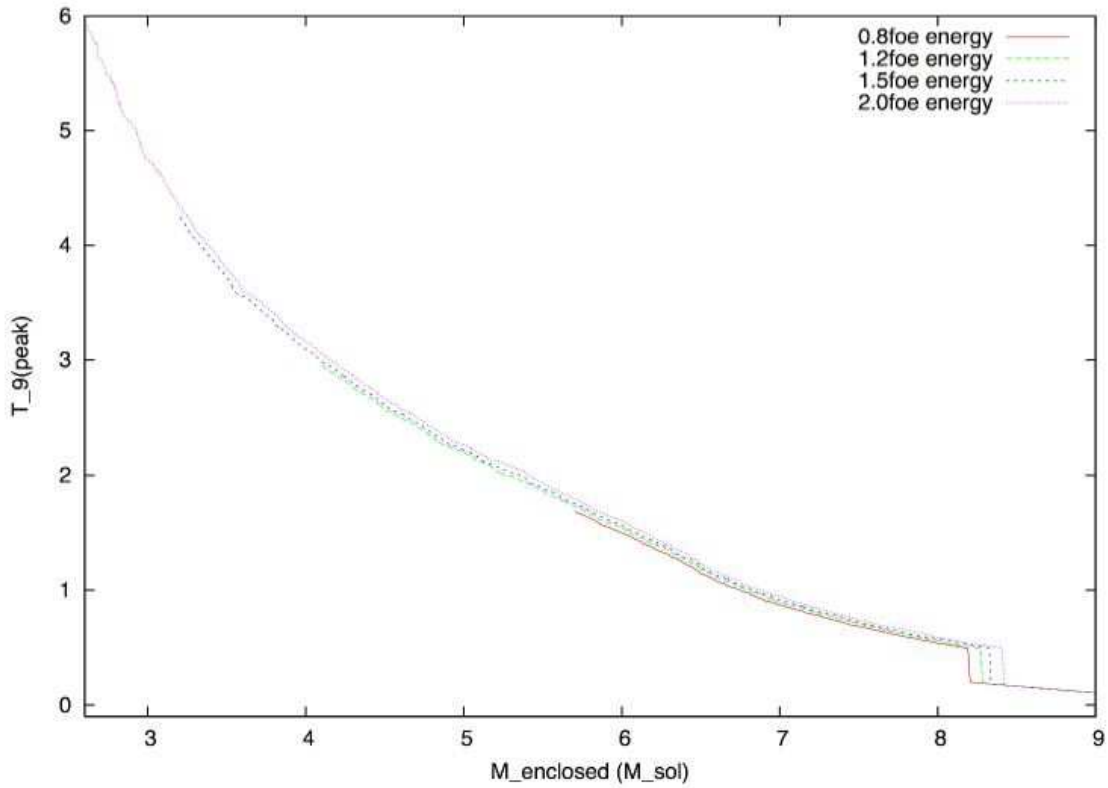


Fig. 14.— Peak $T/10^9$ reached by each mass zone in the ejecta vs. mass coordinate of the progenitor for the thermal bomb models. With increasing energy more material escapes and the extra material is heated to higher temperatures. Only the 2.0 foe explosion ejects material exposed to NSE conditions. The 1.5 foe explosion reaches temperatures sufficient for QSE explosive Si burning.

This trend is exactly what we already expect with increasing explosion energy. At this stellar mass, a range of energies is possible, and we must consider the entire range of yields. The more interesting comparison, however, is between a thermal bomb and a piston explosion of the same final energy. In terms of yields, the piston explosion mimics a higher energy thermal bomb explosion because the piston is more efficient at accelerating material where the explosion is imposed. Figure 15 shows the peak temperature achieved by the ejecta as a function of initial stellar mass coordinate for 1.2 foe thermal bomb and piston explosions. Material from deeper in the star escapes in the piston explosion. Figure 16 shows the velocities versus initial stellar mass coordinate for the 1.2 foe piston and thermal bomb at the same time during the explosion. High velocities persist deeper in the star for the piston since it begins as a mass motion rather than thermal energy that must be transformed into kinetic energy as in the thermal bomb.

Fryer (2006) developed an analytic method to estimate the explosion energy and remnant mass of a collapsing star based on the critical accretion rate of the infalling star onto the convective region. By varying this critical accretion rate, we can determine the dependence of the remnant mass on explosion energy. This curve is shown along with our 1-dimensional results in Figure 17. The pairs of blue points represent the total energy injected in the thermal bomb models (rightmost point) and the final kinetic energy of the explosion (left point). It is difficult to estimate the total energy injected by the piston. The analytic estimate predicts lower remnant masses for a given *total* energy than the thermal bombs. The piston model predicts the lowest remnant masses for a given explosion energy.

There are several differences between the assumptions in the Fryer (2006) analysis and the assumptions in our artificially driven explosions. First, the energy in the analytic estimate is the energy at the base of the explosion, estimated from the total energy stored in the convective region. This is not the total kinetic energy of the shock as it breaks out of the star. Much of this energy goes into unbinding the star. An alternate way to understand this is that the kinetic energy quoted in our artificial explosion is just a fraction of the total explosion energy. It is the total explosion energy that is quoted in most core-collapse engine calculations, but it is the final kinetic energy that is quoted in most estimates based on observations. So the primary difference between these results is the difference between the definitions of explosion energy between these two models. It is difficult to estimate the energy injected in the piston model, but we can calculate the energy injected in our thermal bomb calculations. Unfortunately, much of the energy injected in our artificial explosions ends up falling back onto the compact remnant, so the energy we deposit is likely to be higher than our analytic analysis that assumed all of that energy escaped. We see that this is true for all of our simulations (Figure 17).

Other differences also exist. In the thermal bomb and piston explosions, the engine continues to be powered even after the explosion is launched. In both the analytic estimate, and in a neutrino-driven explosion, the explosion energy is limited to what can be stored in the convective region before the the launch of the explosion. After this launch, neutrinos will not deposit much more energy into a strong explosion. The continued driving that occurs in our artificial explosions leads to less fallback than we would expect from neutrino-driven explosions. In this respect, the analytic estimate is more realistic than our 1-dimensional simulations.

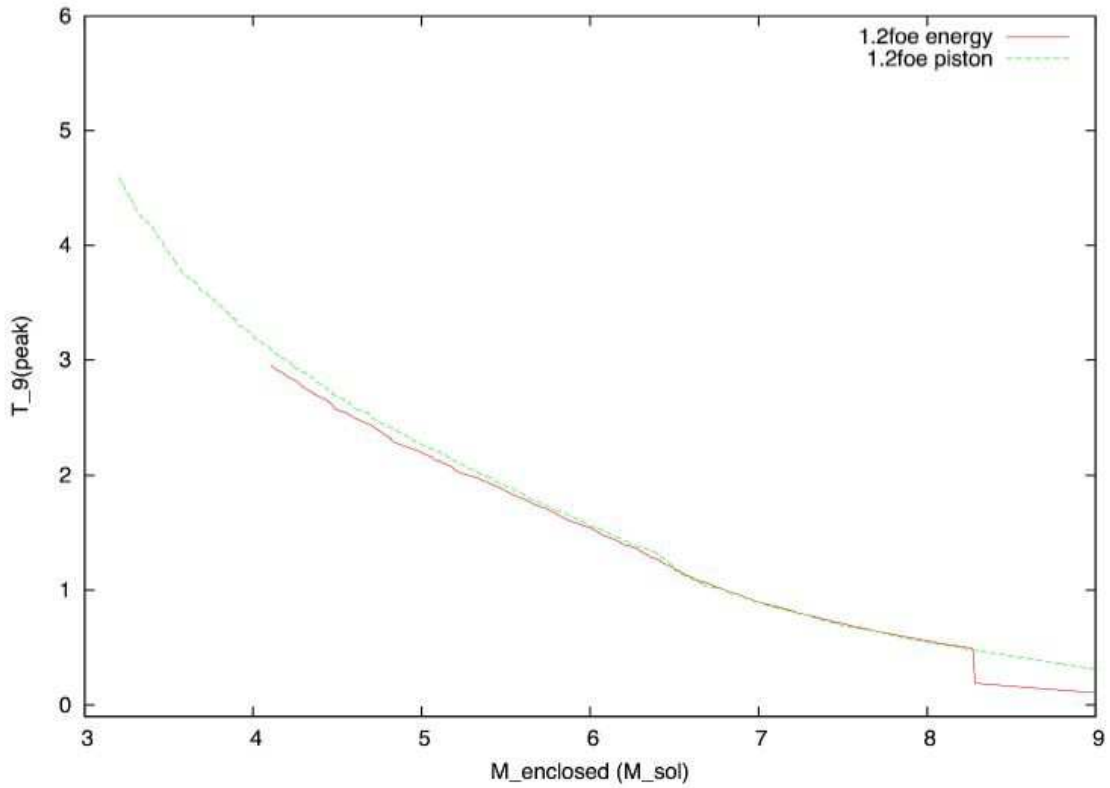


Fig. 15.— Peak $T/10^9$ reached by each mass zone in the ejecta vs. mass coordinate of the progenitor for the 1.2 foe thermal bomb and piston models. The difference in yields is due mostly to the larger amount of material which escapes in the piston explosion. The peak temperatures for the piston begin to become systematically higher in the innermost mass zones, but the difference is small for the portion of the star that escapes in both models.

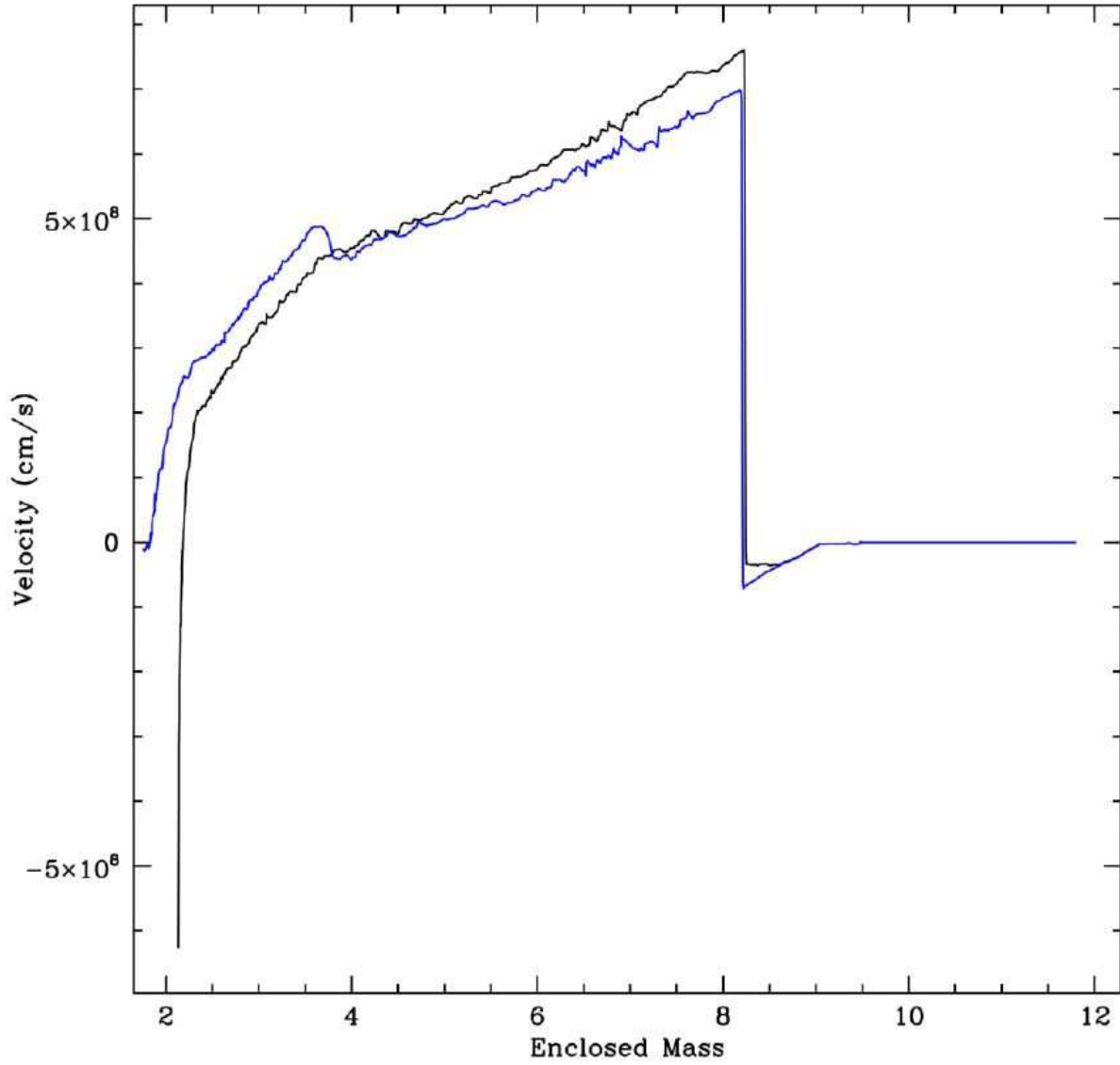


Fig. 16.— Velocity vs. enclosed mass for 1.2 foe piston (blue) and thermal bomb (black) explosions. The piston model generates large velocities deeper in the star, resulting in larger ejecta masses and smaller remnants.

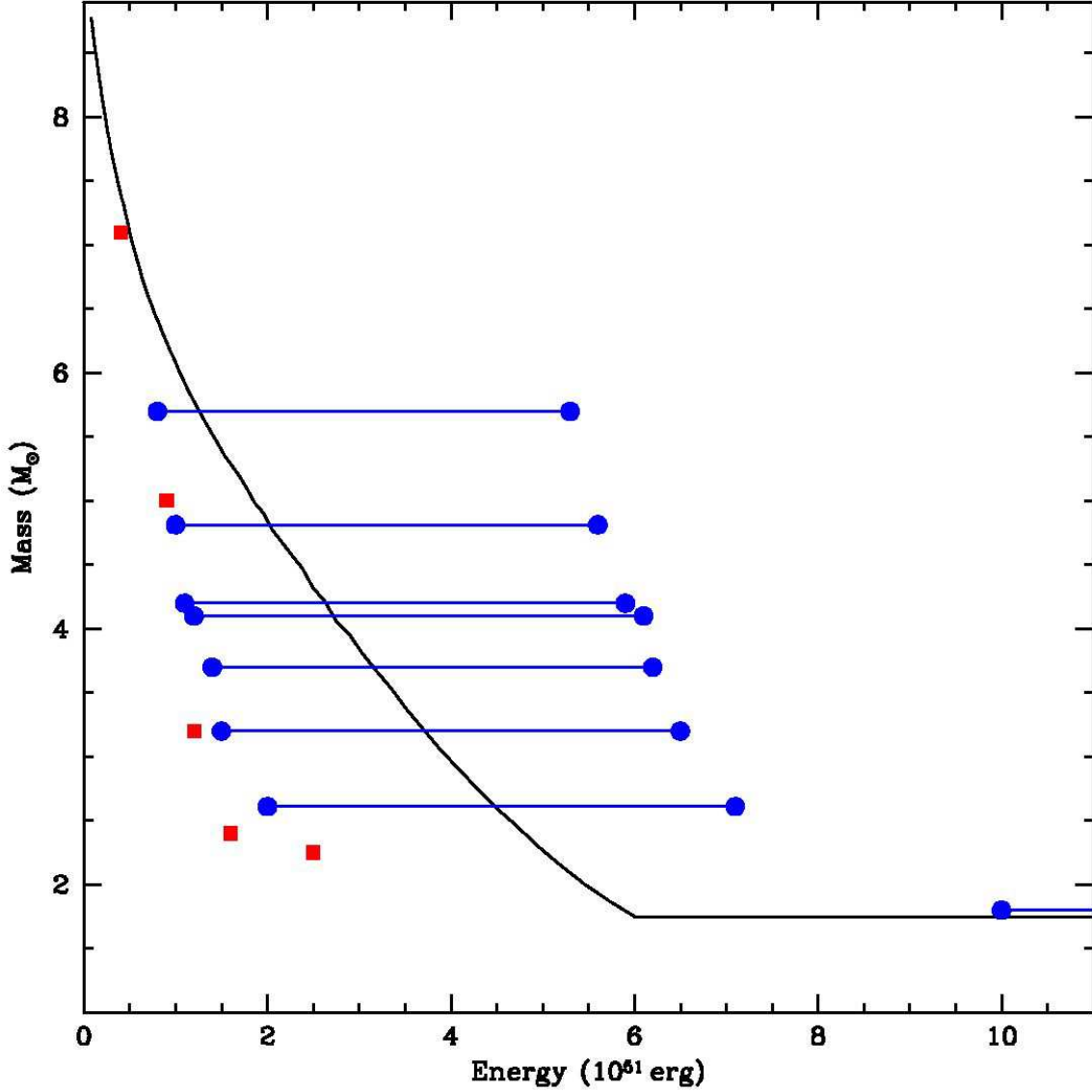


Fig. 17.— Remnant mass vs. energy for thermal bombs (blue pairs), pistons (red) and analytic estimate (solid line). The energies for the piston simulations and the leftmost of each thermal bomb pair are given in kinetic energy when the shock has broken out of the star. The analytic estimate and the rightmost point of each thermal bomb pair gives the energy used to unbind the star, so these two sets of energies are not directly comparable. Much of the injected energy in the thermal bombs ultimately is accreted onto the compact remnant and does not go into exploding the star. So we expect this energy to exceed the energy in our analytic calculation. Piston explosions systematically produce the smallest remnants for a given final kinetic energy, due to the efficient initiation of the shock by imposing mass motion. Larger ejecta masses result in larger yields of highly processed material.

Over the energy range 0.8 - 1.5 foe in the thermal bombs the yield of oxygen increases by 70%, neon by 17%, silicon by 530%, and iron+nickel by 290%. We can also compare thermal bomb and piston explosions of the same energy. At 1.2foe the yields in the piston explosion increase as follows: oxygen 8%, Ne 0.5%, Si 1011%, Fe+Ni 324%. The ^{56}Ni yield increases from essentially zero to $6.6 \times 10^{-3} M_{\odot}$. Figure 18 shows the yields (M_{\odot}) of carbon, oxygen, silicon, ^{54}Fe , ^{56}Ni , and the total iron plus nickel as a function of explosion energy, with thermal bombs in blue and pistons in red. Carbon decreases at higher energies as more ejecta is heated to C burning temperatures. Oxygen increases as a larger fraction of the O-rich mantle is ejected, then decreases at energies that produce O burning temperatures. Silicon has a sharp turn-up where pre-supernova Si is finally ejected. ^{54}Fe rises rapidly for energies that produce Si burning ($T > 3 \times 10^9\text{K}$) and then drops at energies high enough for the equilibrium to favor ^{56}Ni ($T > 5 \times 10^9\text{K}$). Total Fe+Ni of course increases rapidly at energies that produce Si burning temperatures. These trends are the same for both types of explosion, but are shifted to lower energies for the piston models. The effect is especially dramatic for the Fe peak.

We also compare thermal bomb explosions with different explosion delays, as explained in Section 2.2. For a star this massive it is reasonable to expect a long delay in light of 3D simulations (Fryer & Young 2006). Figures 19-22 show the bulk element yields for explosions with additional delays of 0.2 seconds at 0.8 and 1.5 foe and 0.7s at 0.8 and 1.5 foe. These can be compared to Figures 4,8,10,12. The detailed isotopic yields are presented in Table 4. We find that for longer delays the yield of intermediate mass and Fe peak elements increases because the longer energy input raises more material out of the potential well. However, this material is at systematically lower velocities and thus lower shock temperatures (see Section 2.2). As a result, the yield of Fe peak material processed at NSE temperatures is lower in the 1.5 foe explosions with longer delays than the 2.0foe short delay, even though as much or more total material escapes. The ^{56}Ni yield increases by two orders of magnitude for both moderate and long delays. ^{44}Ti increases by a factor of five with 0.2s additional delay and by another factor of five with 0.7s as more material is heated to Si burning QSE and escapes with longer delays. These results should be taken as indicative of the range of yields that can be generated with variation of parameters than a real trend. In 3D a longer delay allows *more* fallback, so this may be the opposite of what nature does.

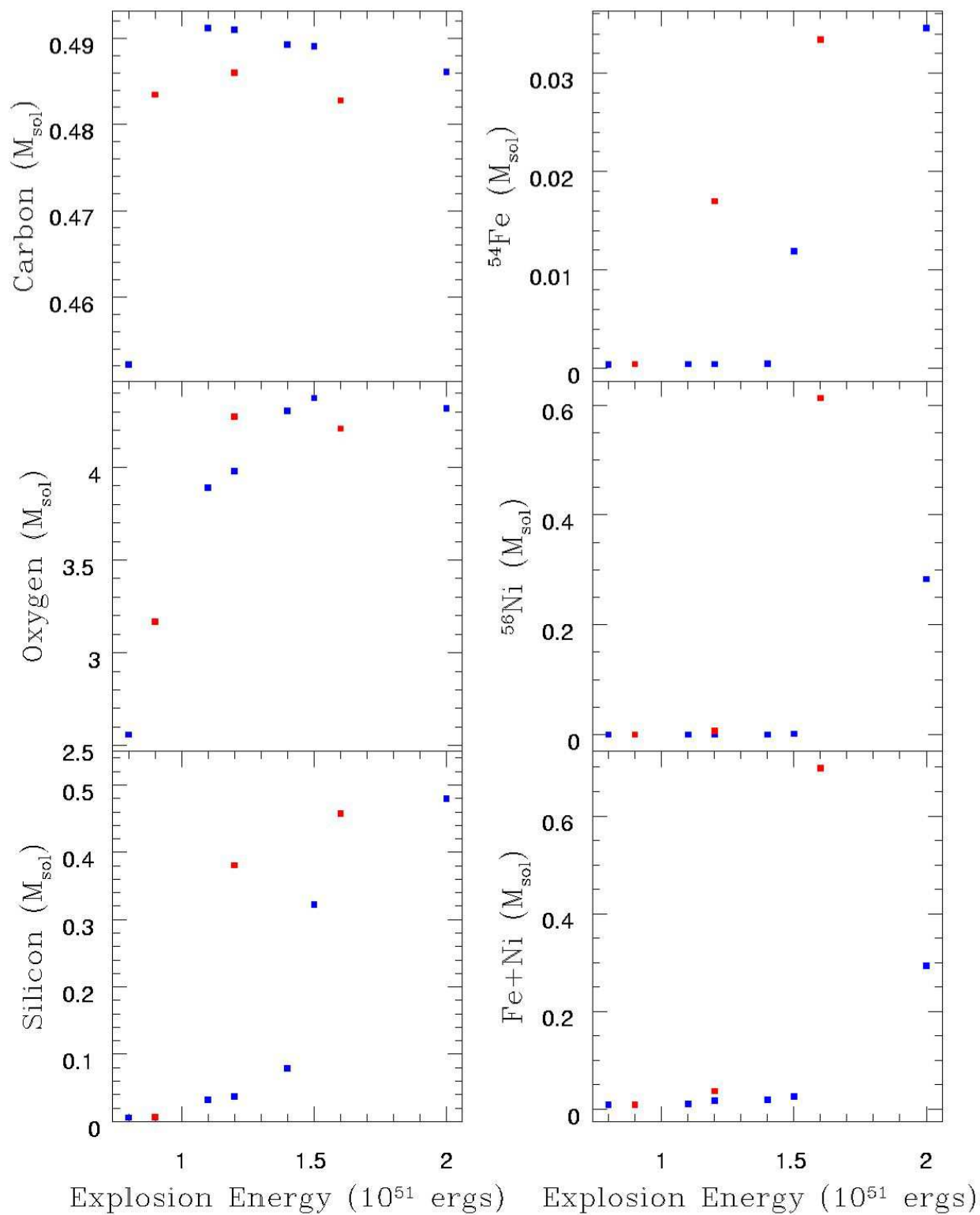


Fig. 18.— Yields (M_{\odot}) of carbon, oxygen, silicon, ^{54}Fe , ^{56}Ni , and the total iron plus nickel as a function of explosion energy, with thermal bombs in blue and pistons in red.

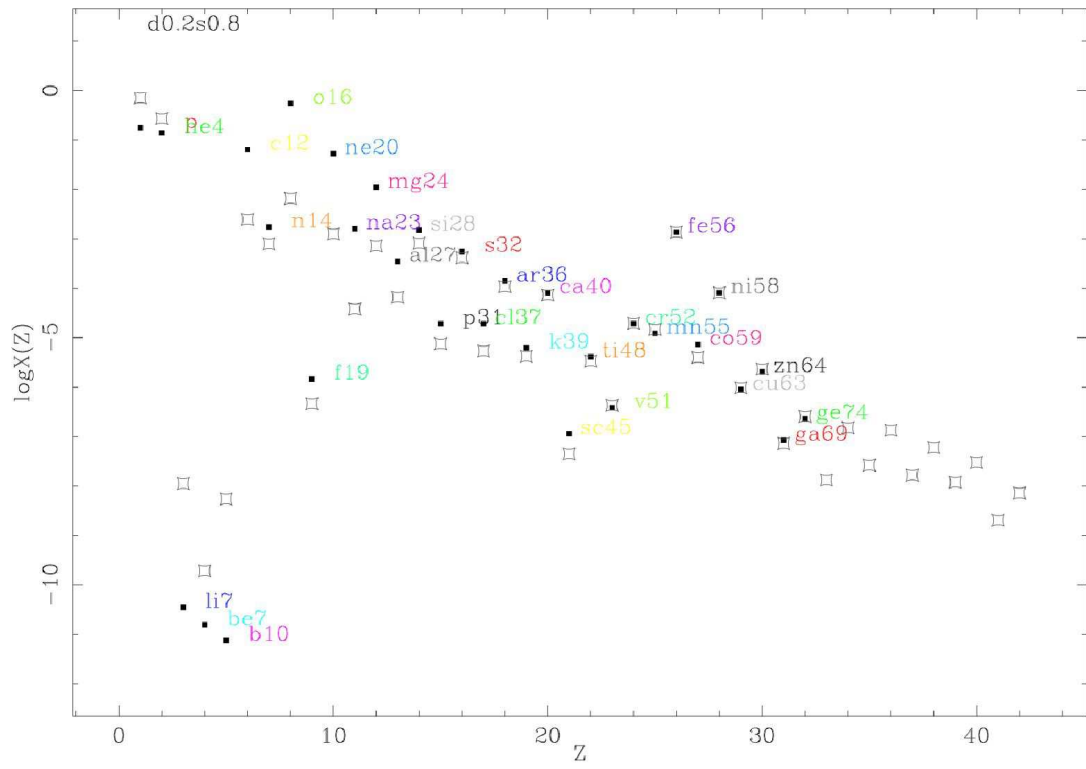


Fig. 19.— Mass fraction of elemental yields X/X_{\odot} versus proton number Z for the 0.8foe thermal bomb model with an additional 0.2s delay.

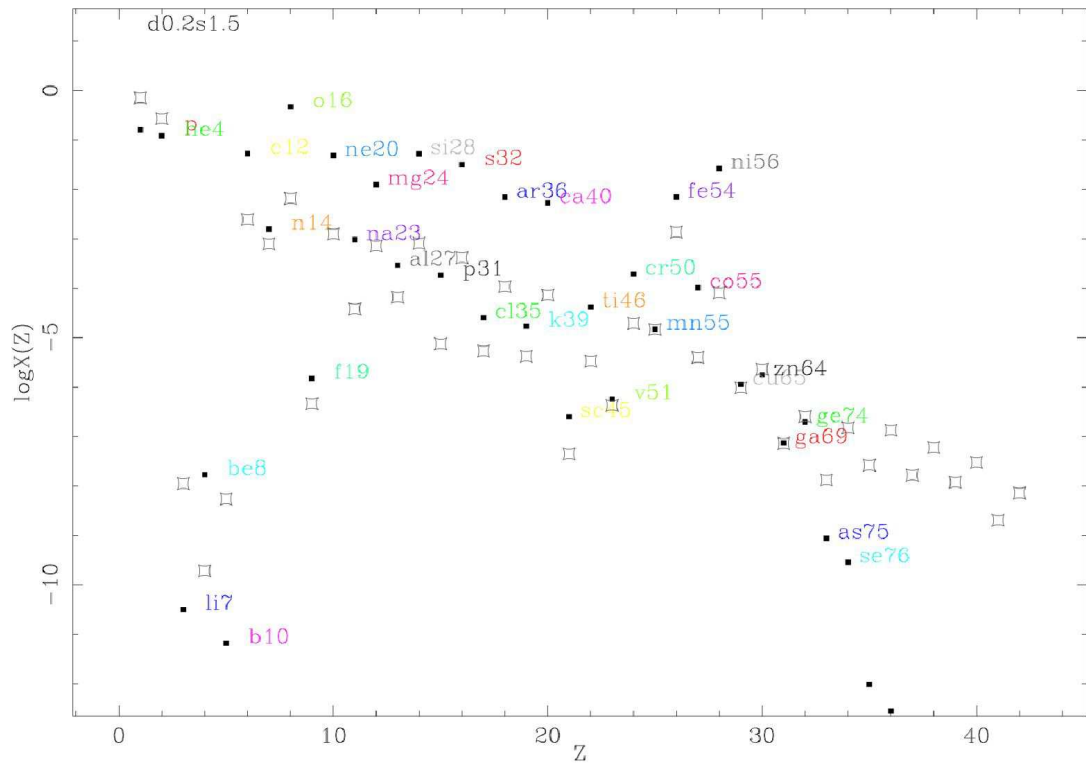


Fig. 20.— Mass fraction of elemental yields X/X_{\odot} versus proton number Z for the 1.5foe thermal bomb model with an additional 0.2s delay.

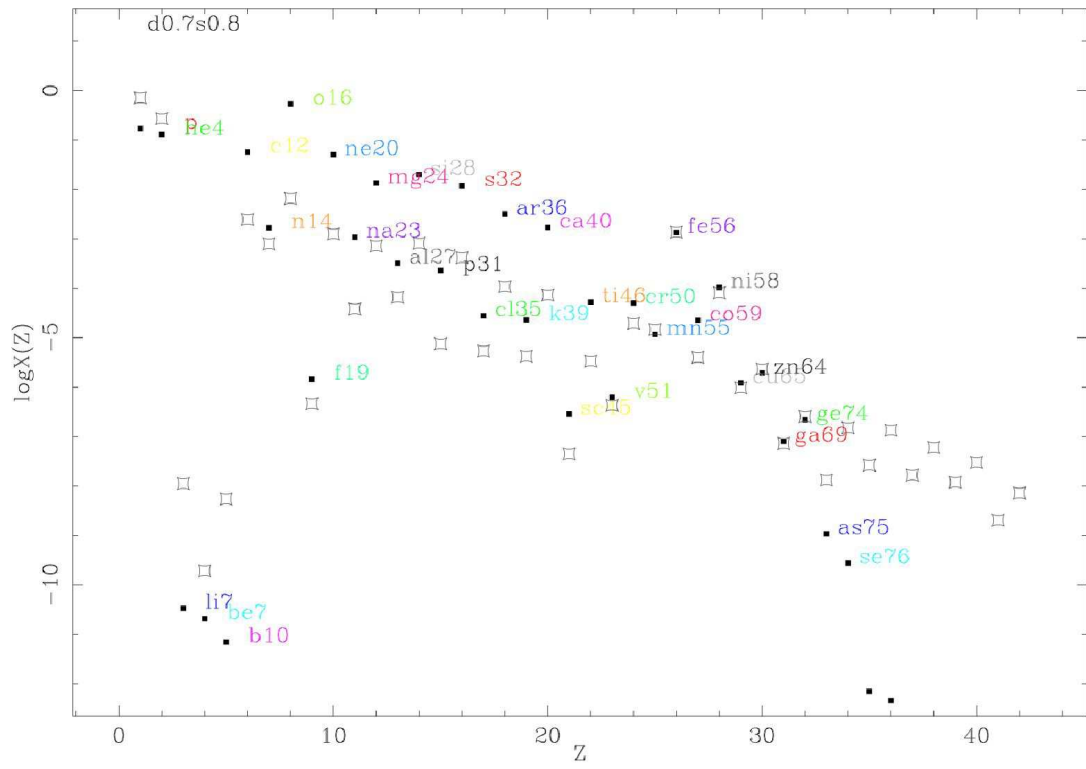


Fig. 21.— Mass fraction of elemental yields X/X_{\odot} versus proton number Z for the 0.8foe thermal bomb model with an additional 0.7s delay.

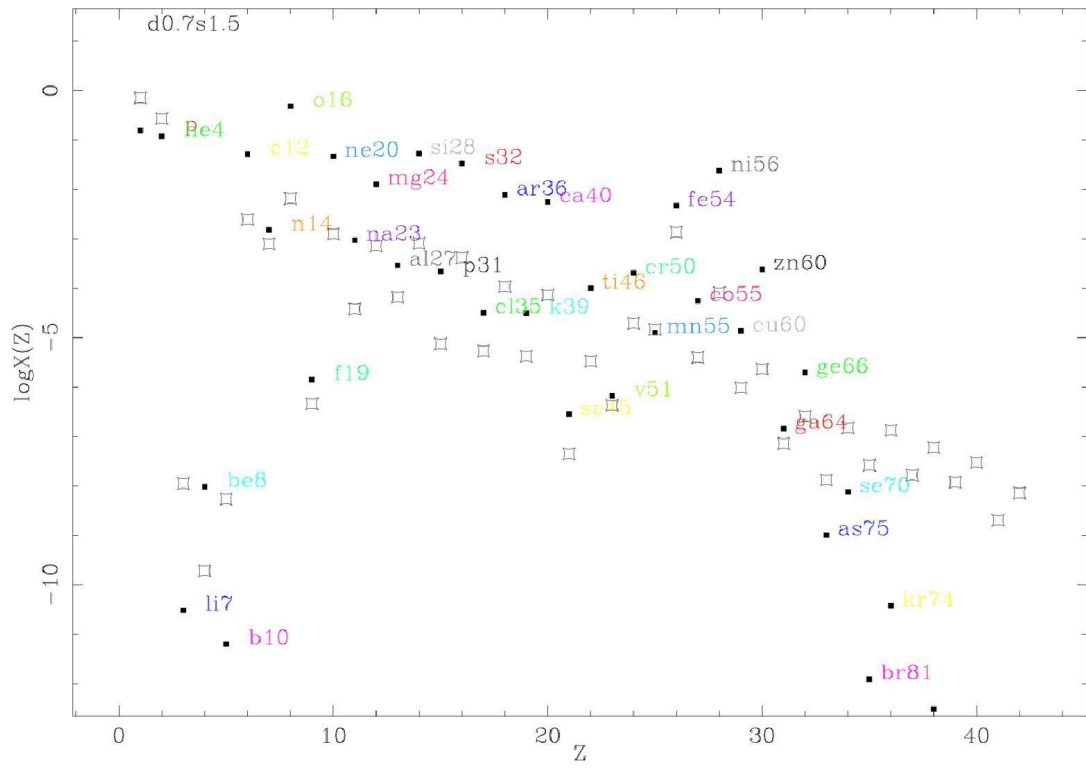


Fig. 22.— Mass fraction of elemental yields X/X_{\odot} versus proton number Z for the 1.5foe thermal bomb model with an additional 0.7s delay.

4. DISCUSSION

This research provides a framework for estimating uncertainties in yields arising from the shortcomings of 1D explosion models. These errors fall roughly into two regimes.

In the low explosion energy regime the variation in yields arises simply from the amount of material processed by hydrostatic burning which escapes from the star. Ignoring multi-D effects (the importance of which should not be underestimated), this can be described by a traditional mass cut.

In the high energy explosion regime we must deal with explosive nucleosynthesis as well. In this case the thermodynamic trajectory of the ejecta is important. The velocity evolution of a piston explosion and a thermal bomb of the same energy or of a piston and a thermal bomb with the same mass cut will differ slightly, imposing an accompanying difference in the thermodynamic evolution. Hence any material which undergoes explosive nucleosynthesis will have different abundances. The 1.2foe piston and 1.5foe thermal bomb produce the same mass compact remnant. If we examine the elemental yields we see that the effect is small, as the difference in the velocities is small. In individual isotopes, however, the difference can be larger. ^{56}Ni is a factor of three larger in the piston driven explosion because its production is dominated by the highest temperature material, in which the largest deviation in thermodynamic histories is seen. This changes the Fe yield by $\sim 25\%$. The evolution would be substantially different for an explosion with a gain region as in the analytic case, and the abundances correspondingly disparate. A small change in energy/compact remnant mass in this regime results in a much larger difference in the yields than a similar change in the low energy regime due to the steep temperature dependence of the burning. In addition, the time delay of the explosion has an effect in this regime. A longer delay *in 1D* results in more material escaping, but with lower shock temperatures, resulting in a higher intermediate mass to Fe peak ratio. In 3D, we would expect more fallback, resulting in a lower overall ejecta mass.

We can choose between two parameters in constructing a grid of yields. If we choose to parameterize by compact remnant mass, which makes more sense in terms of yields, we must still take into account the thermodynamic history of the material which escapes. If we parameterize by explosion energy, which has some hope of being partially constrained by observations of explosions, we are left with a very uncertain remnant mass, amount of ejecta, and thermodynamic history.

Fryer & Kalogera (2001) examine how supernova explosion energy varies with mass. They argued that the supernova explosion energy peaks at an initial progenitor mass of $15M_{\odot}$. At $23M_{\odot}$, they predicted an explosion energy of less than 10^{51} erg. While the progenitors

we have used in this paper are very different from the progenitors used in Fryer & Kalogera (2001), we may still use the trends in that work to guess where the parameter space will open up for the uncertainties identified here. We find that large explosion energies are required to expel explosively processed material at $23 M_{\odot}$ because of the massive core of the star. It is likely that sufficiently large explosion energies only occur if the collapsar engine is driving the explosion. If such stars do have low explosion energies, then our primary uncertainty will be in the O/Ne/Mg to Si/S part of the periodic table, where we may expect changes in O of tens of percent and changes in Si of factors of a few. In this case it is sufficient to examine a range of total ejecta masses to estimate the range of yields, remembering that the energy corresponding to a given remnant mass differs by $\sim 30\%$ between piston and thermal bomb models and is even larger for a neutrino gain region. As our progenitor decreases in mass, explosion energy rises and the amount of energy required to eject explosively processed material declines. By analogy to the models in this work, the mass range where our expected explosion energy crosses into the regime where QSE and NSE processing take place can have uncertainties in Si by a factor of 10 and in Fe peak by factors of several. Useful explosion diagnostics like ^{56}Ni can vary by orders of magnitude. At higher explosion energies the main uncertainties lie in the Fe peak, with a smaller contribution in the amount of Si rich material left unburned. The situation is rendered more difficult by the fact that this parameterization relates progenitor mass to explosion energy, which does not have a one-to-one correspondence with remnant/ejecta mass.

We expect our maximum uncertainties for lower mass, and thus more common, progenitors. For these stars a two parameter grid in remnant mass and thermodynamic history must be calculated to estimate the uncertainties. Without a good understanding of the supernova mechanism and the remnant to explosion energy relation, these grids and their corresponding error bars must be large. Perhaps more importantly, the solutions for a given abundance pattern are not unique, especially if we measure only elemental abundances. Ignoring variations in progenitors, initial mass functions, and 3D complications, we can independently adjust the explosion energy distribution, the energy/remnant mass relation, and the thermodynamic history of an explosion to find a given result. To some extent we can constrain our parameter space by attempting to match the solar abundance pattern (which is itself in dispute! (Asplund et al. 2005)), but this gives us very little leverage in making predictions since it introduces further complications of star formation histories and the non-linearity of enriching intermediate generations of model stars with our own uncertain yields.

It is worth discussing these results in the context of previous studies. We will begin with Woosley & Weaver (1995), which provides the current standard for yields and the template from which later compilations of yields are derived. Globally, we notice that varying the explosion energy or the treatment of the explosion can have very large effects not only

on individual, low abundance diagnostic isotopes, but also on the bulk yields of common elements. Woosley & Weaver (1995) examine different effective gravitational potentials in the piston (broadly equivalent to changing the final explosion kinetic energy while keeping the same energy input) for stars $> 30 M_{\odot}$. Below this mass limit they explore some small changes in the method of implementing the piston, which do have effects on important low abundance isotopes. However, they do not change the bulk energetics, assuming a final explosion kinetic energy of $\sim 1.2 \times 10^{51}$ erg. Woosley & Weaver (1995) do point out that the energies are uncertain, but do not present any resulting uncertainties in the yields. If anything, the assumption of constant energy looks worse now. Our still unsatisfactory understanding of the mechanism at least assures us that the explosion energies for stars in the common 10-20 M_{\odot} range will vary a great deal. Uncertainties of factors of more than ten in silicon and the iron peak can occur for stars of masses common enough to be interesting to population yields, given what we must currently accept as a reasonable range of explosion energies.

More specifically, we can compare our 1.2 foe piston to the Woosley & Weaver (1995) S22A model. Our yield of carbon is almost exactly twice that of S22A. Oxygen is increased by $\sim 80\%$, Si by 10%. The S22A Fe peak is nearly a factor of seven higher than our 23p-1.2, due almost entirely to their much larger yield of ^{56}Ni . Almost all of these changes can be traced to differences in the progenitor model. Our progenitor includes mass loss and, most importantly, a much more realistic treatment of hydrodynamics and mixing, which results in much larger core sizes for a given mass. This contributes to the ^{56}Ni discrepancy as well, but as Woosley & Weaver (1995) point out, this is also sensitive to the details of the piston.

ABT (1991) examine in detail two different methods of launching a 1D explosion with thermal bombs and pistons, and so provide an interesting comparison to this work. Their results at first glance appear to diverge significantly from ours, but when the differing assumptions of the two calculations are taken into account we shall see that the results of both studies are quite consistent. The following discussion highlights some of the vagaries of using 1D explosion models.

ABT (1991) find that the temperature profiles for thermal bombs and pistons are nearly identical in most of the stellar mantle, beginning to diverge increasingly, starting at several percent when T exceeds $2 \times 10^9\text{K}$ (see their Figure 7). The mass represented by very large temperature differences is small. Since they define the ejected material by imposing a uniform mass cut, the bulk yields for a given final kinetic energy are similar.

The principal difference in our results versus those of ABT (1991) results from our treatment of the hydrodynamic evolution. We do not impose a mass cut; rather we let material without sufficient kinetic energy to become unbound fall back onto the compact

object. If we return to Figure 15, which compares the peak temperatures in thermal bomb and piston models with a final kinetic energy of 1.2foe, we see that the temperatures in the ejected material begin to diverge at about $T > 2 \times 10^9\text{K}$, but the difference remains small for the material ejected, just as in the ABT (1991) study. The two models have very different yields, however, because much more material falls back in the thermal bomb case. Indeed, when we compare the 1.2foe piston and 1.5foe thermal bomb or 1.6foe piston and 2.0foe thermal bomb, which have similar compact remnant masses, we find that the yields are reasonably similar, with the exception of NSE species such as ^{56}Ni , which we would expect to show the effects of the initial difference in partition of kinetic and thermal energy between the thermal bomb and piston. Given that we are free to specify the location of the piston, its acceleration, velocity, and duration, we could probably produce more similar kinetic energies for a given compact remnant mass, but this *ad hoc* fine tuning obscures the amount of variation produced by taking an independent “best guess” in setting up the two explosions to reproduce the observable constraint of ejecta kinetic energy.

The other notable difference is the mass coordinate at which corresponding temperatures occur in each study. ABT (1991) use a $20M_{\odot}$ stellar model from Nomoto & Hashimoto (1988). Our progenitor is a $23 M_{\odot}$ model with hydrodynamic that accounts for hydrodynamic mixing processes that produce much larger nuclear processed cores and burning shells. The much more massive $\bar{A} \geq 16$ mantle in our model requires much more energy input to produce a successful explosion, so high temperatures extend to higher mass coordinates, as do the Fe core and O and Si shells. This is exactly as we would expect. Once adjusted for the differences in progenitors, the agreement of our results is surprisingly good.

More recent studies corroborate these results. Umeda & Nomoto (2005) examine nucleosynthesis in population III stars with varying amounts of fallback and mixing. While it is obviously impossible to compare our results directly, since the progenitors are of entirely different mass, metallicity, and input physics, their methodology has some bearing on this study. Their figure 14 is particularly interesting, showing the allowed range of fallback masses required to derive a Mg/Fe ratio consistent with extremely metal-poor stars. They choose an initial mass cut of $2.44M_{\odot}$, but their final allowed values are between $10.2 - 13.6M_{\odot}$. This indicates that an enormous variety of yields can be generated from a single model by choosing the parameters for explosion energy and amount of fallback and mixing. Limongi & Chieffi (2003) examine nucleosynthesis with a variety of explosion parameters and fallback. Their yields are highly variable for Fe peak and intermediate mass elements, depending on the energy of the explosion and the amount of fallback. Their range of variation for CNO and Si is smaller than ours mainly because their range of explosion energies does not extend as low as ours. We cannot compare directly to their results because their progenitors do not include a realistic prescription for mixing during the evolution, and there-

fore the extent of the various nuclear processed regions is smaller. However, if we examine their $35M_{\odot}$ progenitor we can make some approximate comparisons since the extent of the oxygen and heavier core is similar. They show a range of a factor of five in ^{28}Si and about an order of magnitude in ^{32}S , ^{40}Ca , and ^{56}Fe . There is little variation of CNO because the minimum explosion energy is 1.3 foe, which ejects all or nearly all of the CNO mantle. We find similar results for explosion energies this high.

Since we are required by computational limitations to rely on 1D explosion for population yields, the best we can hope for in the near future is use a few 3-dimensional simulations provide some insight into energy distribution, the energy/remnant mass relation and amount of mixing to constrain the size of the 1-dimensional grid. But recall that the current uncertainties in the explosion mechanism, even in 3-dimensions, prevent such results from being the final yields of stars. It is likely that we will have to live with uncertainties in the yields for some time yet, but understanding these uncertainties should help in understanding the current data.

4.1. O-rich Supernova Remnants

An incidental point of interest of this study concerns O-rich supernova remnants. As a class these remnant have very large masses of O dominated ejecta and comparatively small enrichments in Si/S and Fe elements. In particular, N132D in the Large Magellanic Cloud (LMC) and 1E 0102.2-7219 in the SMC show no evidence for the products of oxygen burning, either hydrostatic or explosive (Blair et al. 2000). In addition, Zampieri et al. (2003) present an analysis of two dim supernovae, SN 1997D and SN 1997br, which have small explosion energies (<1 foe) and very small masses of ^{56}Ni ($< 10^{-2}M_{\odot}$). Taken together, these observations are most simply explained by the explosion of a massive star that does not eject material processed by oxygen burning or later stages.

We see from these results that for a $23 M_{\odot}$ progenitor, explosion energies of 1.2 and 1.5 foe for the piston and thermal bomb models, respectively, are needed to produce a significant amount of ^{56}Ni . Small amounts, a few $\times 10^3 M_{\odot}$, can be explained by 3D effects and mixing, even in weak explosions, but there is a very large discrepancy between the energy necessary for significant ^{56}Ni production and the energies predicted for stars above $20 M_{\odot}$ by Fryer & Kalogera (2001). We thus expect most stars between $\sim 20 M_{\odot}$ and the lower mass limit for Wolf-Rayet stars ($30 M_{\odot}$?) to eject very little Si and Fe peak, which represents a significant population of objects that both explode as dim supernovae and produce O-rich remnants.

This work was carried out in part under the auspices of the National Nuclear Security Administration of the U.S. Department of Energy at Los Alamos National Laboratory and supported by Contract No. DE-AC52-06NA25396, by a DOE SciDAC grant DE-FC02-01ER41176, an NNSA ASC grant, and a subcontract to the ASCI FLASH Center at the University of Chicago.

REFERENCES

- Aoki, W. et al. 2006, *ApJ*, 639, 897
- Asplund, Martin, Grevesse, N. & Sauval, A. J. 2005, *astro-ph* 0410214
- Aufderheide, M. B., Baron, E., & Thielemann, F.-K. 1991, *ApJ*, 370, 630
- Benz, W., Thielemann, F.-K., & Hills, J. G. 1989, *ApJ*, 342, 986
- Berger, E. et al. 2006, *astro-ph*/0603689
- Blair, William P. et al. 2000, *ApJ*, 537, 667
- Blöcker, T. 1995, *A&A*, 297, 727
- Blondin, J.M. & Mezzacappa, A. 2006, *ApJ*, 642, 401
- Buras, R., Rampp, M., Janka, H.-Th., Kifonidis, K. 2003, *Phys. Rev. Lett.*, 90, 1101
- Burrows, A., Livne, E., Dessart, L., Ott, C.D., & Murphy, J. 2006, *ApJ*, 640, 878
- Erb, Dawn K. et al. 2006, *ApJ*, in press
- Frölich, C., Hauser, P., Liebendörfer, M., Martinez-Pinedo, G., Thielemann, F.-K., Bravo, E., Zinner, N.T., Hix, W.R., Langanke, K., Mezzacappa, A., & Nomoto, K. 2006, *ApJ*, 637, 415
- Fryer, Chris, Benz, Willy, Herant, Marc, & Colgate, Stirling A. 1999, *ApJ*, 516, 892
- Fryer, C.L., Colgate, S.A., & Pinto, P.A. 1999, *ApJ*, 511, 885
- Fryer, C.L., Heger, A. 2000, *ApJ*, 541, 1033
- Fryer, Chris, L. & Kalogera, Vasiliki 2001, *ApJ*, 554, 548
- Fryer, Chris L. & Warren, Michael S. 2002, *ApJ*, 574, L65

- Fryer, Chris L. & Warren, Michael S. 2004, ApJ, 601, 391
- Fryer, C.L., Kusenko, A. 2006, ApJS, 163, 335
- Fryer, C.L. 2006, submitted in New Astronomy
- Fryer, Chris L., Young, Patrick A., Hungerford, Aimee L. 2006, ApJ, in press
- Fryer, Chris L. & Young, Patrick A. 2006, ApJ, submitted
- Fryer, Chris L. in preparation
- Garnett, Donald R. 2002, ApJ, 581, 1019
- Graboske, H. C., Dewitt, H. E., Grossman, A. S., & Cooper, M. S. 1973, ApJ, 181, 457
- Grevesse, N. & Sauval, A. J., 1998, Space Science Reviews, 85, 161
- Hamuy, Mario 2003, ApJ, 582, 905
- Herant, Marc, Benz, Willy, Hix, W. Raphael, Fryer, Chris L., & Colgate, Stirling A. 1994, ApJ, 435, 339
- Hungerford, Aimee L., Fryer, Chris L., & Warren, Michael S. 2003, ApJ, 594, 390
- Hungerford, Aimee L., Fryer, Chris L., & Rockefeller, G. 2003, ApJ, 635, 487
- Kifonidis, K., Plewa, T., Janka, H.-Th., Müller, E. 2000, ApJ, 531, L123
- Kifonidis, K., Plewa, T., Janka, H.-Th., Müller, E. 2003, A&A, 408, 621
- Kotake, K., Yamada, S., & Sato, K. 2003, ApJ, 595, 304
- Kifonidis, K., Plewa, T., Janka, H.-Th., Müller, E. 2003, A&A, 408, 621
- Kudritzki, R. P., Pauldrach, A., Puls, J., & Abbott, D. C. 1989, A&A, 219, 205
- Langanke, K. & Martinez-Pinedo, G. 2000, Nuclear Physics A, 673, 481
- Limongi, Marco & Chieffi, Alessandro 2003, ApJ, 592, 404
- Meynet, G. & Maeder, A. 2000, A&A, 361, 101
- Meakin, Casey, A. & Arnett, David 2006, ApJ, 637L, 53
- Meakin, Casey, Young, Patrick A., & Arnett, David 2005, ApJ, in prep

- Nagataki, Shigehiro, Hashimoto, Masa-Aki, Sato, Katsuhiko, Yamada, Shoichi, & Mochizuki, Yuko S. 1998, *ApJ*, 492L, 45
- Nomoto, Ken'ichi, Umeda, Hideyuki, Maeda, Keiichi, Ohkubo, Takuya, Deng, Jingsong, & Mazzali, Paolo 2003, *Nucl. Phys. A*, 718, 277
- Nomoto, K. & Hashimoto, M. 1988, *Phys. Repts.*, 163, 13
- Pritzl, Barton, J., Venn, Kim A., & Irwin, Mike 2005, *AJ*, 130, 214
- Rauscher, T. & Thielemann, F.-K. 2001, *Atomic Data Nuclear Tables*, 79, 47
- Shimizu, T., Yamada, S., & Sato, K. 1994, *ApJ*, 432, L119
- Thielemann, Friedrich-Karl et al. 2002, *Ap&SS*, 281, 25
- Thielemann, Friedrich-Karl, Nomoto, Ken'ichi, & Hashimoto, Masa-Aki 1997, *ApJ*, 460, 408
- Umeda, Hideyuki & Nomoto, Ken'ichi 2005, *ApJ*, 619, 427
- Woosley, S. E. 1993, *ApJ*, 405, 273
- Woosley, S. E. & Weaver, Thomas A. 1995, *ApJS*, 101, 181
- Young, Patrick A. & Arnett, David 2005, *ApJ*, 618, 908
- Young, Patrick A., Meakin, Casey, Arnett, David, & Fryer, Chris L. 2005, *ApJ*, 629, 101
- Zampieri, L., Pastorello, A., Turatto, M., Cappellaro, E., Benetti, S., Altavilla, G., Mazzali, P., & Hamuy, M. 2003, *MNRAS*, 338, 711

Table 1. Explosion Simulations

Simulation	type	Energy 10^{51} erg	M_{Rem} (M_{\odot})
23e-0.8	thermal bomb - 20 ms	0.8	5.7
23e-1.1	thermal bomb - 20 ms	1.1	4.2
23e-1.2	thermal bomb - 20 ms	1.2	4.1
23e-1.4	thermal bomb - 20 ms	1.4	3.7
23e-1.5	thermal bomb - 20 ms	1.5	3.2
23e-2.0	thermal bomb - 20 ms	2.0	2.6
23e-0.2-0.8	thermal bomb - 200 ms	0.8	3.5
23e-0.2-1.5	thermal bomb - 200 ms	1.5	2.6
23e-0.7-0.8	thermal bomb - 700 ms	0.8	3.2
23e-0.7-1.5	thermal bomb - 700 ms	1.5	2.3
23p-0.9	piston	0.9	5.0
23p-1.2	piston	1.2	3.2
23p-1.6	piston	1.6	2.4

Table 2. Detailed Yields (M_{\odot}) Before Radioactive Decay For Thermal Bomb Simulations

Species	23e-0.8	23e-1.1	23e-1.2	23e-1.4	23e-1.5	23e-2.0
^1H	1.46E+00	1.46E+00	1.46E+00	1.46E+00	1.46E+00	1.46E+00
^2H	3.86E-16	4.46E-16	4.39E-16	4.78E-16	4.76E-16	5.96E-16
^3H	2.39E-23	1.58E-16	1.58E-16	1.58E-16	1.57E-16	1.55E-16
^3He	6.60E-05	6.60E-05	6.60E-05	6.60E-05	6.60E-05	6.60E-05
^4He	1.13E+00	1.13E+00	1.13E+00	1.13E+00	1.13E+00	1.13E+00
^6Li	2.01E-18	2.35E-18	2.29E-18	2.51E-18	2.50E-18	3.22E-18
^7Li	2.89E-10	2.89E-10	2.89E-10	2.89E-10	2.89E-10	2.89E-10
^7Be	1.28E-10	1.28E-10	1.28E-10	1.28E-10	1.28E-10	1.28E-10
^8Be	1.95E-16	3.82E-11	6.11E-11	1.57E-10	4.10E-09	1.39E-06
^9Be	8.88E-19	1.01E-18	1.03E-18	1.12E-18	1.14E-18	1.27E-18
^8B	1.80E-20	1.80E-20	1.80E-20	1.80E-20	1.80E-20	1.80E-20
^{10}B	3.74E-11	3.74E-11	3.74E-11	3.74E-11	3.74E-11	3.74E-11
^{11}B	2.06E-11	2.27E-11	2.27E-11	2.27E-11	2.27E-11	2.27E-11
^{11}C	4.17E-20	1.32E-17	1.35E-17	1.48E-17	1.56E-17	1.69E-17
^{12}C	4.52E-01	4.91E-01	4.90E-01	4.89E-01	4.89E-01	4.86E-01
^{13}C	4.31E-04	4.29E-04	4.29E-04	4.27E-04	4.27E-04	4.24E-04
^{14}C	4.48E-08	1.70E-06	1.70E-06	1.67E-06	1.67E-06	1.62E-06
^{12}N	1.33E-31	1.81E-31	1.80E-31	2.13E-31	2.25E-31	3.26E-31
^{13}N	1.32E-07	1.44E-07	1.44E-07	1.51E-07	1.55E-07	1.73E-07
^{14}N	1.44E-02	1.44E-02	1.44E-02	1.44E-02	1.44E-02	1.44E-02
^{15}N	5.95E-06	6.14E-06	6.15E-06	6.23E-06	6.26E-06	6.49E-06
^{14}O	6.66E-12	6.67E-12	6.66E-12	6.65E-12	6.56E-12	6.52E-12
^{15}O	4.63E-10	6.22E-10	6.29E-10	6.91E-10	7.16E-10	8.75E-10
^{16}O	2.56E+00	3.89E+00	3.98E+00	4.30E+00	4.37E+00	4.32E+00
^{17}O	5.40E-04	5.40E-04	5.40E-04	5.40E-04	5.40E-04	5.40E-04
^{18}O	1.02E-04	9.99E-05	9.98E-05	9.87E-05	9.85E-05	9.65E-05
^{19}O	2.58E-10	3.10E-10	3.14E-10	3.49E-10	3.64E-10	4.39E-10
^{17}F	4.08E-12	4.59E-12	4.55E-12	4.87E-12	4.71E-12	5.43E-12
^{18}F	3.83E-06	4.40E-06	4.46E-06	4.87E-06	5.06E-06	5.83E-06
^{19}F	9.03E-06	8.93E-06	8.92E-06	8.85E-06	8.84E-06	8.71E-06

Table 2—Continued

Species	23e-0.8	23e-1.1	23e-1.2	23e-1.4	23e-1.5	23e-2.0
²⁰ F	1.83E-08	2.10E-08	2.12E-08	2.28E-08	2.31E-08	2.62E-08
²¹ F	1.17E-10	1.64E-10	1.67E-10	1.91E-10	1.94E-10	2.40E-10
¹⁷ Ne	1.61E-54	1.88E-54	1.93E-54	2.48E-54	2.14E-52	4.13E-51
¹⁸ Ne	4.91E-18	4.83E-18	4.82E-18	4.78E-18	4.77E-18	4.67E-18
¹⁹ Ne	1.42E-11	1.63E-11	1.65E-11	1.80E-11	1.85E-11	2.23E-11
²⁰ Ne	3.21E-01	3.73E-01	3.74E-01	3.78E-01	3.78E-01	3.85E-01
²¹ Ne	4.50E-03	5.25E-03	5.25E-03	5.19E-03	5.18E-03	5.06E-03
²² Ne	5.44E-02	6.30E-02	6.29E-02	6.22E-02	6.21E-02	6.09E-02
²³ Ne	1.17E-05	1.39E-05	1.40E-05	1.43E-05	1.43E-05	1.48E-05
²⁴ Ne	6.93E-10	8.33E-10	8.38E-10	8.73E-10	8.76E-10	9.24E-10
¹⁹ Na	1.55E-39	1.55E-39	1.61E-39	1.69E-39	1.75E-39	1.78E-39
²⁰ Na	2.56E-21	2.77E-21	2.83E-21	3.00E-21	3.07E-21	3.76E-21
²¹ Na	4.15E-08	4.76E-08	4.80E-08	5.18E-08	5.21E-08	5.79E-08
²² Na	7.95E-07	1.96E-06	1.96E-06	1.93E-06	1.93E-06	1.87E-06
²³ Na	6.89E-03	9.08E-03	9.07E-03	8.95E-03	8.94E-03	8.73E-03
²⁴ Na	3.24E-05	5.44E-05	5.47E-05	5.66E-05	5.69E-05	5.96E-05
²⁵ Na	5.14E-07	7.14E-07	7.23E-07	7.85E-07	7.93E-07	8.96E-07
²⁶ Na	2.70E-11	3.27E-11	3.30E-11	3.65E-11	3.67E-11	4.23E-11
²⁷ Na	8.02E-18	8.74E-18	8.87E-18	9.46E-18	9.36E-18	9.80E-18
²⁰ Mg	1.75E-52	2.30E-52	2.43E-52	2.94E-52	3.56E-52	4.70E-52
²¹ Mg	3.01E-31	2.94E-31	3.22E-31	3.13E-31	3.11E-31	3.39E-31
²² Mg	2.53E-13	2.72E-13	2.73E-13	2.83E-13	2.84E-13	2.98E-13
²³ Mg	3.13E-08	3.36E-06	3.36E-06	3.35E-06	3.35E-06	3.35E-06
²⁴ Mg	5.16E-02	7.31E-02	7.55E-02	8.30E-02	8.35E-02	8.63E-02
²⁵ Mg	8.92E-03	1.35E-02	1.35E-02	1.39E-02	1.39E-02	1.46E-02
²⁶ Mg	1.34E-02	2.09E-02	2.09E-02	2.08E-02	2.08E-02	2.07E-02
²⁷ Mg	3.28E-06	7.63E-06	7.71E-06	8.18E-06	8.29E-06	9.19E-06
²⁸ Mg	5.52E-08	1.01E-07	1.03E-07	1.16E-07	1.18E-07	1.45E-07
²⁹ Mg	2.00E-12	2.74E-12	2.80E-12	3.34E-12	3.39E-12	4.44E-12
²² Al	1.07E-58	9.17E-59	1.16E-58	9.43E-59	9.34E-59	8.31E-59

Table 2—Continued

Species	23e-0.8	23e-1.1	23e-1.2	23e-1.4	23e-1.5	23e-2.0
²³ Al	1.67E-30	1.53E-30	1.53E-30	1.45E-30	1.46E-30	1.29E-30
²⁴ Al	3.18E-18	3.15E-18	3.13E-18	3.06E-18	3.04E-18	2.95E-18
²⁵ Al	6.04E-07	6.00E-07	6.00E-07	5.96E-07	5.96E-07	5.91E-07
²⁶ Al	1.29E-05	2.83E-05	2.84E-05	2.93E-05	2.94E-05	3.10E-05
²⁷ Al	8.96E-04	2.60E-03	2.64E-03	2.68E-03	2.69E-03	2.70E-03
²⁸ Al	9.67E-06	4.80E-05	4.84E-05	5.00E-05	5.09E-05	5.47E-05
²⁹ Al	4.22E-07	1.58E-06	1.60E-06	1.72E-06	1.76E-06	2.03E-06
³⁰ Al	7.76E-10	1.43E-09	1.46E-09	1.75E-09	1.79E-09	2.40E-09
³¹ Al	2.64E-13	4.28E-13	4.41E-13	5.53E-13	5.64E-13	8.05E-13
²³ Si	1.86E-76	1.57E-76	2.01E-76	1.72E-76	1.83E-76	1.88E-76
²⁴ Si	3.91E-38	3.22E-38	3.33E-38	2.97E-38	2.98E-38	2.33E-38
²⁵ Si	1.94E-27	1.69E-27	1.80E-27	1.65E-27	1.64E-27	1.31E-27
²⁶ Si	6.34E-13	6.80E-13	6.78E-13	6.71E-13	6.66E-13	6.51E-13
²⁷ Si	3.16E-09	5.50E-07	5.57E-07	5.74E-07	5.80E-07	5.80E-07
²⁸ Si	5.18E-03	1.86E-02	2.17E-02	5.98E-02	3.03E-01	4.61E-01
²⁹ Si	5.74E-04	5.36E-03	5.56E-03	5.94E-03	6.06E-03	6.09E-03
³⁰ Si	2.64E-04	8.65E-03	1.04E-02	1.32E-02	1.32E-02	1.30E-02
³¹ Si	6.83E-06	4.73E-05	4.75E-05	4.89E-05	4.94E-05	5.27E-05
³² Si	1.39E-07	2.80E-06	2.81E-06	2.89E-06	2.91E-06	3.09E-06
³³ Si	1.87E-10	2.76E-10	2.85E-10	3.56E-10	3.65E-10	5.24E-10
³⁴ Si	2.16E-13	3.45E-13	3.59E-13	4.69E-13	4.82E-13	7.44E-13
²⁷ P	1.17E-25	1.03E-25	1.10E-25	1.02E-25	1.01E-25	8.22E-26
²⁸ P	1.81E-19	1.69E-19	1.78E-19	1.70E-19	1.69E-19	1.46E-19
²⁹ P	7.46E-10	8.79E-10	8.90E-10	9.76E-10	9.87E-10	1.17E-09
³⁰ P	1.93E-08	2.51E-06	2.51E-06	2.56E-06	2.65E-06	2.75E-06
³¹ P	5.28E-05	1.19E-03	1.31E-03	1.62E-03	1.70E-03	1.69E-03
³² P	3.77E-07	1.22E-05	1.25E-05	1.29E-05	1.29E-05	1.31E-05
³³ P	4.72E-07	1.12E-05	1.20E-05	1.28E-05	1.28E-05	1.29E-05
³⁴ P	6.64E-09	4.28E-08	4.30E-08	4.47E-08	4.53E-08	4.90E-08
³⁵ P	2.18E-10	2.07E-09	2.09E-09	2.18E-09	2.21E-09	2.45E-09

Table 2—Continued

Species	23e-0.8	23e-1.1	23e-1.2	23e-1.4	23e-1.5	23e-2.0
³⁶ P	1.61E-13	2.60E-13	2.70E-13	3.54E-13	3.65E-13	5.62E-13
³⁷ P	1.45E-17	2.35E-17	2.44E-17	3.20E-17	3.28E-17	5.05E-17
³⁸ P	2.30E-26	2.69E-26	3.00E-26	3.23E-26	3.17E-26	3.10E-26
²⁸ S	3.87E-40	3.23E-40	3.18E-40	2.93E-40	2.92E-40	3.32E-40
²⁹ S	2.30E-29	1.97E-29	2.04E-29	1.91E-29	1.89E-29	1.59E-29
³⁰ S	8.21E-17	2.64E-16	2.64E-16	2.69E-16	6.08E-16	1.49E-14
³¹ S	9.15E-14	1.13E-08	1.85E-08	4.48E-08	4.98E-08	7.25E-08
³² S	2.11E-03	6.54E-03	7.75E-03	2.27E-02	1.50E-01	2.53E-01
³³ S	8.89E-05	2.20E-04	2.49E-04	3.81E-04	4.96E-04	5.02E-04
³⁴ S	1.21E-04	2.03E-03	2.90E-03	9.14E-03	1.21E-02	1.25E-02
³⁵ S	2.90E-06	1.31E-05	1.31E-05	1.34E-05	1.35E-05	1.39E-05
³⁶ S	2.28E-06	2.22E-05	2.28E-05	2.33E-05	2.33E-05	2.37E-05
³⁷ S	5.30E-09	6.73E-09	6.87E-09	7.89E-09	8.01E-09	1.01E-08
³⁸ S	4.53E-11	6.43E-11	6.61E-11	8.07E-11	8.24E-11	1.14E-10
³⁹ S	1.20E-13	1.89E-13	1.96E-13	2.53E-13	2.61E-13	3.95E-13
⁴⁰ S	1.03E-15	1.80E-15	1.88E-15	2.59E-15	2.69E-15	4.49E-15
⁴¹ S	5.09E-21	8.80E-21	9.19E-21	1.25E-20	1.29E-20	2.10E-20
⁴² S	1.64E-22	3.49E-22	3.71E-22	5.67E-22	5.94E-22	1.17E-21
³¹ Cl	2.77E-32	2.56E-32	2.51E-32	2.39E-32	2.42E-32	8.46E-30
³² Cl	7.53E-24	7.01E-24	7.13E-24	6.94E-24	6.95E-24	2.91E-22
³³ Cl	2.36E-10	2.36E-10	2.36E-10	2.35E-10	2.34E-10	2.45E-10
³⁴ Cl	7.69E-12	1.00E-09	1.04E-09	1.95E-09	6.65E-09	1.63E-08
³⁵ Cl	3.96E-05	8.02E-05	8.14E-05	1.14E-04	1.63E-04	1.66E-04
³⁶ Cl	1.42E-06	2.63E-06	2.70E-06	2.85E-06	2.90E-06	2.89E-06
³⁷ Cl	4.25E-05	6.43E-05	6.49E-05	6.59E-05	6.61E-05	6.66E-05
³⁸ Cl	3.22E-07	5.91E-07	5.98E-07	6.42E-07	6.49E-07	7.34E-07
³⁹ Cl	3.12E-08	8.76E-08	8.88E-08	9.66E-08	9.83E-08	1.15E-07
⁴⁰ Cl	5.88E-10	1.10E-09	1.13E-09	1.36E-09	1.39E-09	1.91E-09
⁴¹ Cl	3.16E-11	9.23E-11	9.46E-11	1.12E-10	1.15E-10	1.60E-10
⁴² Cl	3.31E-13	6.55E-13	6.86E-13	9.49E-13	9.84E-13	1.68E-12

Table 2—Continued

Species	23e-0.8	23e-1.1	23e-1.2	23e-1.4	23e-1.5	23e-2.0
⁴³ Cl	8.77E-15	2.37E-14	2.49E-14	3.47E-14	3.62E-14	6.51E-14
⁴⁴ Cl	1.48E-20	2.88E-20	3.04E-20	4.41E-20	4.55E-20	8.18E-20
⁴⁵ Cl	7.80E-21	1.98E-20	2.14E-20	3.60E-20	3.81E-20	8.77E-20
³² Ar	6.26E-45	6.19E-45	6.15E-45	6.12E-45	6.08E-45	8.12E-36
³³ Ar	1.46E-34	1.24E-34	1.25E-34	1.17E-34	1.15E-34	3.72E-33
³⁴ Ar	3.02E-17	3.01E-17	2.99E-17	2.96E-17	3.75E-17	5.98E-14
³⁵ Ar	4.00E-17	1.36E-13	1.36E-13	1.94E-13	5.63E-11	1.00E-09
³⁶ Ar	4.65E-04	5.50E-04	5.65E-04	2.05E-03	2.30E-02	4.62E-02
³⁷ Ar	2.88E-06	3.98E-06	4.21E-06	1.49E-05	4.55E-05	4.65E-05
³⁸ Ar	1.12E-04	2.26E-04	2.78E-04	3.81E-03	8.00E-03	8.28E-03
³⁹ Ar	2.96E-06	4.67E-06	4.69E-06	4.80E-06	4.83E-06	5.04E-06
⁴⁰ Ar	5.93E-07	2.78E-06	2.84E-06	2.90E-06	2.92E-06	3.00E-06
⁴¹ Ar	9.13E-09	2.45E-08	2.47E-08	2.65E-08	2.68E-08	3.07E-08
⁴² Ar	4.22E-10	1.49E-08	1.50E-08	1.52E-08	1.52E-08	1.56E-08
⁴³ Ar	6.92E-12	1.58E-11	1.62E-11	1.94E-11	1.99E-11	2.74E-11
⁴⁴ Ar	1.62E-13	1.20E-12	1.21E-12	1.32E-12	1.34E-12	1.63E-12
⁴⁵ Ar	9.86E-16	2.15E-15	2.26E-15	3.14E-15	3.27E-15	5.71E-15
⁴⁶ Ar	7.89E-18	3.75E-17	3.85E-17	4.80E-17	4.94E-17	7.78E-17
³⁵ K	6.63E-35	5.91E-35	5.94E-35	5.55E-35	5.55E-35	3.25E-31
³⁶ K	2.95E-28	2.69E-28	2.69E-28	2.57E-28	2.55E-28	2.11E-22
³⁷ K	2.40E-12	2.36E-12	2.36E-12	2.34E-12	2.36E-12	2.58E-12
³⁸ K	6.52E-13	2.29E-11	2.35E-11	2.18E-10	2.47E-09	1.03E-08
³⁹ K	2.34E-05	2.90E-05	2.91E-05	6.48E-05	1.40E-04	1.43E-04
⁴⁰ K	1.37E-06	1.84E-06	1.84E-06	1.85E-06	1.85E-06	1.84E-06
⁴¹ K	3.52E-06	5.08E-06	5.10E-06	5.10E-06	5.10E-06	5.08E-06
⁴² K	1.83E-07	7.71E-07	7.74E-07	7.92E-07	8.00E-07	8.41E-07
⁴³ K	7.55E-08	6.55E-07	6.57E-07	6.74E-07	6.79E-07	7.21E-07
⁴⁴ K	6.97E-09	1.63E-07	1.64E-07	1.68E-07	1.70E-07	1.80E-07
⁴⁵ K	1.02E-09	1.41E-07	1.41E-07	1.44E-07	1.45E-07	1.52E-07
⁴⁶ K	1.68E-11	8.39E-09	8.39E-09	8.66E-09	8.74E-09	9.28E-09

Table 2—Continued

Species	23e-0.8	23e-1.1	23e-1.2	23e-1.4	23e-1.5	23e-2.0
⁴⁷ K	1.85E-13	6.86E-10	6.85E-10	7.02E-10	7.06E-10	7.44E-10
⁴⁸ K	3.90E-16	8.77E-16	9.27E-16	1.39E-15	1.46E-15	2.83E-15
⁴⁹ K	1.71E-18	4.30E-18	4.59E-18	7.23E-18	7.60E-18	1.60E-17
³⁶ Ca	2.50E-42	2.16E-42	2.13E-42	1.97E-42	1.87E-42	2.30E-39
³⁷ Ca	4.26E-38	3.65E-38	3.61E-38	3.38E-38	3.24E-38	1.96E-32
³⁸ Ca	1.10E-20	1.02E-20	1.02E-20	9.82E-21	9.87E-21	1.01E-16
³⁹ Ca	2.27E-20	6.77E-18	6.73E-18	1.87E-16	2.03E-13	1.65E-11
⁴⁰ Ca	3.85E-04	4.35E-04	4.35E-04	7.54E-04	1.39E-02	3.74E-02
⁴¹ Ca	1.12E-05	1.31E-05	1.31E-05	1.36E-05	1.71E-05	1.69E-05
⁴² Ca	5.78E-06	8.39E-06	9.11E-06	1.48E-04	3.11E-04	3.18E-04
⁴³ Ca	1.11E-06	1.68E-06	1.69E-06	1.80E-06	1.82E-06	1.84E-06
⁴⁴ Ca	9.44E-06	1.39E-05	1.45E-05	1.61E-05	1.62E-05	1.60E-05
⁴⁵ Ca	3.84E-07	1.21E-06	1.21E-06	1.23E-06	1.24E-06	1.28E-06
⁴⁶ Ca	8.41E-08	1.58E-06	1.66E-06	1.69E-06	1.69E-06	1.70E-06
⁴⁷ Ca	3.82E-09	1.63E-07	1.63E-07	1.65E-07	1.66E-07	1.73E-07
⁴⁸ Ca	9.18E-07	1.19E-06	1.21E-06	1.22E-06	1.22E-06	1.21E-06
⁴⁹ Ca	1.52E-09	1.86E-09	1.88E-09	2.08E-09	2.10E-09	2.48E-09
⁴⁰ Sc	1.44E-33	1.30E-33	1.29E-33	1.21E-33	1.22E-33	2.17E-24
⁴¹ Sc	1.47E-15	1.42E-15	1.43E-15	1.41E-15	1.45E-15	1.61E-15
⁴² Sc	1.75E-15	3.19E-15	3.12E-15	3.21E-15	3.58E-15	8.04E-13
⁴³ Sc	9.51E-12	3.80E-10	3.80E-10	8.15E-10	1.61E-09	1.50E-07
⁴⁴ Sc	2.73E-12	1.63E-09	1.67E-09	8.90E-09	1.29E-08	1.30E-08
⁴⁵ Sc	4.34E-07	7.13E-07	7.27E-07	8.02E-07	8.17E-07	8.04E-07
⁴⁶ Sc	8.38E-08	3.97E-07	4.02E-07	4.07E-07	4.07E-07	4.05E-07
⁴⁷ Sc	2.41E-08	5.65E-07	6.06E-07	6.17E-07	6.16E-07	6.15E-07
⁴⁸ Sc	6.66E-09	3.18E-07	3.20E-07	3.21E-07	3.22E-07	3.25E-07
⁴⁹ Sc	7.08E-10	1.58E-07	1.60E-07	1.61E-07	1.61E-07	1.62E-07
⁵⁰ Sc	1.21E-11	1.48E-10	1.48E-10	1.53E-10	1.54E-10	1.68E-10
⁵¹ Sc	1.76E-13	5.71E-12	5.72E-12	5.86E-12	5.91E-12	6.26E-12
⁴¹ Ti	1.36E-45	1.08E-45	1.13E-45	9.73E-46	9.98E-46	1.26E-36

Table 2—Continued

Species	23e-0.8	23e-1.1	23e-1.2	23e-1.4	23e-1.5	23e-2.0
⁴² Ti	4.46E-26	3.88E-26	4.00E-26	3.77E-26	3.89E-26	1.31E-25
⁴³ Ti	5.56E-23	9.32E-22	8.66E-22	9.20E-22	1.71E-21	1.51E-13
⁴⁴ Ti	2.31E-13	2.91E-10	3.37E-10	2.57E-07	5.13E-06	6.95E-05
⁴⁵ Ti	1.16E-14	7.65E-11	1.00E-10	2.21E-08	1.87E-07	1.99E-07
⁴⁶ Ti	1.66E-06	2.06E-06	2.20E-06	3.13E-05	3.01E-04	3.13E-04
⁴⁷ Ti	1.57E-06	1.98E-06	2.05E-06	2.74E-06	4.38E-06	4.42E-06
⁴⁸ Ti	1.58E-05	1.83E-05	1.89E-05	2.18E-05	2.35E-05	2.36E-05
⁴⁹ Ti	3.48E-06	4.47E-06	4.48E-06	4.50E-06	4.50E-06	4.50E-06
⁵⁰ Ti	2.01E-06	5.20E-06	5.46E-06	5.72E-06	5.73E-06	5.83E-06
⁵¹ Ti	3.18E-08	9.33E-08	9.41E-08	9.93E-08	1.00E-07	1.11E-07
⁵² Ti	1.28E-09	2.10E-08	2.11E-08	2.15E-08	2.17E-08	2.28E-08
⁵³ Ti	2.15E-11	3.71E-11	3.83E-11	4.83E-11	4.96E-11	7.28E-11
⁴³ V	5.75E-43	5.86E-43	6.09E-43	6.54E-43	7.44E-43	1.76E-42
⁴⁴ V	2.56E-35	2.14E-35	2.30E-35	2.06E-35	2.00E-35	8.65E-26
⁴⁵ V	4.67E-23	4.76E-23	4.77E-23	4.79E-23	4.95E-23	1.16E-14
⁴⁶ V	5.15E-25	7.77E-21	8.05E-21	4.94E-18	1.85E-16	9.28E-15
⁴⁷ V	3.47E-13	3.69E-11	3.79E-11	1.90E-09	4.52E-08	3.80E-07
⁴⁸ V	4.94E-13	1.06E-09	1.40E-09	5.82E-08	2.75E-07	3.42E-07
⁴⁹ V	3.06E-11	5.50E-08	6.35E-08	2.57E-07	5.47E-07	5.83E-07
⁵⁰ V	4.34E-09	4.03E-08	4.49E-08	5.62E-08	5.79E-08	6.04E-08
⁵¹ V	2.18E-06	3.00E-06	3.17E-06	3.35E-06	3.37E-06	3.35E-06
⁵² V	1.09E-07	3.93E-07	3.95E-07	4.05E-07	4.09E-07	4.27E-07
⁵³ V	1.55E-08	3.27E-07	3.27E-07	3.31E-07	3.32E-07	3.43E-07
⁵⁴ V	5.44E-10	1.80E-09	1.82E-09	1.99E-09	2.02E-09	2.40E-09
⁵⁵ V	7.39E-12	4.30E-11	4.32E-11	4.67E-11	4.72E-11	5.52E-11
⁴⁴ Cr	3.28E-55	4.64E-55	4.92E-55	6.35E-55	8.60E-55	1.22E-54
⁴⁵ Cr	9.84E-47	6.96E-47	7.45E-47	6.41E-47	6.15E-47	4.95E-38
⁴⁶ Cr	4.60E-34	4.38E-34	4.41E-34	5.22E-34	1.86E-29	3.75E-20
⁴⁷ Cr	7.62E-31	1.81E-24	1.77E-24	1.56E-22	2.91E-18	9.51E-12
⁴⁸ Cr	1.95E-19	2.09E-12	3.67E-12	5.56E-08	1.49E-05	4.60E-04

Table 2—Continued

Species	23e-0.8	23e-1.1	23e-1.2	23e-1.4	23e-1.5	23e-2.0
⁴⁹ Cr	1.01E-18	2.26E-12	3.55E-12	2.03E-08	1.18E-06	7.66E-06
⁵⁰ Cr	3.93E-06	4.26E-06	4.27E-06	1.70E-05	6.30E-04	9.26E-04
⁵¹ Cr	3.24E-07	4.21E-07	4.52E-07	1.26E-06	7.50E-06	7.85E-06
⁵² Cr	8.99E-05	1.01E-04	1.01E-04	1.08E-04	1.84E-04	1.89E-04
⁵³ Cr	1.45E-05	1.65E-05	1.65E-05	1.64E-05	1.64E-05	1.62E-05
⁵⁴ Cr	8.25E-06	2.20E-05	2.29E-05	2.35E-05	2.36E-05	2.38E-05
⁵⁵ Cr	2.61E-07	5.22E-07	5.28E-07	5.68E-07	5.74E-07	6.51E-07
⁵⁶ Cr	2.46E-08	1.63E-07	1.64E-07	1.71E-07	1.72E-07	1.88E-07
⁵⁷ Cr	7.56E-11	1.11E-10	1.15E-10	1.43E-10	1.46E-10	2.06E-10
⁵⁸ Cr	9.80E-12	1.79E-11	1.86E-11	2.47E-11	2.55E-11	4.06E-11
⁴⁶ Mn	1.34E-64	9.06E-65	9.71E-65	8.43E-65	8.77E-65	6.43E-56
⁴⁷ Mn	5.28E-50	4.38E-50	4.87E-50	4.45E-50	4.43E-50	5.00E-36
⁴⁸ Mn	8.94E-46	8.80E-46	9.31E-46	8.54E-46	8.42E-46	1.63E-25
⁴⁹ Mn	8.48E-31	6.14E-30	6.22E-30	2.61E-28	2.66E-22	2.45E-15
⁵⁰ Mn	1.06E-30	2.01E-23	2.16E-23	3.42E-19	2.54E-15	1.40E-13
⁵¹ Mn	2.18E-13	4.62E-12	4.71E-12	7.17E-10	2.03E-06	2.17E-05
⁵² Mn	3.88E-14	9.37E-11	1.57E-10	2.45E-08	4.13E-07	2.96E-06
⁵³ Mn	5.52E-11	1.51E-08	1.70E-08	1.95E-07	5.08E-06	7.09E-06
⁵⁴ Mn	5.30E-11	6.34E-08	7.56E-08	8.92E-08	1.14E-07	1.16E-07
⁵⁵ Mn	6.84E-05	7.90E-05	7.95E-05	7.89E-05	7.87E-05	7.72E-05
⁵⁶ Mn	2.28E-06	6.73E-06	6.77E-06	6.90E-06	6.95E-06	7.16E-06
⁵⁷ Mn	8.39E-07	1.13E-05	1.13E-05	1.15E-05	1.15E-05	1.19E-05
⁵⁸ Mn	3.43E-08	1.64E-07	1.65E-07	1.73E-07	1.75E-07	1.94E-07
⁵⁹ Mn	8.18E-09	2.49E-07	2.49E-07	2.54E-07	2.57E-07	2.71E-07
⁶⁰ Mn	9.72E-11	1.73E-10	1.80E-10	2.37E-10	2.44E-10	3.81E-10
⁶¹ Mn	5.46E-12	1.13E-11	1.18E-11	1.64E-11	1.70E-11	2.91E-11
⁴⁷ Fe	1.32E-78	1.45E-78	1.57E-78	2.03E-78	3.05E-78	1.75E-70
⁴⁸ Fe	6.09E-64	4.42E-64	5.11E-64	4.44E-64	4.62E-64	4.17E-50
⁴⁹ Fe	2.92E-58	2.59E-58	2.58E-58	2.43E-58	9.31E-56	1.72E-38
⁵⁰ Fe	5.07E-45	4.31E-45	4.70E-45	6.38E-45	1.81E-38	6.32E-29

Table 2—Continued

Species	23e-0.8	23e-1.1	23e-1.2	23e-1.4	23e-1.5	23e-2.0
⁵¹ Fe	8.16E-40	5.62E-32	5.11E-32	2.65E-28	5.93E-22	3.67E-17
⁵² Fe	2.45E-20	1.00E-14	2.57E-14	1.91E-09	1.30E-04	8.50E-03
⁵³ Fe	4.59E-21	3.95E-14	8.29E-14	2.50E-09	7.86E-06	1.40E-04
⁵⁴ Fe	4.02E-04	4.38E-04	4.38E-04	4.52E-04	1.19E-02	3.46E-02
⁵⁵ Fe	2.71E-05	3.34E-05	3.37E-05	3.58E-05	9.00E-05	9.44E-05
⁵⁶ Fe	6.94E-03	7.71E-03	7.72E-03	8.08E-03	8.58E-03	8.51E-03
⁵⁷ Fe	7.03E-04	8.70E-04	8.71E-04	8.70E-04	8.71E-04	8.68E-04
⁵⁸ Fe	2.33E-04	1.08E-03	1.18E-03	1.29E-03	1.29E-03	1.31E-03
⁵⁹ Fe	2.59E-05	7.13E-05	7.17E-05	7.47E-05	7.53E-05	8.19E-05
⁶⁰ Fe	5.25E-06	1.12E-04	1.15E-04	1.17E-04	1.17E-04	1.21E-04
⁶¹ Fe	2.21E-07	3.41E-07	3.50E-07	4.21E-07	4.30E-07	5.89E-07
⁶² Fe	1.50E-08	4.78E-08	4.86E-08	5.53E-08	5.63E-08	7.24E-08
⁶³ Fe	2.18E-10	3.66E-10	3.82E-10	5.16E-10	5.34E-10	8.72E-10
⁵⁰ Co	1.67E-73	1.23E-73	1.35E-73	1.19E-73	1.08E-73	1.28E-53
⁵¹ Co	7.86E-61	6.13E-61	6.73E-61	5.88E-61	5.98E-61	1.44E-44
⁵² Co	3.43E-57	2.93E-57	3.04E-57	2.65E-57	3.53E-56	2.73E-32
⁵³ Co	1.05E-36	1.08E-36	1.09E-36	5.82E-35	1.00E-26	1.02E-19
⁵⁴ Co	1.46E-34	8.10E-27	9.88E-27	1.49E-21	7.88E-16	9.54E-14
⁵⁵ Co	6.21E-12	1.91E-10	1.91E-10	4.33E-10	2.51E-05	5.41E-04
⁵⁶ Co	3.98E-13	1.84E-10	2.21E-10	2.60E-09	6.09E-07	8.91E-06
⁵⁷ Co	9.94E-10	1.84E-07	1.91E-07	6.72E-07	2.86E-06	3.14E-06
⁵⁸ Co	4.86E-10	3.24E-07	4.61E-07	6.76E-07	6.91E-07	6.97E-07
⁵⁹ Co	3.11E-05	9.13E-05	1.05E-04	1.15E-04	1.15E-04	1.15E-04
⁶⁰ Co	3.34E-06	1.01E-05	1.01E-05	1.02E-05	1.03E-05	1.04E-05
⁶¹ Co	1.49E-06	4.36E-05	4.49E-05	4.53E-05	4.54E-05	4.61E-05
⁶² Co	2.51E-07	2.01E-06	2.02E-06	2.07E-06	2.08E-06	2.21E-06
⁶³ Co	9.53E-08	8.64E-06	8.64E-06	8.68E-06	8.72E-06	8.90E-06
⁶⁴ Co	8.28E-14	1.01E-13	1.04E-13	1.15E-13	1.15E-13	1.28E-13
⁶⁵ Co	1.02E-09	4.19E-08	4.20E-08	4.31E-08	4.36E-08	4.65E-08
⁵¹ Ni	2.86E-89	1.77E-89	1.99E-89	1.76E-89	1.56E-89	1.62E-69

Table 2—Continued

Species	23e-0.8	23e-1.1	23e-1.2	23e-1.4	23e-1.5	23e-2.0
⁵² Ni	9.99E-77	6.81E-77	7.61E-77	6.49E-77	6.67E-77	1.16E-60
⁵³ Ni	2.16E-71	1.61E-71	1.67E-71	1.48E-71	1.34E-64	4.95E-47
⁵⁴ Ni	1.62E-50	1.34E-50	1.36E-50	1.21E-48	2.15E-39	7.36E-32
⁵⁵ Ni	9.49E-45	3.80E-37	3.38E-37	2.24E-32	3.10E-24	2.24E-19
⁵⁶ Ni	2.19E-19	2.98E-14	6.08E-14	7.02E-10	1.32E-03	2.83E-01
⁵⁷ Ni	5.70E-20	6.44E-14	1.50E-13	9.34E-10	2.09E-05	1.56E-03
⁵⁸ Ni	2.88E-04	3.12E-04	3.13E-04	3.26E-04	1.10E-03	1.01E-02
⁵⁹ Ni	1.99E-05	2.46E-05	2.57E-05	2.79E-05	2.95E-05	3.35E-05
⁶⁰ Ni	1.34E-04	1.59E-04	1.70E-04	2.47E-04	2.74E-04	2.84E-04
⁶¹ Ni	1.94E-05	2.42E-05	2.42E-05	2.44E-05	2.44E-05	2.44E-05
⁶² Ni	2.70E-05	5.70E-05	6.49E-05	8.55E-05	8.55E-05	8.91E-05
⁶³ Ni	5.25E-06	1.35E-05	1.36E-05	1.39E-05	1.40E-05	1.49E-05
⁶⁴ Ni	7.52E-06	3.42E-05	3.64E-05	3.77E-05	3.78E-05	3.85E-05
⁶⁵ Ni	2.28E-07	4.75E-07	4.81E-07	5.22E-07	5.28E-07	6.15E-07
⁶⁶ Ni	3.61E-08	3.56E-07	3.69E-07	3.83E-07	3.85E-07	4.13E-07
⁶⁷ Ni	9.27E-10	1.57E-09	1.62E-09	2.01E-09	2.06E-09	2.95E-09
⁵⁵ Cu	2.69E-78	1.81E-78	2.02E-78	1.77E-78	1.77E-78	6.27E-60
⁵⁶ Cu	3.80E-61	3.14E-61	3.25E-61	2.83E-61	1.34E-58	1.23E-34
⁵⁷ Cu	1.51E-36	1.38E-36	1.46E-36	1.36E-36	1.36E-29	1.27E-17
⁵⁸ Cu	4.33E-29	7.54E-25	7.52E-25	2.51E-23	1.45E-15	1.57E-08
⁵⁹ Cu	1.16E-12	7.74E-12	7.69E-12	7.45E-12	2.46E-11	4.41E-05
⁶⁰ Cu	2.86E-14	9.18E-12	9.28E-12	9.53E-12	2.31E-11	5.60E-05
⁶¹ Cu	1.72E-12	1.33E-10	1.36E-10	2.22E-10	3.81E-10	1.74E-06
⁶² Cu	4.91E-13	6.55E-10	6.76E-10	7.90E-10	8.00E-10	1.15E-07
⁶³ Cu	3.10E-06	3.44E-06	3.44E-06	3.42E-06	3.41E-06	3.35E-06
⁶⁴ Cu	4.12E-08	1.37E-07	1.38E-07	1.39E-07	1.38E-07	1.38E-07
⁶⁵ Cu	1.99E-06	4.27E-06	4.73E-06	4.90E-06	4.89E-06	4.94E-06
⁶⁶ Cu	8.28E-08	1.91E-07	1.91E-07	1.95E-07	1.95E-07	1.98E-07
⁶⁷ Cu	1.01E-07	1.47E-06	1.48E-06	1.49E-06	1.50E-06	1.54E-06
⁶⁸ Cu	1.81E-08	5.22E-08	5.27E-08	5.63E-08	5.72E-08	6.44E-08

Table 2—Continued

Species	23e-0.8	23e-1.1	23e-1.2	23e-1.4	23e-1.5	23e-2.0
⁶⁹ Cu	9.42E-09	1.67E-07	1.67E-07	1.70E-07	1.72E-07	1.82E-07
⁵⁷ Zn	1.87E-76	1.37E-76	1.59E-76	1.35E-76	7.27E-76	3.84E-50
⁵⁸ Zn	8.53E-52	7.07E-52	7.90E-52	7.12E-52	1.18E-47	3.65E-33
⁵⁹ Zn	1.01E-43	5.89E-41	4.91E-41	5.10E-41	7.80E-33	1.45E-20
⁶⁰ Zn	1.42E-20	7.47E-19	7.46E-19	6.33E-18	5.25E-12	1.27E-03
⁶¹ Zn	8.22E-22	6.66E-17	6.81E-17	1.10E-16	2.90E-13	2.64E-05
⁶² Zn	6.56E-19	2.74E-13	3.33E-13	7.54E-12	2.20E-10	6.55E-04
⁶³ Zn	2.46E-19	2.43E-13	2.94E-13	1.72E-12	2.25E-12	9.10E-08
⁶⁴ Zn	4.94E-06	5.37E-06	5.41E-06	5.39E-06	5.38E-06	5.31E-06
⁶⁵ Zn	2.37E-07	2.86E-07	2.86E-07	2.84E-07	2.82E-07	2.77E-07
⁶⁶ Zn	3.67E-06	4.31E-06	4.50E-06	4.76E-06	4.75E-06	4.77E-06
⁶⁷ Zn	6.96E-07	7.73E-07	7.73E-07	7.67E-07	7.66E-07	7.54E-07
⁶⁸ Zn	2.71E-06	3.76E-06	3.93E-06	4.09E-06	4.09E-06	4.09E-06
⁶⁹ Zn	7.81E-08	1.53E-07	1.54E-07	1.61E-07	1.62E-07	1.73E-07
⁷⁰ Zn	1.37E-07	7.80E-07	7.89E-07	8.00E-07	8.04E-07	8.30E-07
⁷¹ Zn	9.00E-09	1.62E-08	1.65E-08	1.88E-08	1.92E-08	2.40E-08
⁷² Zn	2.96E-09	2.09E-08	2.11E-08	2.24E-08	2.26E-08	2.55E-08
⁵⁹ Ga	8.90E-85	5.87E-85	7.24E-85	6.33E-85	6.39E-85	9.32E-67
⁶⁰ Ga	2.28E-68	2.01E-68	2.08E-68	1.85E-68	1.83E-68	6.49E-44
⁶¹ Ga	7.79E-40	6.96E-40	7.52E-40	6.73E-40	6.68E-40	1.02E-19
⁶² Ga	4.64E-39	1.05E-38	8.52E-39	9.74E-39	1.58E-36	5.20E-21
⁶³ Ga	3.81E-27	1.59E-23	1.59E-23	1.65E-23	3.95E-20	6.17E-08
⁶⁴ Ga	3.40E-26	8.07E-20	8.14E-20	1.23E-19	1.72E-18	5.16E-07
⁶⁵ Ga	4.11E-14	9.47E-13	9.42E-13	9.28E-13	9.18E-13	4.16E-08
⁶⁶ Ga	5.54E-16	9.39E-13	9.59E-13	9.89E-13	9.81E-13	6.59E-09
⁶⁷ Ga	1.29E-13	4.66E-11	4.82E-11	5.08E-11	5.08E-11	8.08E-11
⁶⁸ Ga	3.34E-14	2.00E-11	2.21E-11	2.41E-11	2.40E-11	2.40E-11
⁶⁹ Ga	2.95E-07	3.24E-07	3.25E-07	3.22E-07	3.21E-07	3.14E-07
⁷⁰ Ga	7.59E-09	1.31E-08	1.31E-08	1.32E-08	1.31E-08	1.33E-08
⁷¹ Ga	1.60E-07	2.13E-07	2.13E-07	2.12E-07	2.12E-07	2.09E-07

Table 2—Continued

Species	23e-0.8	23e-1.1	23e-1.2	23e-1.4	23e-1.5	23e-2.0
⁷² Ga	8.44E-09	1.49E-08	1.50E-08	1.50E-08	1.49E-08	1.47E-08
⁷³ Ga	1.72E-08	7.64E-08	7.67E-08	7.81E-08	7.84E-08	8.05E-08
⁷⁴ Ga	5.36E-09	1.04E-08	1.05E-08	1.12E-08	1.14E-08	1.25E-08
⁷⁵ Ga	4.25E-09	2.99E-08	3.00E-08	3.12E-08	3.16E-08	3.43E-08
⁶² Ge	2.49E-56	1.97E-56	2.37E-56	1.99E-56	1.98E-56	2.89E-36
⁶³ Ge	2.46E-46	7.26E-42	5.78E-42	6.42E-42	1.91E-39	1.78E-21
⁶⁴ Ge	2.93E-35	1.70E-28	1.79E-28	1.03E-25	7.74E-20	4.83E-06
⁶⁵ Ge	1.23E-33	1.97E-25	1.98E-25	2.60E-25	5.93E-22	2.03E-07
⁶⁶ Ge	3.85E-21	1.02E-17	1.13E-17	1.35E-17	1.79E-17	9.43E-06
⁶⁷ Ge	3.78E-23	9.36E-17	9.88E-17	1.07E-16	1.07E-16	5.75E-09
⁶⁸ Ge	7.32E-20	1.26E-11	1.92E-11	2.47E-11	2.47E-11	1.38E-09
⁶⁹ Ge	8.42E-18	1.58E-12	1.81E-12	1.98E-12	1.98E-12	2.31E-12
⁷⁰ Ge	2.93E-07	3.13E-07	3.17E-07	3.19E-07	3.18E-07	3.12E-07
⁷¹ Ge	1.95E-08	2.21E-08	2.21E-08	2.18E-08	2.17E-08	2.12E-08
⁷² Ge	3.71E-07	4.09E-07	4.15E-07	4.38E-07	4.37E-07	4.31E-07
⁷³ Ge	1.18E-07	1.32E-07	1.32E-07	1.31E-07	1.31E-07	1.29E-07
⁷⁴ Ge	5.46E-07	6.32E-07	6.50E-07	6.72E-07	6.70E-07	6.60E-07
⁷⁵ Ge	3.43E-08	5.95E-08	5.98E-08	6.19E-08	6.22E-08	6.53E-08
⁷⁶ Ge	2.62E-08	1.65E-07	1.69E-07	1.73E-07	1.74E-07	1.82E-07
⁷⁷ Ge	3.11E-09	5.47E-09	5.58E-09	6.38E-09	6.50E-09	8.12E-09
⁷⁸ Ge	1.02E-09	5.38E-09	5.45E-09	5.90E-09	5.98E-09	7.02E-09
⁶⁵ As	1.34E-54	1.28E-54	1.26E-54	1.19E-54	1.39E-54	9.48E-23
⁶⁶ As	3.32E-54	1.03E-50	7.01E-51	1.07E-50	1.33E-47	7.19E-24
⁶⁷ As	2.95E-31	1.26E-28	1.24E-28	1.17E-28	1.22E-28	1.22E-11
⁶⁸ As	1.50E-30	3.57E-25	3.57E-25	3.57E-25	3.50E-25	2.28E-10
⁶⁹ As	1.81E-27	7.52E-21	7.75E-21	8.21E-21	8.22E-21	5.66E-11
⁷⁰ As	1.72E-24	1.16E-17	1.19E-17	1.25E-17	1.25E-17	1.34E-10
⁷¹ As	2.32E-15	1.42E-13	1.42E-13	1.42E-13	1.40E-13	2.03E-12
⁷² As	9.49E-17	7.35E-14	7.38E-14	7.46E-14	7.35E-14	7.43E-14
⁷³ As	1.21E-14	1.22E-11	1.36E-11	1.97E-11	1.96E-11	2.01E-11

Table 2—Continued

Species	23e-0.8	23e-1.1	23e-1.2	23e-1.4	23e-1.5	23e-2.0
⁷⁴ As	3.40E-15	4.06E-12	4.29E-12	4.57E-12	4.56E-12	4.57E-12
⁷⁵ As	1.73E-11	1.88E-09	2.94E-09	4.00E-09	3.98E-09	3.98E-09
⁷⁶ As	6.99E-13	5.87E-11	5.97E-11	6.02E-11	6.02E-11	6.03E-11
⁷⁷ As	2.09E-12	2.33E-09	2.60E-09	2.65E-09	2.65E-09	2.69E-09
⁷⁸ As	9.08E-13	2.72E-11	2.73E-11	2.76E-11	2.77E-11	2.89E-11
⁷⁹ As	1.64E-13	1.25E-09	1.25E-09	1.25E-09	1.25E-09	1.25E-09
⁶⁸ Se	3.10E-39	2.89E-34	2.95E-34	6.41E-34	6.25E-29	3.39E-09
⁶⁹ Se	3.99E-38	9.77E-31	9.85E-31	1.03E-30	2.25E-30	1.85E-10
⁷⁰ Se	1.31E-34	5.54E-23	6.35E-23	8.21E-23	8.14E-23	5.73E-08
⁷¹ Se	1.46E-30	2.15E-21	2.31E-21	3.03E-21	3.00E-21	9.27E-11
⁷² Se	3.42E-22	9.69E-16	3.03E-15	4.50E-14	4.48E-14	1.62E-10
⁷³ Se	2.05E-23	2.19E-16	4.00E-16	2.21E-15	2.21E-15	1.58E-14
⁷⁴ Se	7.04E-21	2.70E-11	1.04E-10	6.20E-10	6.18E-10	6.65E-10
⁷⁵ Se	2.25E-21	2.18E-12	3.74E-12	8.59E-12	8.56E-12	8.83E-12
⁷⁶ Se	2.68E-17	2.02E-10	4.42E-10	1.39E-09	1.40E-09	1.59E-09
⁷⁷ Se	4.40E-17	5.91E-12	6.59E-12	7.84E-12	7.84E-12	8.21E-12
⁷⁸ Se	4.00E-16	1.66E-10	2.42E-10	3.30E-10	3.31E-10	3.71E-10
⁷⁹ Se	1.38E-15	1.62E-11	1.62E-11	1.62E-11	1.62E-11	1.63E-11
⁸⁰ Se	2.56E-17	2.89E-11	3.55E-11	4.01E-11	4.03E-11	4.36E-11
⁸¹ Se	1.43E-18	3.74E-13	3.74E-13	3.72E-13	3.72E-13	3.71E-13
⁸² Se	2.21E-19	7.50E-12	7.61E-12	7.79E-12	7.80E-12	8.01E-12
⁸³ Se	1.11E-20	9.02E-16	8.99E-16	8.93E-16	8.94E-16	8.87E-16
⁷⁰ Br	3.96E-59	9.54E-59	7.68E-59	8.27E-59	9.21E-59	1.40E-27
⁷¹ Br	3.05E-44	6.27E-36	6.32E-36	6.76E-36	6.65E-36	4.27E-14
⁷² Br	1.90E-38	1.74E-31	1.75E-31	1.86E-31	1.83E-31	5.96E-13
⁷³ Br	7.72E-30	5.32E-25	5.38E-25	5.94E-25	5.81E-25	5.62E-13
⁷⁴ Br	3.85E-31	1.08E-21	1.18E-21	2.80E-21	2.77E-21	2.88E-12
⁷⁵ Br	1.11E-28	3.99E-18	6.45E-18	3.11E-17	3.11E-17	2.86E-14
⁷⁶ Br	6.13E-29	1.98E-16	2.63E-16	5.67E-16	5.66E-16	9.12E-16
⁷⁷ Br	5.58E-27	2.03E-14	2.76E-14	8.83E-14	8.82E-14	9.98E-14

Table 2—Continued

Species	23e-0.8	23e-1.1	23e-1.2	23e-1.4	23e-1.5	23e-2.0
⁷⁸ Br	5.44E-27	5.19E-15	5.82E-15	7.51E-15	7.50E-15	8.05E-15
⁷⁹ Br	7.44E-25	1.08E-12	1.55E-12	2.02E-12	2.03E-12	2.32E-12
⁸⁰ Br	4.57E-25	1.24E-13	1.34E-13	1.44E-13	1.45E-13	1.55E-13
⁸¹ Br	2.76E-21	2.72E-12	3.81E-12	4.32E-12	4.34E-12	4.88E-12
⁸² Br	3.79E-23	4.75E-14	4.94E-14	5.16E-14	5.15E-14	5.44E-14
⁸³ Br	4.86E-23	1.17E-12	1.29E-12	1.38E-12	1.38E-12	1.50E-12
⁷² Kr	4.63E-53	1.35E-40	1.36E-40	1.56E-40	3.96E-38	1.60E-12
⁷³ Kr	8.18E-46	4.14E-36	4.18E-36	4.55E-36	4.58E-36	1.30E-12
⁷⁴ Kr	2.66E-37	9.85E-29	1.51E-28	9.10E-27	8.95E-27	3.42E-10
⁷⁵ Kr	1.33E-38	4.76E-26	5.67E-26	5.84E-25	5.77E-25	1.32E-12
⁷⁶ Kr	5.46E-36	1.81E-19	4.18E-19	6.80E-17	6.73E-17	2.87E-12
⁷⁷ Kr	2.95E-36	1.46E-19	3.13E-19	2.41E-17	2.37E-17	4.53E-15
⁷⁸ Kr	3.77E-34	3.54E-15	1.39E-14	4.78E-13	4.76E-13	5.50E-13
⁷⁹ Kr	1.79E-34	1.89E-15	3.95E-15	2.14E-14	2.15E-14	2.62E-14
⁸⁰ Kr	1.70E-27	5.39E-14	1.72E-13	1.21E-12	1.23E-12	1.63E-12
⁸¹ Kr	1.70E-29	1.40E-15	2.26E-15	4.88E-15	4.93E-15	6.28E-15
⁸² Kr	2.28E-27	4.96E-14	1.04E-13	2.75E-13	2.81E-13	3.99E-13
⁸³ Kr	1.47E-26	1.25E-15	1.39E-15	1.56E-15	1.57E-15	1.74E-15
⁸⁴ Kr	1.06E-28	1.05E-14	1.60E-14	2.46E-14	2.50E-14	3.42E-14
⁸⁵ Kr	3.42E-30	2.64E-17	2.71E-17	2.84E-17	2.84E-17	2.99E-17
⁸⁶ Kr	3.62E-31	7.50E-16	9.37E-16	1.14E-15	1.15E-15	1.41E-15
⁸⁷ Kr	3.73E-33	1.16E-21	1.16E-21	1.16E-21	1.16E-21	1.15E-21

Table 3. Detailed Yields (M_{\odot}) Before Radioactive Decay For Piston Simulations

Species	23p-0.9	23p-1.2	23p-1.6
^1H	1.46E+00	1.46E+00	1.46E+00
^2H	1.75E-16	1.67E-16	1.89E-16
^3H	6.77E-18	1.77E-16	1.75E-16
^3He	6.60E-05	6.60E-05	6.60E-05
^4He	1.13E+00	1.13E+00	1.15E+00
^6Li	1.26E-18	4.24E-18	7.05E-18
^7Li	2.89E-10	2.89E-10	2.89E-10
^7Be	1.28E-10	1.28E-10	1.28E-10
^8Be	3.29E-15	1.82E-08	1.68E-06
^9Be	8.77E-19	2.52E-19	1.69E-19
^8B	1.80E-20	1.80E-20	1.80E-20
^{10}B	3.74E-11	3.74E-11	3.74E-11
^{11}B	2.18E-11	2.26E-11	2.26E-11
^{11}C	2.49E-18	1.65E-17	1.77E-17
^{12}C	4.83E-01	4.86E-01	4.82E-01
^{13}C	4.29E-04	4.25E-04	4.23E-04
^{14}C	1.08E-06	1.61E-06	1.51E-06
^{12}N	9.79E-32	3.46E-34	3.87E-35
^{13}N	1.37E-07	1.58E-07	1.67E-07
^{14}N	1.44E-02	1.44E-02	1.44E-02
^{15}N	6.03E-06	6.19E-06	6.24E-06
^{14}O	6.57E-12	6.05E-12	5.86E-12
^{15}O	5.28E-10	6.71E-10	7.17E-10
^{16}O	3.17E+00	4.28E+00	4.21E+00
^{17}O	5.40E-04	5.40E-04	5.40E-04
^{18}O	1.01E-04	9.94E-05	9.80E-05
^{19}O	2.78E-10	3.00E-10	3.22E-10
^{17}F	2.82E-11	1.57E-10	1.72E-10
^{18}F	4.22E-06	4.85E-06	5.40E-06
^{19}F	9.00E-06	8.90E-06	8.78E-06

Table 3—Continued

Species	23p-0.9	23p-1.2	23p-1.6
²⁰ F	1.71E-08	1.34E-08	1.29E-08
²¹ F	9.58E-11	4.51E-11	3.79E-11
¹⁷ Ne	1.97E-56	4.58E-63	1.27E-66
¹⁸ Ne	2.26E-18	2.64E-19	9.94E-20
¹⁹ Ne	1.49E-11	1.32E-11	1.27E-11
²⁰ Ne	3.61E-01	3.78E-01	3.83E-01
²¹ Ne	5.22E-03	5.14E-03	5.02E-03
²² Ne	6.24E-02	6.16E-02	6.03E-02
²³ Ne	1.29E-05	1.20E-05	1.17E-05
²⁴ Ne	7.97E-10	8.29E-10	8.50E-10
¹⁹ Na	2.62E-40	3.11E-43	1.65E-44
²⁰ Na	1.67E-22	3.30E-25	4.54E-27
²¹ Na	4.26E-08	3.85E-08	4.07E-08
²² Na	1.77E-06	1.90E-06	1.83E-06
²³ Na	8.56E-03	8.82E-03	8.58E-03
²⁴ Na	4.83E-05	5.54E-05	5.79E-05
²⁵ Na	6.37E-07	6.87E-07	7.66E-07
²⁶ Na	6.00E-12	1.31E-13	2.27E-14
²⁷ Na	7.52E-20	6.90E-24	1.25E-25
²⁰ Mg	1.47E-53	1.10E-58	8.26E-61
²¹ Mg	1.28E-33	1.62E-38	4.37E-41
²² Mg	1.86E-13	6.28E-14	4.22E-14
²³ Mg	9.60E-07	1.87E-06	1.59E-06
²⁴ Mg	5.83E-02	8.16E-02	8.42E-02
²⁵ Mg	1.09E-02	1.34E-02	1.40E-02
²⁶ Mg	1.75E-02	2.02E-02	2.00E-02
²⁷ Mg	5.33E-06	7.56E-06	8.39E-06
²⁸ Mg	7.65E-08	1.05E-07	1.31E-07
²⁹ Mg	5.55E-13	2.20E-14	6.03E-15
²² Al	8.02E-63	7.89E-73	3.38E-77

Table 3—Continued

Species	23p-0.9	23p-1.2	23p-1.6
²³ Al	5.89E-31	2.94E-32	6.34E-33
²⁴ Al	1.69E-18	2.12E-19	8.15E-20
²⁵ Al	5.38E-07	2.81E-07	2.12E-07
²⁶ Al	1.73E-05	2.82E-05	2.96E-05
²⁷ Al	1.17E-03	2.61E-03	2.59E-03
²⁸ Al	1.72E-05	4.55E-05	4.75E-05
²⁹ Al	6.77E-07	1.55E-06	1.76E-06
³⁰ Al	6.27E-10	2.65E-10	2.26E-10
³¹ Al	6.36E-14	1.79E-15	4.16E-16
²³ Si	2.55E-81	1.13E-93	2.02E-98
²⁴ Si	5.69E-40	3.83E-44	5.76E-46
²⁵ Si	3.20E-29	3.82E-33	1.63E-34
²⁶ Si	3.37E-13	4.83E-14	1.97E-14
²⁷ Si	1.88E-08	1.30E-07	8.39E-08
²⁸ Si	5.80E-03	3.62E-01	4.39E-01
²⁹ Si	7.22E-04	5.88E-03	5.83E-03
³⁰ Si	3.17E-04	1.25E-02	1.23E-02
³¹ Si	1.02E-05	4.73E-05	4.91E-05
³² Si	2.15E-07	2.86E-06	2.91E-06
³³ Si	1.61E-10	1.05E-10	1.21E-10
³⁴ Si	1.38E-13	4.40E-14	4.00E-14
²⁷ P	2.74E-27	3.45E-31	7.62E-33
²⁸ P	7.16E-21	3.74E-24	2.29E-25
²⁹ P	5.27E-10	1.93E-10	1.57E-10
³⁰ P	4.48E-08	2.54E-06	2.52E-06
³¹ P	6.02E-05	1.64E-03	1.62E-03
³² P	5.20E-07	1.27E-05	1.25E-05
³³ P	1.33E-06	1.24E-05	1.23E-05
³⁴ P	1.59E-08	2.55E-08	2.38E-08
³⁵ P	6.06E-10	1.76E-09	1.86E-09

Table 3—Continued

Species	23p-0.9	23p-1.2	23p-1.6
³⁶ P	1.39E-13	9.21E-14	1.14E-13
³⁷ P	2.47E-18	3.62E-20	6.14E-21
³⁸ P	1.72E-28	1.91E-33	3.25E-35
²⁸ S	2.32E-42	5.30E-47	1.93E-50
²⁹ S	4.91E-32	2.98E-37	3.14E-39
³⁰ S	2.41E-17	1.88E-17	5.54E-17
³¹ S	7.52E-13	4.80E-09	2.82E-09
³² S	2.34E-03	1.79E-01	2.38E-01
³³ S	1.01E-04	4.88E-04	4.92E-04
³⁴ S	1.36E-04	1.19E-02	1.23E-02
³⁵ S	4.07E-06	1.31E-05	1.32E-05
³⁶ S	3.44E-06	2.28E-05	2.26E-05
³⁷ S	5.83E-09	6.95E-09	8.90E-09
³⁸ S	5.13E-11	6.74E-11	9.71E-11
³⁹ S	1.20E-13	1.17E-13	1.65E-13
⁴⁰ S	1.05E-15	1.14E-15	1.85E-15
⁴¹ S	7.16E-22	7.20E-24	1.00E-24
⁴² S	6.76E-23	8.44E-24	6.22E-24
³¹ Cl	7.31E-33	8.83E-35	1.96E-32
³² Cl	1.38E-25	1.60E-29	1.16E-28
³³ Cl	1.30E-10	2.55E-11	1.65E-11
³⁴ Cl	1.43E-11	4.32E-10	2.48E-10
³⁵ Cl	4.36E-05	1.63E-04	1.67E-04
³⁶ Cl	1.72E-06	2.86E-06	2.82E-06
³⁷ Cl	5.03E-05	6.47E-05	6.47E-05
³⁸ Cl	4.68E-07	6.01E-07	6.84E-07
³⁹ Cl	4.65E-08	8.76E-08	1.03E-07
⁴⁰ Cl	7.64E-10	1.04E-09	1.45E-09
⁴¹ Cl	4.14E-11	7.65E-11	1.03E-10
⁴² Cl	3.24E-13	2.75E-13	4.04E-13

Table 3—Continued

Species	23p-0.9	23p-1.2	23p-1.6
⁴³ Cl	1.09E-14	2.05E-14	3.79E-14
⁴⁴ Cl	1.30E-21	4.43E-24	3.26E-25
⁴⁵ Cl	3.74E-21	6.48E-22	6.76E-22
³² Ar	1.56E-46	4.93E-50	7.25E-44
³³ Ar	2.04E-37	4.12E-43	3.41E-43
³⁴ Ar	5.69E-18	1.97E-19	4.98E-17
³⁵ Ar	3.56E-16	7.45E-12	1.42E-11
³⁶ Ar	5.13E-04	2.78E-02	4.33E-02
³⁷ Ar	3.22E-06	4.47E-05	4.57E-05
³⁸ Ar	1.26E-04	7.87E-03	8.14E-03
³⁹ Ar	3.54E-06	4.65E-06	4.84E-06
⁴⁰ Ar	7.39E-07	2.83E-06	2.87E-06
⁴¹ Ar	1.29E-08	2.46E-08	2.79E-08
⁴² Ar	7.02E-10	1.48E-08	1.50E-08
⁴³ Ar	8.83E-12	1.57E-11	2.19E-11
⁴⁴ Ar	2.13E-13	1.19E-12	1.39E-12
⁴⁵ Ar	1.09E-15	1.51E-15	2.61E-15
⁴⁶ Ar	7.74E-18	1.71E-17	2.05E-17
³⁵ K	2.59E-36	8.27E-41	8.01E-38
³⁶ K	5.91E-30	1.56E-33	5.40E-27
³⁷ K	7.51E-13	3.97E-14	1.21E-14
³⁸ K	4.36E-12	4.04E-09	1.08E-08
³⁹ K	2.62E-05	1.39E-04	1.54E-04
⁴⁰ K	1.59E-06	1.83E-06	1.80E-06
⁴¹ K	4.12E-06	5.02E-06	4.97E-06
⁴² K	3.18E-07	7.60E-07	7.87E-07
⁴³ K	1.23E-07	6.48E-07	6.76E-07
⁴⁴ K	1.22E-08	1.61E-07	1.67E-07
⁴⁵ K	1.84E-09	1.40E-07	1.44E-07
⁴⁶ K	3.46E-11	7.97E-09	8.05E-09

Table 3—Continued

Species	23p-0.9	23p-1.2	23p-1.6
⁴⁷ K	3.60E-13	4.81E-10	4.48E-10
⁴⁸ K	3.30E-16	2.47E-16	3.96E-16
⁴⁹ K	1.04E-18	3.37E-19	3.98E-19
³⁶ Ca	7.81E-45	8.84E-50	4.29E-51
³⁷ Ca	4.09E-41	7.96E-47	2.85E-44
³⁸ Ca	5.02E-22	5.40E-25	5.16E-23
³⁹ Ca	4.90E-20	1.57E-15	9.40E-15
⁴⁰ Ca	4.26E-04	1.73E-02	3.53E-02
⁴¹ Ca	1.29E-05	1.69E-05	1.67E-05
⁴² Ca	6.45E-06	3.06E-04	3.14E-04
⁴³ Ca	1.26E-06	1.80E-06	1.81E-06
⁴⁴ Ca	1.05E-05	1.57E-05	1.55E-05
⁴⁵ Ca	4.84E-07	1.20E-06	1.23E-06
⁴⁶ Ca	1.09E-07	1.63E-06	1.64E-06
⁴⁷ Ca	5.80E-09	1.63E-07	1.66E-07
⁴⁸ Ca	1.02E-06	1.20E-06	1.19E-06
⁴⁹ Ca	1.70E-09	1.94E-09	2.31E-09
⁴⁰ Sc	5.20E-35	1.83E-39	6.46E-31
⁴¹ Sc	1.69E-16	9.42E-19	5.67E-20
⁴² Sc	3.62E-16	3.41E-18	4.18E-17
⁴³ Sc	1.33E-10	1.63E-09	1.04E-06
⁴⁴ Sc	5.86E-11	1.31E-08	1.32E-08
⁴⁵ Sc	4.89E-07	8.03E-07	7.86E-07
⁴⁶ Sc	1.06E-07	3.97E-07	3.91E-07
⁴⁷ Sc	3.39E-08	5.91E-07	5.90E-07
⁴⁸ Sc	1.02E-08	3.15E-07	3.13E-07
⁴⁹ Sc	1.19E-09	1.57E-07	1.56E-07
⁵⁰ Sc	1.86E-11	1.35E-10	1.37E-10
⁵¹ Sc	2.46E-13	3.59E-12	3.18E-12
⁴¹ Ti	3.33E-48	1.63E-55	4.02E-47

Table 3—Continued

Species	23p-0.9	23p-1.2	23p-1.6
⁴² Ti	3.61E-28	9.41E-33	3.79E-35
⁴³ Ti	4.07E-23	1.49E-25	9.97E-20
⁴⁴ Ti	2.42E-12	6.55E-06	2.35E-04
⁴⁵ Ti	1.64E-13	1.85E-07	2.00E-07
⁴⁶ Ti	1.82E-06	2.99E-04	3.10E-04
⁴⁷ Ti	1.72E-06	4.30E-06	4.35E-06
⁴⁸ Ti	1.74E-05	2.35E-05	2.35E-05
⁴⁹ Ti	4.07E-06	4.43E-06	4.42E-06
⁵⁰ Ti	2.37E-06	5.56E-06	5.62E-06
⁵¹ Ti	4.86E-08	9.12E-08	1.01E-07
⁵² Ti	2.09E-09	1.95E-08	1.97E-08
⁵³ Ti	2.44E-11	3.15E-11	4.63E-11
⁴³ V	1.43E-44	3.32E-50	2.29E-53
⁴⁴ V	4.72E-38	3.79E-44	2.43E-36
⁴⁵ V	7.05E-24	8.71E-26	5.19E-18
⁴⁶ V	2.53E-25	1.12E-20	4.45E-21
⁴⁷ V	8.76E-12	8.19E-08	1.21E-06
⁴⁸ V	1.58E-11	2.80E-07	3.50E-07
⁴⁹ V	2.72E-09	5.65E-07	6.17E-07
⁵⁰ V	6.56E-09	5.85E-08	6.01E-08
⁵¹ V	2.42E-06	3.33E-06	3.31E-06
⁵² V	2.05E-07	3.81E-07	3.92E-07
⁵³ V	2.94E-08	3.02E-07	3.01E-07
⁵⁴ V	8.00E-10	1.47E-09	1.67E-09
⁵⁵ V	4.69E-12	2.82E-12	1.45E-12
⁴⁴ Cr	1.77E-57	5.77E-66	5.59E-70
⁴⁵ Cr	4.45E-51	4.98E-59	2.38E-53
⁴⁶ Cr	2.61E-36	3.63E-36	4.35E-32
⁴⁷ Cr	9.88E-29	4.58E-21	4.16E-16
⁴⁸ Cr	1.36E-16	5.70E-05	5.43E-04

Table 3—Continued

Species	23p-0.9	23p-1.2	23p-1.6
⁴⁹ Cr	5.56E-16	2.33E-06	7.50E-06
⁵⁰ Cr	4.28E-06	7.39E-04	9.15E-04
⁵¹ Cr	3.76E-07	7.52E-06	7.90E-06
⁵² Cr	9.94E-05	1.90E-04	1.94E-04
⁵³ Cr	1.62E-05	1.63E-05	1.60E-05
⁵⁴ Cr	9.91E-06	2.28E-05	2.29E-05
⁵⁵ Cr	3.69E-07	5.16E-07	5.84E-07
⁵⁶ Cr	3.57E-08	1.60E-07	1.71E-07
⁵⁷ Cr	3.93E-11	7.01E-12	4.50E-12
⁵⁸ Cr	8.62E-12	6.45E-12	8.33E-12
⁴⁶ Mn	1.26E-68	6.37E-78	3.80E-72
⁴⁷ Mn	5.54E-54	2.42E-63	6.79E-55
⁴⁸ Mn	3.58E-48	3.67E-54	1.50E-34
⁴⁹ Mn	6.09E-32	1.15E-25	9.31E-21
⁵⁰ Mn	6.06E-29	1.43E-20	3.94E-22
⁵¹ Mn	4.25E-12	6.12E-06	2.16E-05
⁵² Mn	3.44E-12	6.71E-07	4.61E-06
⁵³ Mn	4.03E-09	6.00E-06	9.56E-06
⁵⁴ Mn	1.79E-08	1.12E-07	1.12E-07
⁵⁵ Mn	7.67E-05	7.80E-05	7.64E-05
⁵⁶ Mn	4.76E-06	6.52E-06	6.64E-06
⁵⁷ Mn	1.62E-06	1.04E-05	1.04E-05
⁵⁸ Mn	4.51E-08	5.16E-08	3.99E-08
⁵⁹ Mn	1.35E-08	1.11E-07	9.18E-08
⁶⁰ Mn	6.63E-11	2.65E-11	2.85E-11
⁶¹ Mn	2.81E-12	4.85E-13	3.52E-13
⁴⁷ Fe	1.01E-82	3.96E-95	4.48E-91
⁴⁸ Fe	3.06E-69	5.92E-82	1.95E-73
⁴⁹ Fe	5.16E-63	2.57E-69	4.14E-53
⁵⁰ Fe	7.83E-48	3.34E-50	2.21E-39

Table 3—Continued

Species	23p-0.9	23p-1.2	23p-1.6
⁵¹ Fe	1.15E-37	3.53E-28	3.61E-28
⁵² Fe	9.88E-18	6.17E-04	8.95E-03
⁵³ Fe	3.06E-17	2.24E-05	1.42E-04
⁵⁴ Fe	4.40E-04	1.70E-02	3.34E-02
⁵⁵ Fe	3.22E-05	9.27E-05	9.70E-05
⁵⁶ Fe	7.66E-03	8.53E-03	8.44E-03
⁵⁷ Fe	8.22E-04	8.59E-04	8.54E-04
⁵⁸ Fe	2.93E-04	1.24E-03	1.25E-03
⁵⁹ Fe	3.55E-05	7.08E-05	7.65E-05
⁶⁰ Fe	7.18E-06	1.15E-04	1.17E-04
⁶¹ Fe	2.52E-07	3.45E-07	4.85E-07
⁶² Fe	1.67E-08	4.43E-08	5.49E-08
⁶³ Fe	2.21E-10	2.39E-10	3.77E-10
⁵⁰ Co	1.28E-79	3.22E-91	7.63E-73
⁵¹ Co	8.23E-65	2.86E-75	2.27E-60
⁵² Co	8.12E-61	2.32E-66	3.19E-48
⁵³ Co	1.25E-38	3.67E-33	7.02E-25
⁵⁴ Co	2.32E-32	4.88E-23	1.16E-25
⁵⁵ Co	1.80E-10	8.38E-05	5.76E-04
⁵⁶ Co	6.12E-11	1.02E-06	2.03E-05
⁵⁷ Co	9.17E-08	2.95E-06	3.64E-06
⁵⁸ Co	5.05E-08	6.89E-07	6.94E-07
⁵⁹ Co	3.65E-05	1.12E-04	1.12E-04
⁶⁰ Co	4.85E-06	9.92E-06	9.96E-06
⁶¹ Co	2.56E-06	4.44E-05	4.44E-05
⁶² Co	4.50E-07	1.91E-06	1.97E-06
⁶³ Co	1.73E-07	6.95E-06	6.59E-06
⁶⁴ Co	2.24E-15	1.12E-18	9.68E-20
⁶⁵ Co	1.44E-09	2.11E-08	1.79E-08
⁵¹ Ni	1.09E-96	1.03-111	2.35E-93

Table 3—Continued

Species	23p-0.9	23p-1.2	23p-1.6
⁵² Ni	6.46E-82	5.07E-95	7.18E-81
⁵³ Ni	3.66E-77	3.25E-82	4.36E-68
⁵⁴ Ni	2.69E-54	3.95E-51	1.61E-44
⁵⁵ Ni	2.68E-42	7.19E-32	4.29E-33
⁵⁶ Ni	2.22E-16	6.62E-03	6.13E-01
⁵⁷ Ni	5.49E-16	6.06E-05	4.35E-03
⁵⁸ Ni	3.14E-04	1.46E-03	2.74E-02
⁵⁹ Ni	2.27E-05	2.97E-05	6.22E-05
⁶⁰ Ni	1.48E-04	2.85E-04	3.11E-04
⁶¹ Ni	2.24E-05	2.42E-05	2.41E-05
⁶² Ni	3.11E-05	8.77E-05	9.17E-05
⁶³ Ni	6.95E-06	1.50E-05	1.60E-05
⁶⁴ Ni	8.70E-06	3.68E-05	3.72E-05
⁶⁵ Ni	2.99E-07	5.02E-07	5.83E-07
⁶⁶ Ni	4.78E-08	3.75E-07	3.96E-07
⁶⁷ Ni	1.01E-09	1.16E-09	1.59E-09
⁵⁵ Cu	6.65E-84	4.18E-96	2.30E-80
⁵⁶ Cu	3.37E-65	2.96E-70	1.05E-53
⁵⁷ Cu	1.25E-37	2.03E-35	2.35E-20
⁵⁸ Cu	2.89E-25	1.15E-15	5.97E-09
⁵⁹ Cu	8.90E-12	6.50E-11	1.53E-04
⁶⁰ Cu	6.93E-12	3.96E-11	4.97E-04
⁶¹ Cu	8.17E-11	4.16E-10	1.62E-05
⁶² Cu	4.55E-11	8.06E-10	1.04E-06
⁶³ Cu	3.40E-06	3.40E-06	3.34E-06
⁶⁴ Cu	9.72E-08	1.35E-07	1.33E-07
⁶⁵ Cu	2.23E-06	4.87E-06	4.91E-06
⁶⁶ Cu	1.41E-07	1.86E-07	1.86E-07
⁶⁷ Cu	1.87E-07	1.47E-06	1.48E-06
⁶⁸ Cu	2.98E-08	4.38E-08	4.72E-08

Table 3—Continued

Species	23p-0.9	23p-1.2	23p-1.6
⁶⁹ Cu	1.86E-08	1.60E-07	1.64E-07
⁵⁷ Zn	3.22E-82	6.48E-92	1.44E-74
⁵⁸ Zn	1.09E-54	3.72E-59	4.59E-41
⁵⁹ Zn	5.92E-43	7.09E-40	1.74E-29
⁶⁰ Zn	8.80E-19	3.34E-11	4.90E-03
⁶¹ Zn	1.34E-17	1.10E-12	1.03E-04
⁶² Zn	1.12E-15	3.86E-10	2.64E-03
⁶³ Zn	3.75E-16	2.65E-12	4.39E-07
⁶⁴ Zn	5.35E-06	5.37E-06	5.50E-06
⁶⁵ Zn	2.79E-07	2.82E-07	2.79E-07
⁶⁶ Zn	4.02E-06	4.83E-06	4.84E-06
⁶⁷ Zn	7.72E-07	7.62E-07	7.49E-07
⁶⁸ Zn	3.06E-06	4.03E-06	4.02E-06
⁶⁹ Zn	1.18E-07	1.59E-07	1.71E-07
⁷⁰ Zn	1.85E-07	7.78E-07	7.94E-07
⁷¹ Zn	1.19E-08	1.62E-08	2.06E-08
⁷² Zn	3.98E-09	2.13E-08	2.35E-08
⁵⁹ Ga	3.36E-90	5.23E-103	2.50E-86
⁶⁰ Ga	5.77E-72	2.72E-80	2.63E-57
⁶¹ Ga	1.76E-41	6.12E-46	8.04E-25
⁶² Ga	1.17E-40	7.35E-45	5.42E-26
⁶³ Ga	5.89E-24	1.05E-19	2.17E-07
⁶⁴ Ga	7.23E-22	3.05E-18	4.31E-06
⁶⁵ Ga	9.58E-13	9.12E-13	4.00E-07
⁶⁶ Ga	3.33E-13	9.77E-13	6.32E-08
⁶⁷ Ga	2.01E-11	5.02E-11	3.54E-10
⁶⁸ Ga	6.20E-12	2.39E-11	2.36E-11
⁶⁹ Ga	3.15E-07	3.21E-07	3.14E-07
⁷⁰ Ga	1.18E-08	1.28E-08	1.27E-08
⁷¹ Ga	1.76E-07	2.10E-07	2.07E-07

Table 3—Continued

Species	23p-0.9	23p-1.2	23p-1.6
⁷² Ga	1.42E-08	1.46E-08	1.42E-08
⁷³ Ga	2.83E-08	7.62E-08	7.71E-08
⁷⁴ Ga	8.17E-09	1.07E-08	1.19E-08
⁷⁵ Ga	6.75E-09	2.85E-08	3.04E-08
⁶² Ge	1.00E-59	4.52E-68	7.63E-47
⁶³ Ge	5.27E-44	1.08E-46	1.49E-34
⁶⁴ Ge	6.75E-31	4.45E-19	1.85E-05
⁶⁵ Ge	3.77E-28	1.64E-21	7.67E-07
⁶⁶ Ge	1.92E-18	2.45E-17	3.98E-05
⁶⁷ Ge	1.08E-18	1.12E-16	2.60E-08
⁶⁸ Ge	2.54E-15	2.67E-11	5.62E-09
⁶⁹ Ge	2.06E-15	2.03E-12	6.31E-12
⁷⁰ Ge	3.10E-07	3.19E-07	3.13E-07
⁷¹ Ge	2.19E-08	2.17E-08	2.11E-08
⁷² Ge	4.00E-07	4.36E-07	4.30E-07
⁷³ Ge	1.32E-07	1.30E-07	1.28E-07
⁷⁴ Ge	5.96E-07	6.62E-07	6.52E-07
⁷⁵ Ge	5.09E-08	6.09E-08	6.44E-08
⁷⁶ Ge	3.93E-08	1.66E-07	1.73E-07
⁷⁷ Ge	4.12E-09	5.74E-09	7.37E-09
⁷⁸ Ge	1.38E-09	5.46E-09	6.33E-09
⁶⁵ As	5.37E-56	8.08E-60	1.08E-28
⁶⁶ As	4.79E-55	4.24E-59	4.21E-29
⁶⁷ As	1.59E-28	1.42E-28	5.14E-11
⁶⁸ As	2.22E-25	3.49E-25	2.07E-09
⁶⁹ As	8.46E-22	8.34E-21	4.83E-10
⁷⁰ As	5.90E-21	1.28E-17	1.27E-09
⁷¹ As	1.31E-13	1.37E-13	1.88E-11
⁷² As	3.79E-14	7.16E-14	8.16E-14
⁷³ As	2.54E-12	2.03E-11	2.06E-11

Table 3—Continued

Species	23p-0.9	23p-1.2	23p-1.6
⁷⁴ As	1.26E-12	4.44E-12	4.33E-12
⁷⁵ As	4.40E-11	3.92E-09	3.97E-09
⁷⁶ As	7.05E-12	5.78E-11	5.61E-11
⁷⁷ As	1.57E-11	2.59E-09	2.61E-09
⁷⁸ As	4.48E-12	3.30E-11	3.58E-11
⁷⁹ As	1.23E-11	1.24E-09	1.20E-09
⁶⁸ Se	3.14E-35	4.61E-28	1.42E-08
⁶⁹ Se	8.73E-32	5.05E-30	7.15E-10
⁷⁰ Se	1.44E-27	9.72E-23	2.38E-07
⁷¹ Se	2.31E-26	3.38E-21	3.98E-10
⁷² Se	5.11E-18	5.33E-14	6.68E-10
⁷³ Se	1.30E-18	2.57E-15	1.81E-13
⁷⁴ Se	2.22E-16	6.96E-10	7.59E-10
⁷⁵ Se	1.84E-16	9.01E-12	9.28E-12
⁷⁶ Se	1.73E-15	1.67E-09	1.92E-09
⁷⁷ Se	3.33E-15	8.11E-12	8.28E-12
⁷⁸ Se	9.38E-15	3.78E-10	4.09E-10
⁷⁹ Se	1.92E-13	3.10E-11	3.37E-11
⁸⁰ Se	4.37E-15	4.49E-11	4.68E-11
⁸¹ Se	1.15E-15	3.81E-13	3.65E-13
⁸² Se	5.56E-16	8.28E-12	8.09E-12
⁸³ Se	8.47E-18	9.45E-16	8.66E-16
⁷⁰ Br	2.45E-60	1.20E-64	7.40E-33
⁷¹ Br	4.76E-38	5.78E-36	1.58E-13
⁷² Br	3.97E-34	1.80E-31	4.87E-12
⁷³ Br	3.50E-25	6.06E-25	3.86E-12
⁷⁴ Br	1.30E-24	3.31E-21	2.78E-11
⁷⁵ Br	5.51E-22	3.88E-17	2.75E-13
⁷⁶ Br	6.10E-22	6.47E-16	3.76E-15
⁷⁷ Br	3.31E-20	1.13E-13	1.31E-13

Table 3—Continued

Species	23p-0.9	23p-1.2	23p-1.6
⁷⁸ Br	2.51E-20	8.04E-15	8.41E-15
⁷⁹ Br	2.43E-19	2.41E-12	2.64E-12
⁸⁰ Br	2.97E-19	1.48E-13	1.51E-13
⁸¹ Br	4.70E-18	4.88E-12	5.20E-12
⁸² Br	4.63E-19	5.14E-14	5.12E-14
⁸³ Br	1.66E-18	1.48E-12	1.51E-12
⁷² Kr	4.67E-45	2.62E-37	4.76E-12
⁷³ Kr	1.42E-40	4.18E-36	4.62E-12
⁷⁴ Kr	1.94E-31	1.32E-26	1.45E-09
⁷⁵ Kr	8.24E-31	8.01E-25	5.53E-12
⁷⁶ Kr	5.06E-27	8.55E-17	1.24E-11
⁷⁷ Kr	3.18E-27	3.14E-17	4.42E-14
⁷⁸ Kr	1.79E-24	6.61E-13	8.41E-13
⁷⁹ Kr	2.15E-24	3.15E-14	3.87E-14
⁸⁰ Kr	1.97E-21	1.99E-12	2.70E-12
⁸¹ Kr	2.28E-23	7.28E-15	9.15E-15
⁸² Kr	1.15E-22	4.79E-13	6.63E-13
⁸³ Kr	1.49E-21	2.74E-15	3.12E-15
⁸⁴ Kr	9.81E-23	3.92E-14	4.98E-14
⁸⁵ Kr	3.21E-23	2.95E-17	2.86E-17
⁸⁶ Kr	2.68E-23	1.57E-15	1.75E-15
⁸⁷ Kr	7.51E-26	1.24E-21	1.13E-21

Table 4. Detailed Yields (M_{\odot}) Before Radioactive Decay For Delayed Thermal Bombs

Species	d0.2s0.8	d0.2s1.5	d0.7s0.8	d0.7s1.5
^1H	1.47E+00	1.47E+00	1.47E+00	1.47E+00
^2H	3.03E-16	4.79E-16	3.86E-16	5.27E-16
^3H	1.63E-16	1.66E-16	1.52E-16	1.66E-16
^3He	6.63E-05	6.63E-05	6.63E-05	6.63E-05
^4He	1.13E+00	1.12E+00	1.13E+00	1.13E+00
^6Li	1.45E-18	2.45E-18	1.79E-18	2.53E-18
^7Li	2.90E-10	2.90E-10	2.90E-10	2.90E-10
^7Be	1.29E-10	1.29E-10	1.29E-10	1.29E-10
^8Be	2.48E-10	1.56E-07	4.96E-11	9.19E-08
^9Be	8.50E-19	1.19E-18	7.24E-19	9.68E-19
^8B	1.81E-20	1.81E-20	1.81E-20	1.81E-20
^{10}B	3.76E-11	3.76E-11	3.76E-11	3.76E-11
^{11}B	2.30E-11	2.29E-11	2.28E-11	2.27E-11
^{11}C	1.77E-17	1.83E-17	1.78E-17	1.78E-17
^{12}C	4.94E-01	4.86E-01	4.94E-01	4.89E-01
^{13}C	4.34E-04	4.28E-04	4.35E-04	4.30E-04
^{14}C	1.70E-06	1.58E-06	1.68E-06	1.60E-06
^{12}N	7.77E-32	2.03E-31	7.06E-32	1.47E-31
^{13}N	1.19E-07	1.52E-07	1.21E-07	1.44E-07
^{14}N	1.44E-02	1.44E-02	1.44E-02	1.44E-02
^{15}N	5.91E-06	6.28E-06	5.95E-06	6.25E-06
^{14}O	6.45E-12	6.48E-12	6.75E-12	6.73E-12
^{15}O	4.97E-10	7.10E-10	5.28E-10	7.02E-10
^{16}O	4.42E+00	4.31E+00	4.63E+00	4.61E+00
^{17}O	5.43E-04	5.43E-04	5.44E-04	5.43E-04
^{18}O	1.03E-04	9.86E-05	1.02E-04	9.86E-05
^{19}O	2.19E-10	3.56E-10	2.10E-10	3.18E-10
^{17}F	3.00E-12	4.31E-12	2.17E-12	2.92E-12
^{18}F	3.51E-06	4.98E-06	3.45E-06	4.65E-06
^{19}F	9.15E-06	8.85E-06	9.09E-06	8.84E-06

Table 4—Continued

Species	d0.2s0.8	d0.2s1.5	d0.7s0.8	d0.7s1.5
²⁰ F	1.65E-08	2.30E-08	1.79E-08	2.34E-08
²¹ F	1.09E-10	1.97E-10	1.31E-10	2.10E-10
¹⁷ Ne	1.60E-54	4.04E-53	8.13E-54	4.10E-53
¹⁸ Ne	5.04E-18	4.85E-18	6.22E-18	5.83E-18
¹⁹ Ne	1.31E-11	1.87E-11	1.40E-11	1.86E-11
²⁰ Ne	3.59E-01	3.76E-01	3.64E-01	3.79E-01
²¹ Ne	5.38E-03	5.13E-03	5.40E-03	5.19E-03
²² Ne	6.43E-02	6.16E-02	6.45E-02	6.22E-02
²³ Ne	1.27E-05	1.42E-05	1.32E-05	1.45E-05
²⁴ Ne	7.21E-10	8.75E-10	7.57E-10	8.84E-10
¹⁹ Na	2.31E-39	2.00E-39	3.83E-39	2.98E-39
²⁰ Na	2.78E-21	3.57E-21	5.47E-21	5.92E-21
²¹ Na	3.70E-08	5.22E-08	3.98E-08	5.27E-08
²² Na	1.95E-06	1.83E-06	1.97E-06	1.90E-06
²³ Na	9.27E-03	8.77E-03	9.29E-03	8.91E-03
²⁴ Na	4.79E-05	5.54E-05	4.89E-05	5.56E-05
²⁵ Na	5.44E-07	7.96E-07	5.77E-07	7.92E-07
²⁶ Na	2.41E-11	3.87E-11	3.67E-11	5.17E-11
²⁷ Na	8.58E-18	1.07E-17	2.57E-17	2.51E-17
²⁰ Mg	2.56E-52	4.00E-52	5.13E-52	4.75E-52
²¹ Mg	5.17E-31	4.62E-31	1.81E-30	1.37E-30
²² Mg	2.42E-13	2.90E-13	2.76E-13	3.16E-13
²³ Mg	3.21E-06	3.18E-06	3.26E-06	3.36E-06
²⁴ Mg	7.62E-02	8.22E-02	8.29E-02	8.81E-02
²⁵ Mg	1.25E-02	1.36E-02	1.26E-02	1.37E-02
²⁶ Mg	2.09E-02	2.03E-02	2.09E-02	2.06E-02
²⁷ Mg	6.33E-06	8.01E-06	6.37E-06	7.85E-06
²⁸ Mg	6.94E-08	1.16E-07	7.20E-08	1.12E-07
²⁹ Mg	1.54E-12	3.45E-12	2.28E-12	4.30E-12
²² Al	5.24E-58	2.16E-58	3.12E-57	1.63E-57

Table 4—Continued

Species	d0.2s0.8	d0.2s1.5	d0.7s0.8	d0.7s1.5
²³ Al	2.02E-30	1.56E-30	2.62E-30	2.07E-30
²⁴ Al	3.55E-18	3.15E-18	4.30E-18	3.77E-18
²⁵ Al	6.13E-07	6.07E-07	6.59E-07	6.42E-07
²⁶ Al	2.57E-05	2.83E-05	2.58E-05	2.85E-05
²⁷ Al	2.67E-03	2.60E-03	2.70E-03	2.70E-03
²⁸ Al	4.37E-05	4.83E-05	4.29E-05	4.75E-05
²⁹ Al	1.30E-06	1.68E-06	1.28E-06	1.61E-06
³⁰ Al	8.35E-10	1.75E-09	9.69E-10	1.81E-09
³¹ Al	2.03E-13	5.52E-13	3.12E-13	6.98E-13
²³ Si	1.42E-75	4.86E-76	1.46E-74	5.41E-75
²⁴ Si	6.82E-38	3.99E-38	1.72E-37	9.47E-38
²⁵ Si	3.61E-27	2.21E-27	8.27E-27	5.15E-27
²⁶ Si	7.04E-13	6.89E-13	8.53E-13	8.12E-13
²⁷ Si	5.58E-07	5.55E-07	6.03E-07	6.24E-07
²⁸ Si	1.08E-01	4.63E-01	1.48E-01	4.82E-01
²⁹ Si	5.96E-03	5.91E-03	6.35E-03	6.66E-03
³⁰ Si	1.31E-02	1.29E-02	1.66E-02	1.62E-02
³¹ Si	4.41E-05	4.79E-05	4.30E-05	4.81E-05
³² Si	2.73E-06	2.87E-06	2.66E-06	2.95E-06
³³ Si	1.32E-10	3.57E-10	1.54E-10	3.54E-10
³⁴ Si	1.39E-13	4.61E-13	1.76E-13	4.77E-13
²⁷ P	2.09E-25	1.31E-25	4.16E-25	2.74E-25
²⁸ P	2.79E-19	2.05E-19	5.55E-19	4.13E-19
²⁹ P	6.58E-10	1.01E-09	7.53E-10	1.09E-09
³⁰ P	2.52E-06	2.73E-06	2.55E-06	2.98E-06
³¹ P	1.62E-03	1.66E-03	1.95E-03	2.05E-03
³² P	1.28E-05	1.27E-05	1.32E-05	1.40E-05
³³ P	1.26E-05	1.27E-05	1.37E-05	1.40E-05
³⁴ P	3.84E-08	4.34E-08	3.84E-08	4.34E-08
³⁵ P	1.83E-09	2.12E-09	1.78E-09	2.03E-09

Table 4—Continued

Species	d0.2s0.8	d0.2s1.5	d0.7s0.8	d0.7s1.5
³⁶ P	1.03E-13	3.50E-13	1.23E-13	3.44E-13
³⁷ P	9.19E-18	3.14E-17	1.56E-17	4.14E-17
³⁸ P	3.31E-26	4.00E-26	9.77E-26	1.08E-25
²⁸ S	5.16E-40	3.70E-40	1.63E-39	6.83E-39
²⁹ S	3.94E-29	2.63E-29	1.48E-28	8.19E-29
³⁰ S	2.54E-16	1.42E-14	3.05E-16	3.39E-14
³¹ S	4.55E-08	8.30E-08	8.32E-08	1.04E-07
³² S	5.34E-02	2.80E-01	8.92E-02	3.00E-01
³³ S	4.33E-04	4.87E-04	5.26E-04	6.36E-04
³⁴ S	9.81E-03	1.18E-02	1.27E-02	1.64E-02
³⁵ S	1.25E-05	1.31E-05	1.23E-05	1.35E-05
³⁶ S	2.25E-05	2.29E-05	2.28E-05	2.40E-05
³⁷ S	4.34E-09	8.00E-09	4.64E-09	7.76E-09
³⁸ S	3.35E-11	8.11E-11	3.66E-11	7.71E-11
³⁹ S	7.86E-14	2.50E-13	9.04E-14	2.40E-13
⁴⁰ S	5.84E-16	2.47E-15	6.85E-16	2.32E-15
⁴¹ S	2.92E-21	1.18E-20	5.22E-21	1.59E-20
⁴² S	7.18E-23	4.98E-22	1.06E-22	5.33E-22
³¹ Cl	3.06E-32	2.55E-32	4.36E-32	1.26E-28
³² Cl	9.82E-24	8.35E-24	2.27E-23	3.08E-20
³³ Cl	2.34E-10	2.39E-10	2.77E-10	3.20E-10
³⁴ Cl	3.40E-09	2.24E-08	5.63E-09	1.85E-08
³⁵ Cl	1.38E-04	1.64E-04	1.72E-04	2.33E-04
³⁶ Cl	2.86E-06	2.87E-06	2.92E-06	3.00E-06
³⁷ Cl	6.48E-05	6.52E-05	6.53E-05	6.63E-05
³⁸ Cl	4.69E-07	6.30E-07	4.82E-07	6.24E-07
³⁹ Cl	6.78E-08	9.38E-08	6.84E-08	9.08E-08
⁴⁰ Cl	6.17E-10	1.33E-09	6.61E-10	1.28E-09
⁴¹ Cl	5.74E-11	1.07E-10	5.93E-11	1.02E-10
⁴² Cl	2.19E-13	8.86E-13	2.58E-13	8.47E-13

Table 4—Continued

Species	d0.2s0.8	d0.2s1.5	d0.7s0.8	d0.7s1.5
⁴³ Cl	9.08E-15	3.05E-14	9.72E-15	2.78E-14
⁴⁴ Cl	6.96E-21	3.78E-20	1.45E-20	5.53E-20
⁴⁵ Cl	2.52E-21	2.79E-20	3.77E-21	2.85E-20
³² Ar	5.96E-45	7.34E-44	1.40E-44	2.36E-34
³³ Ar	2.17E-34	1.61E-34	8.99E-34	3.48E-30
³⁴ Ar	3.06E-17	5.57E-16	4.59E-17	3.46E-13
³⁵ Ar	2.69E-13	1.43E-09	5.53E-13	8.03E-10
³⁶ Ar	7.85E-03	5.60E-02	1.87E-02	6.13E-02
³⁷ Ar	3.27E-05	4.51E-05	5.68E-05	8.16E-05
³⁸ Ar	6.08E-03	7.84E-03	8.55E-03	1.29E-02
³⁹ Ar	4.34E-06	4.70E-06	4.33E-06	4.67E-06
⁴⁰ Ar	2.77E-06	2.86E-06	2.81E-06	2.97E-06
⁴¹ Ar	1.97E-08	2.57E-08	1.99E-08	2.51E-08
⁴² Ar	1.48E-08	1.50E-08	1.47E-08	1.57E-08
⁴³ Ar	9.49E-12	1.88E-11	9.86E-12	1.78E-11
⁴⁴ Ar	1.01E-12	1.28E-12	9.84E-13	1.26E-12
⁴⁵ Ar	7.57E-16	2.87E-15	8.42E-16	2.65E-15
⁴⁶ Ar	2.43E-17	4.37E-17	2.49E-17	4.27E-17
³⁵ K	9.02E-35	6.45E-35	1.64E-34	1.28E-29
³⁶ K	3.50E-28	4.66E-28	8.29E-28	1.20E-20
³⁷ K	2.57E-12	2.48E-12	3.33E-12	4.94E-12
³⁸ K	6.74E-10	1.38E-08	1.67E-09	9.75E-09
³⁹ K	1.10E-04	1.48E-04	1.90E-04	2.90E-04
⁴⁰ K	1.87E-06	1.82E-06	1.87E-06	1.86E-06
⁴¹ K	5.11E-06	5.03E-06	5.14E-06	5.12E-06
⁴² K	7.09E-07	7.67E-07	6.98E-07	7.70E-07
⁴³ K	6.15E-07	6.58E-07	5.98E-07	6.68E-07
⁴⁴ K	1.58E-07	1.65E-07	1.52E-07	1.64E-07
⁴⁵ K	1.41E-07	1.45E-07	1.35E-07	1.52E-07
⁴⁶ K	8.37E-09	8.77E-09	8.03E-09	8.79E-09

Table 4—Continued

Species	d0.2s0.8	d0.2s1.5	d0.7s0.8	d0.7s1.5
⁴⁷ K	6.84E-10	7.23E-10	6.65E-10	7.76E-10
⁴⁸ K	2.05E-16	1.19E-15	2.53E-16	1.13E-15
⁴⁹ K	8.90E-19	5.82E-18	1.15E-18	5.78E-18
³⁶ Ca	2.64E-42	2.13E-42	1.00E-41	3.74E-37
³⁷ Ca	5.03E-38	3.97E-38	2.39E-37	9.09E-30
³⁸ Ca	1.25E-20	2.51E-20	2.51E-20	7.08E-16
³⁹ Ca	6.31E-16	7.42E-12	3.08E-15	4.08E-11
⁴⁰ Ca	4.05E-03	4.87E-02	1.43E-02	5.27E-02
⁴¹ Ca	1.63E-05	1.72E-05	2.14E-05	2.44E-05
⁴² Ca	2.51E-04	3.13E-04	4.11E-04	5.86E-04
⁴³ Ca	1.77E-06	1.80E-06	1.78E-06	1.89E-06
⁴⁴ Ca	1.63E-05	1.59E-05	1.79E-05	1.77E-05
⁴⁵ Ca	1.16E-06	1.21E-06	1.14E-06	1.23E-06
⁴⁶ Ca	1.66E-06	1.68E-06	1.76E-06	1.81E-06
⁴⁷ Ca	1.60E-07	1.65E-07	1.54E-07	1.71E-07
⁴⁸ Ca	1.23E-06	1.21E-06	1.25E-06	1.23E-06
⁴⁹ Ca	1.35E-09	2.11E-09	1.43E-09	2.07E-09
⁴⁰ Sc	1.78E-33	1.37E-33	2.91E-33	2.66E-23
⁴¹ Sc	1.73E-15	1.61E-15	2.70E-15	5.46E-15
⁴² Sc	3.05E-15	6.23E-15	4.91E-15	1.79E-12
⁴³ Sc	1.32E-09	1.81E-09	2.50E-09	1.51E-07
⁴⁴ Sc	1.15E-08	1.30E-08	1.70E-08	2.35E-08
⁴⁵ Sc	8.31E-07	8.08E-07	9.05E-07	9.13E-07
⁴⁶ Sc	4.05E-07	4.00E-07	4.11E-07	4.25E-07
⁴⁷ Sc	6.11E-07	6.15E-07	6.69E-07	6.66E-07
⁴⁸ Sc	3.13E-07	3.18E-07	3.05E-07	3.42E-07
⁴⁹ Sc	1.57E-07	1.60E-07	1.56E-07	1.72E-07
⁵⁰ Sc	1.34E-10	1.48E-10	1.31E-10	1.46E-10
⁵¹ Sc	5.40E-12	5.49E-12	5.29E-12	5.46E-12
⁴¹ Ti	3.18E-45	1.45E-45	7.83E-45	5.61E-34

Table 4—Continued

Species	d0.2s0.8	d0.2s1.5	d0.7s0.8	d0.7s1.5
⁴² Ti	6.87E-26	5.12E-26	2.01E-25	2.48E-24
⁴³ Ti	5.98E-22	4.14E-20	1.03E-21	6.18E-13
⁴⁴ Ti	1.72E-06	2.62E-05	8.17E-06	1.00E-04
⁴⁵ Ti	1.09E-07	2.32E-07	4.49E-07	7.42E-07
⁴⁶ Ti	1.94E-04	3.19E-04	4.09E-04	8.14E-04
⁴⁷ Ti	3.96E-06	4.34E-06	4.64E-06	5.88E-06
⁴⁸ Ti	2.30E-05	2.36E-05	2.39E-05	2.51E-05
⁴⁹ Ti	4.42E-06	4.44E-06	4.43E-06	4.47E-06
⁵⁰ Ti	5.49E-06	5.67E-06	5.81E-06	5.94E-06
⁵¹ Ti	7.77E-08	9.57E-08	7.80E-08	9.42E-08
⁵² Ti	2.01E-08	2.08E-08	1.95E-08	2.15E-08
⁵³ Ti	1.77E-11	4.74E-11	1.94E-11	4.49E-11
⁴³ V	9.13E-43	9.08E-43	2.60E-42	1.22E-40
⁴⁴ V	5.17E-35	2.99E-35	1.84E-34	1.43E-23
⁴⁵ V	4.62E-23	1.50E-22	7.09E-23	1.14E-13
⁴⁶ V	1.85E-17	2.64E-15	1.73E-16	2.21E-14
⁴⁷ V	1.50E-08	1.91E-07	4.23E-08	4.30E-07
⁴⁸ V	2.19E-07	3.44E-07	4.04E-07	6.73E-07
⁴⁹ V	4.50E-07	5.91E-07	5.98E-07	9.16E-07
⁵⁰ V	5.10E-08	5.96E-08	5.54E-08	6.15E-08
⁵¹ V	3.37E-06	3.38E-06	3.59E-06	3.54E-06
⁵² V	3.57E-07	3.89E-07	3.54E-07	3.91E-07
⁵³ V	3.16E-07	3.24E-07	3.06E-07	3.40E-07
⁵⁴ V	1.36E-09	1.92E-09	1.39E-09	1.89E-09
⁵⁵ V	3.54E-11	4.49E-11	3.96E-11	4.90E-11
⁴⁴ Cr	5.17E-55	1.06E-54	1.14E-54	2.69E-52
⁴⁵ Cr	2.25E-46	1.20E-46	1.87E-45	4.28E-34
⁴⁶ Cr	6.81E-34	3.84E-27	4.33E-33	3.69E-19
⁴⁷ Cr	8.48E-22	3.54E-16	9.22E-21	2.54E-11
⁴⁸ Cr	8.43E-07	5.83E-04	3.41E-06	3.05E-04

Table 4—Continued

Species	d0.2s0.8	d0.2s1.5	d0.7s0.8	d0.7s1.5
⁴⁹ Cr	2.47E-07	1.00E-05	9.29E-07	6.68E-06
⁵⁰ Cr	2.03E-04	9.77E-04	2.67E-04	1.41E-03
⁵¹ Cr	4.92E-06	7.49E-06	4.63E-06	1.17E-05
⁵² Cr	1.29E-04	1.69E-04	1.18E-04	1.70E-04
⁵³ Cr	1.68E-05	1.63E-05	1.68E-05	1.64E-05
⁵⁴ Cr	2.29E-05	2.32E-05	2.40E-05	2.43E-05
⁵⁵ Cr	4.15E-07	5.56E-07	4.25E-07	5.50E-07
⁵⁶ Cr	1.47E-07	1.66E-07	1.45E-07	1.70E-07
⁵⁷ Cr	5.44E-11	1.44E-10	7.10E-11	1.58E-10
⁵⁸ Cr	7.00E-12	2.40E-11	8.22E-12	2.34E-11
⁴⁶ Mn	3.88E-64	1.76E-64	3.84E-63	4.09E-51
⁴⁷ Mn	1.51E-49	7.57E-50	8.70E-49	4.57E-33
⁴⁸ Mn	1.74E-45	1.85E-45	5.29E-45	2.07E-23
⁴⁹ Mn	5.16E-27	3.43E-20	2.19E-26	2.20E-14
⁵⁰ Mn	4.49E-18	1.80E-13	3.45E-17	1.54E-13
⁵¹ Mn	1.32E-08	2.90E-05	2.35E-08	1.36E-05
⁵² Mn	1.89E-07	3.30E-06	2.41E-07	2.07E-06
⁵³ Mn	1.10E-06	7.00E-06	6.36E-07	6.54E-06
⁵⁴ Mn	9.43E-08	1.09E-07	1.05E-07	1.16E-07
⁵⁵ Mn	8.19E-05	7.84E-05	8.29E-05	7.97E-05
⁵⁶ Mn	6.11E-06	6.58E-06	6.10E-06	6.60E-06
⁵⁷ Mn	1.08E-05	1.12E-05	1.05E-05	1.17E-05
⁵⁸ Mn	1.40E-07	1.68E-07	1.46E-07	1.72E-07
⁵⁹ Mn	2.41E-07	2.46E-07	2.41E-07	2.54E-07
⁶⁰ Mn	6.52E-11	2.31E-10	8.45E-11	2.41E-10
⁶¹ Mn	3.62E-12	1.54E-11	4.93E-12	1.66E-11
⁴⁷ Fe	5.63E-78	4.94E-78	7.04E-77	7.09E-64
⁴⁸ Fe	3.56E-63	1.07E-63	3.08E-62	2.16E-45
⁴⁹ Fe	2.95E-58	2.13E-54	3.58E-57	5.05E-35
⁵⁰ Fe	1.20E-44	2.23E-36	4.97E-44	3.82E-26

Table 4—Continued

Species	d0.2s0.8	d0.2s1.5	d0.7s0.8	d0.7s1.5
⁵¹ Fe	1.02E-27	1.30E-19	1.60E-26	2.11E-16
⁵² Fe	7.80E-08	1.16E-02	2.03E-07	5.05E-03
⁵³ Fe	6.94E-08	1.90E-04	1.63E-07	8.73E-05
⁵⁴ Fe	8.56E-04	4.15E-02	6.63E-04	2.80E-02
⁵⁵ Fe	4.56E-05	8.67E-05	3.96E-05	9.48E-05
⁵⁶ Fe	8.39E-03	8.48E-03	8.56E-03	8.85E-03
⁵⁷ Fe	8.65E-04	8.58E-04	8.68E-04	8.64E-04
⁵⁸ Fe	1.24E-03	1.27E-03	1.37E-03	1.39E-03
⁵⁹ Fe	6.21E-05	7.22E-05	6.19E-05	7.11E-05
⁶⁰ Fe	1.10E-04	1.16E-04	1.10E-04	1.20E-04
⁶¹ Fe	1.92E-07	4.18E-07	2.05E-07	3.98E-07
⁶² Fe	3.47E-08	5.40E-08	3.48E-08	5.40E-08
⁶³ Fe	1.32E-10	4.92E-10	1.51E-10	4.62E-10
⁵⁰ Co	4.25E-73	2.24E-73	9.24E-72	2.56E-48
⁵¹ Co	2.23E-60	9.83E-61	8.65E-60	5.62E-41
⁵² Co	7.21E-57	1.48E-50	3.95E-56	9.21E-30
⁵³ Co	2.02E-33	1.55E-24	6.37E-33	7.05E-18
⁵⁴ Co	4.88E-20	1.21E-13	2.55E-19	1.66E-13
⁵⁵ Co	7.14E-09	7.52E-04	4.95E-09	3.30E-04
⁵⁶ Co	2.23E-08	7.27E-06	1.39E-08	4.85E-06
⁵⁷ Co	1.14E-06	3.14E-06	1.43E-06	4.25E-06
⁵⁸ Co	6.32E-07	6.98E-07	8.42E-07	8.41E-07
⁵⁹ Co	1.12E-04	1.16E-04	1.29E-04	1.25E-04
⁶⁰ Co	9.65E-06	9.93E-06	9.50E-06	1.01E-05
⁶¹ Co	4.33E-05	4.53E-05	4.41E-05	4.67E-05
⁶² Co	1.84E-06	1.99E-06	1.80E-06	1.97E-06
⁶³ Co	8.54E-06	8.53E-06	8.26E-06	9.16E-06
⁶⁴ Co	8.93E-14	1.25E-13	2.03E-13	2.46E-13
⁶⁵ Co	3.98E-08	4.01E-08	3.93E-08	3.97E-08
⁵¹ Ni	1.58E-88	4.86E-89	5.32E-87	2.30E-62

Table 4—Continued

Species	d0.2s0.8	d0.2s1.5	d0.7s0.8	d0.7s1.5
⁵² Ni	5.65E-76	1.44E-76	3.38E-75	2.57E-55
⁵³ Ni	4.00E-71	3.66E-64	7.73E-70	1.56E-42
⁵⁴ Ni	3.14E-49	5.57E-37	8.56E-48	9.66E-30
⁵⁵ Ni	9.52E-32	1.08E-21	1.19E-30	2.14E-18
⁵⁶ Ni	4.95E-08	2.40E-01	5.07E-08	2.16E-01
⁵⁷ Ni	1.90E-08	8.76E-04	2.57E-08	1.39E-03
⁵⁸ Ni	3.75E-04	4.90E-03	4.15E-04	9.58E-03
⁵⁹ Ni	2.80E-05	2.96E-05	2.97E-05	3.63E-05
⁶⁰ Ni	2.46E-04	2.80E-04	2.92E-04	3.28E-04
⁶¹ Ni	2.41E-05	2.42E-05	2.42E-05	2.43E-05
⁶² Ni	7.75E-05	8.75E-05	8.87E-05	9.49E-05
⁶³ Ni	1.22E-05	1.35E-05	1.20E-05	1.34E-05
⁶⁴ Ni	3.64E-05	3.76E-05	3.84E-05	3.96E-05
⁶⁵ Ni	3.71E-07	5.09E-07	3.78E-07	4.97E-07
⁶⁶ Ni	3.38E-07	3.84E-07	3.42E-07	3.93E-07
⁶⁷ Ni	7.96E-10	1.97E-09	8.76E-10	1.89E-09
⁵⁵ Cu	1.29E-77	4.08E-78	1.44E-76	1.52E-55
⁵⁶ Cu	7.21E-61	1.42E-52	4.87E-60	4.97E-32
⁵⁷ Cu	2.63E-36	4.90E-27	3.92E-36	1.13E-16
⁵⁸ Cu	4.10E-22	3.58E-13	9.23E-22	2.37E-08
⁵⁹ Cu	7.96E-12	1.09E-09	8.29E-12	5.84E-05
⁶⁰ Cu	9.23E-12	2.90E-10	9.49E-12	5.96E-05
⁶¹ Cu	2.49E-10	5.05E-10	4.08E-10	1.79E-06
⁶² Cu	7.08E-10	8.05E-10	7.46E-10	1.26E-07
⁶³ Cu	3.55E-06	3.41E-06	3.57E-06	3.45E-06
⁶⁴ Cu	1.30E-07	1.33E-07	1.30E-07	1.35E-07
⁶⁵ Cu	4.72E-06	5.02E-06	5.12E-06	5.09E-06
⁶⁶ Cu	1.77E-07	1.88E-07	1.78E-07	1.91E-07
⁶⁷ Cu	1.40E-06	1.48E-06	1.37E-06	1.52E-06
⁶⁸ Cu	4.21E-08	5.52E-08	4.30E-08	5.49E-08

Table 4—Continued

Species	d0.2s0.8	d0.2s1.5	d0.7s0.8	d0.7s1.5
⁶⁹ Cu	1.58E-07	1.64E-07	1.53E-07	1.71E-07
⁵⁷ Zn	5.88E-76	2.88E-72	7.79E-75	1.08E-45
⁵⁸ Zn	2.28E-51	1.86E-45	8.06E-51	2.62E-30
⁵⁹ Zn	1.39E-41	4.75E-30	4.76E-41	1.72E-19
⁶⁰ Zn	5.08E-17	2.15E-09	1.60E-16	1.48E-03
⁶¹ Zn	1.70E-16	2.61E-11	3.51E-16	2.92E-05
⁶² Zn	1.48E-11	1.91E-09	5.47E-11	7.72E-04
⁶³ Zn	1.88E-12	2.65E-12	3.79E-12	8.81E-08
⁶⁴ Zn	5.55E-06	5.39E-06	5.59E-06	5.45E-06
⁶⁵ Zn	2.90E-07	2.79E-07	2.89E-07	2.80E-07
⁶⁶ Zn	4.70E-06	4.82E-06	4.84E-06	4.87E-06
⁶⁷ Zn	7.86E-07	7.61E-07	7.88E-07	7.68E-07
⁶⁸ Zn	4.04E-06	4.06E-06	4.26E-06	4.23E-06
⁶⁹ Zn	1.31E-07	1.57E-07	1.33E-07	1.56E-07
⁷⁰ Zn	7.56E-07	7.89E-07	7.55E-07	8.10E-07
⁷¹ Zn	1.07E-08	1.87E-08	1.12E-08	1.81E-08
⁷² Zn	1.83E-08	2.20E-08	1.80E-08	2.24E-08
⁵⁹ Ga	8.86E-84	1.71E-84	7.63E-83	7.58E-61
⁶⁰ Ga	4.73E-68	2.85E-68	2.38E-67	2.91E-41
⁶¹ Ga	1.73E-39	9.75E-40	3.23E-39	5.14E-18
⁶² Ga	1.05E-38	1.25E-34	2.07E-38	2.60E-19
⁶³ Ga	1.59E-23	1.73E-18	1.83E-23	8.59E-08
⁶⁴ Ga	1.25E-19	2.18E-17	2.20E-19	5.59E-07
⁶⁵ Ga	9.28E-13	8.77E-13	9.42E-13	4.48E-08
⁶⁶ Ga	8.71E-13	9.68E-13	8.64E-13	7.17E-09
⁶⁷ Ga	4.57E-11	4.93E-11	4.60E-11	7.87E-11
⁶⁸ Ga	2.22E-11	2.39E-11	2.50E-11	2.47E-11
⁶⁹ Ga	3.37E-07	3.21E-07	3.39E-07	3.24E-07
⁷⁰ Ga	1.24E-08	1.27E-08	1.24E-08	1.28E-08
⁷¹ Ga	2.17E-07	2.11E-07	2.19E-07	2.13E-07

Table 4—Continued

Species	d0.2s0.8	d0.2s1.5	d0.7s0.8	d0.7s1.5
⁷² Ga	1.43E-08	1.42E-08	1.44E-08	1.45E-08
⁷³ Ga	7.16E-08	7.67E-08	7.13E-08	7.81E-08
⁷⁴ Ga	8.32E-09	1.11E-08	8.58E-09	1.11E-08
⁷⁵ Ga	2.68E-08	3.03E-08	2.62E-08	3.13E-08
⁶² Ge	1.18E-55	3.59E-56	4.14E-55	1.57E-32
⁶³ Ge	1.20E-42	2.78E-36	3.57E-42	1.89E-20
⁶⁴ Ge	3.24E-25	3.26E-17	3.01E-24	5.68E-06
⁶⁵ Ge	2.57E-25	4.21E-20	5.13E-25	2.36E-07
⁶⁶ Ge	1.14E-17	1.12E-16	1.59E-17	1.10E-05
⁶⁷ Ge	8.55E-17	1.12E-16	8.86E-17	6.43E-09
⁶⁸ Ge	2.10E-11	2.68E-11	2.89E-11	1.54E-09
⁶⁹ Ge	1.75E-12	2.05E-12	2.07E-12	2.23E-12
⁷⁰ Ge	3.31E-07	3.19E-07	3.34E-07	3.23E-07
⁷¹ Ge	2.27E-08	2.14E-08	2.25E-08	2.15E-08
⁷² Ge	4.47E-07	4.36E-07	4.68E-07	4.57E-07
⁷³ Ge	1.34E-07	1.30E-07	1.34E-07	1.31E-07
⁷⁴ Ge	6.86E-07	6.66E-07	7.21E-07	6.97E-07
⁷⁵ Ge	5.22E-08	6.02E-08	5.30E-08	6.04E-08
⁷⁶ Ge	1.56E-07	1.70E-07	1.58E-07	1.74E-07
⁷⁷ Ge	3.55E-09	6.37E-09	3.75E-09	6.18E-09
⁷⁸ Ge	4.43E-09	5.78E-09	4.40E-09	5.84E-09
⁶⁵ As	1.98E-54	3.80E-49	2.39E-54	7.78E-22
⁶⁶ As	1.06E-52	4.35E-46	1.34E-51	4.74E-22
⁶⁷ As	1.36E-28	7.40E-28	1.41E-28	1.52E-11
⁶⁸ As	3.38E-25	3.44E-25	3.38E-25	2.49E-10
⁶⁹ As	6.81E-21	8.55E-21	6.85E-21	7.14E-11
⁷⁰ As	1.07E-17	1.29E-17	1.06E-17	1.42E-10
⁷¹ As	1.38E-13	1.34E-13	1.37E-13	2.13E-12
⁷² As	6.85E-14	7.01E-14	6.68E-14	6.98E-14
⁷³ As	1.76E-11	1.97E-11	2.40E-11	2.55E-11

Table 4—Continued

Species	d0.2s0.8	d0.2s1.5	d0.7s0.8	d0.7s1.5
⁷⁴ As	4.22E-12	4.39E-12	4.49E-12	4.51E-12
⁷⁵ As	3.74E-09	4.00E-09	5.34E-09	5.06E-09
⁷⁶ As	5.71E-11	5.77E-11	5.71E-11	5.87E-11
⁷⁷ As	2.49E-09	2.71E-09	2.70E-09	2.70E-09
⁷⁸ As	2.60E-11	2.66E-11	2.51E-11	2.70E-11
⁷⁹ As	1.23E-09	1.22E-09	1.18E-09	1.29E-09
⁶⁸ Se	7.12E-34	7.66E-26	4.69E-33	3.86E-09
⁶⁹ Se	8.39E-31	2.13E-28	8.24E-31	2.57E-10
⁷⁰ Se	6.69E-23	9.65E-23	1.03E-22	6.50E-08
⁷¹ Se	2.55E-21	3.36E-21	3.62E-21	1.05E-10
⁷² Se	3.72E-14	4.74E-14	7.94E-14	1.70E-10
⁷³ Se	1.85E-15	2.30E-15	3.61E-15	1.91E-14
⁷⁴ Se	5.14E-10	6.42E-10	8.58E-10	9.97E-10
⁷⁵ Se	7.45E-12	8.51E-12	1.19E-11	1.25E-11
⁷⁶ Se	1.07E-09	1.55E-09	1.22E-09	1.55E-09
⁷⁷ Se	6.80E-12	7.91E-12	7.09E-12	7.58E-12
⁷⁸ Se	2.53E-10	3.68E-10	2.41E-10	3.17E-10
⁷⁹ Se	1.57E-11	1.57E-11	1.46E-11	1.59E-11
⁸⁰ Se	3.25E-11	4.35E-11	3.18E-11	3.94E-11
⁸¹ Se	3.69E-13	3.60E-13	3.56E-13	3.74E-13
⁸² Se	6.98E-12	7.82E-12	6.85E-12	7.71E-12
⁸³ Se	8.97E-16	8.51E-16	8.60E-16	8.59E-16
⁷⁰ Br	1.80E-58	7.84E-59	3.65E-58	1.46E-25
⁷¹ Br	5.27E-36	1.82E-35	5.27E-36	5.17E-14
⁷² Br	1.49E-31	1.97E-31	1.46E-31	6.73E-13
⁷³ Br	5.56E-25	5.64E-25	6.41E-25	6.68E-13
⁷⁴ Br	2.37E-21	2.94E-21	5.05E-21	2.75E-12
⁷⁵ Br	2.69E-17	3.40E-17	5.36E-17	2.59E-14
⁷⁶ Br	4.94E-16	5.91E-16	8.64E-16	1.24E-15
⁷⁷ Br	7.27E-14	1.01E-13	1.16E-13	1.28E-13

Table 4—Continued

Species	d0.2s0.8	d0.2s1.5	d0.7s0.8	d0.7s1.5
⁷⁸ Br	6.15E-15	7.74E-15	6.69E-15	7.43E-15
⁷⁹ Br	1.48E-12	2.31E-12	1.49E-12	1.92E-12
⁸⁰ Br	1.17E-13	1.47E-13	1.17E-13	1.25E-13
⁸¹ Br	3.14E-12	4.84E-12	3.18E-12	4.15E-12
⁸² Br	4.21E-14	5.05E-14	4.09E-14	4.40E-14
⁸³ Br	1.08E-12	1.46E-12	1.09E-12	1.28E-12
⁷² Kr	1.29E-40	1.16E-34	2.23E-40	1.97E-12
⁷³ Kr	3.65E-36	3.00E-35	4.26E-36	1.66E-12
⁷⁴ Kr	7.87E-27	9.43E-27	5.27E-26	3.49E-10
⁷⁵ Kr	5.15E-25	6.16E-25	2.42E-24	1.28E-12
⁷⁶ Kr	5.81E-17	7.42E-17	7.94E-16	2.69E-12
⁷⁷ Kr	2.08E-17	2.71E-17	1.43E-16	4.42E-15
⁷⁸ Kr	3.92E-13	5.39E-13	3.02E-12	1.48E-12
⁷⁹ Kr	1.60E-14	2.54E-14	3.17E-14	3.24E-14
⁸⁰ Kr	8.31E-13	1.58E-12	8.07E-13	1.21E-12
⁸¹ Kr	3.20E-15	5.97E-15	2.55E-15	4.09E-15
⁸² Kr	1.55E-13	3.79E-13	8.88E-14	1.86E-13
⁸³ Kr	1.17E-15	1.66E-15	1.11E-15	1.33E-15
⁸⁴ Kr	1.35E-14	3.24E-14	1.07E-14	1.91E-14
⁸⁵ Kr	2.28E-17	2.74E-17	2.17E-17	2.34E-17
⁸⁶ Kr	7.13E-16	1.35E-15	6.60E-16	9.95E-16
⁸⁷ Kr	1.05E-21	1.11E-21	1.02E-21	1.07E-21